AD-A147 650 AUXILIARY GAS LOADING OF EXPLOSIVES AND THEIR SENSITIVITY TO DDT (DEFLAGR..(U) NAVAL SURFACE WEAPONS CENTER SILVER SPRING MD D PRICE ET AL. 25 JUN 84 1/1

UNCLASSIFIED NSWC/TR-83-330 F/G 19/1 NL

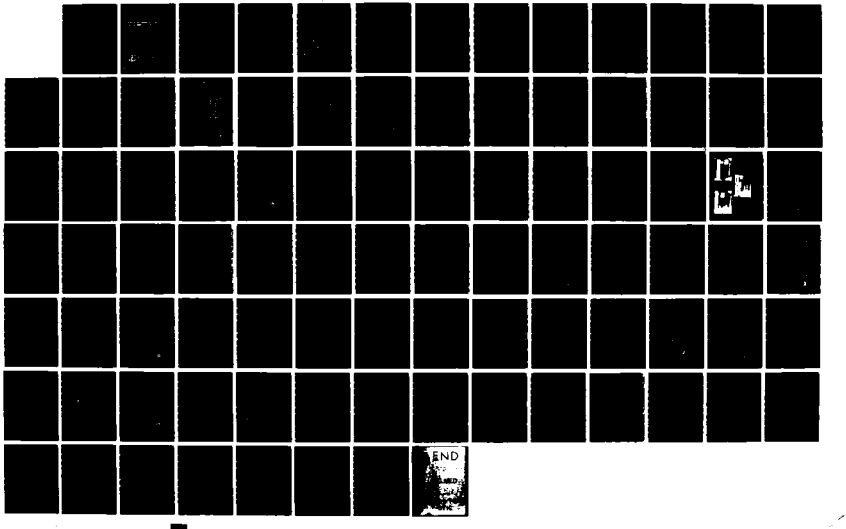

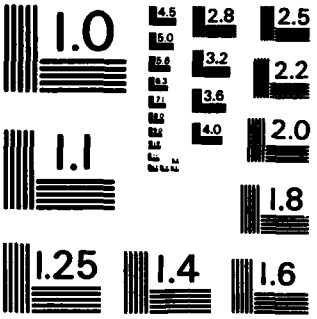

NSWC TR 83-330

AUXILIARY GAS LOADING OF EXPLOSIVES AND THEIR SENSITIVITY TO DDT

BY D. PRICE R. BERNECKER

RESEARCH AND TECHNOLOGY DEPARTMENT

25 JUNE 1984

Approved for public release, distribution unlimited

NAVAL SURFACE WEAPONS CENTER

Dahlgren, Virginia 22448 • Silver Spring, Maryland 20910

UNCLASSIFIED

SECURITY CLASSIFICATION OF THIS PAGE *(When Data Entered)*

REPORT DOCUMENTATION PAGE		READ INSTRUCTIONS BEFORE COMPLETING FORM
1. REPORT NUMBER NSWC/TR 83-330	2. GOVT ACCESSION NO. AD-A147 650	3. RECIPIENT'S CATALOG NUMBER
4. TITLE *(and Subtitle)* AUXILIARY GAS LOADING OF EXPLOSIVES AND THEIR SENSITIVITY TO DDT		5. TYPE OF REPORT & PERIOD COVERED 6. PERFORMING ORG. REPORT NUMBER
7. AUTHOR(s) Donna Price and Richard R. Bernecker		8. CONTRACT OR GRANT NUMBER(s)
9. PERFORMING ORGANIZATION NAME AND ADDRESS Naval Surface Weapons Center (Code R13) White Oak Silver Spring, MD 20910		10. PROGRAM ELEMENT, PROJECT, TASK AREA & WORK UNIT NUMBERS 62633N,SF33354,SF33354314, SEA1846220323
11. CONTROLLING OFFICE NAME AND ADDRESS		12. REPORT DATE 25 June 1984 13. NUMBER OF PAGES 90
14. MONITORING AGENCY NAME & ADDRESS*(if different from Controlling Office)*		15. SECURITY CLASS. *(of this report)* Unclassified 15a. DECLASSIFICATION/DOWNGRADING SCHEDULE

16. DISTRIBUTION STATEMENT *(of this Report)*

Approved for public release, distribution unlimited.

17. DISTRIBUTION STATEMENT *(of the abstract entered in Block 20, if different from Report)*

18. SUPPLEMENTARY NOTES

19. KEY WORDS *(Continue on reverse side if necessary and identify by block number)*

Gas loading	RDX	Expl D	PBXN103
Sensitivity	91/9 RDX/wax	Cast H-6	PBXW-108
DDT	tetryl	Cast Comp B	PBXN-106
TNT	Cast cyclotol 75/25	Cast pentolite 50/50	AFX 108

20. ABSTRACT *(Continue on reverse side if necessary and identify by block number)*

The object of this report is to present all previously unreported work on the auxiliary gas loading experiments in the studies of the deflagration to detonation transition (DDT) in high explosives (HE). The study was directed toward methods to rate quantitatively both cast and porous HE for their susceptibility to undergoing DDT. Granular explosives studied were RDX, waxed RDX, tetryl, TNT, and Explosive D; cast HE, TNT based compositions and plastic bonded explosives (PBXs). Sensitivity of an explosive to DDT has been rated

cont'd

DD FORM 1 JAN 73 1473 EDITION OF 1 NOV 65 IS OBSOLETE
S/N 0102-LF-014-6601

UNCLASSIFIED

SECURITY CLASSIFICATION OF THIS PAGE *(When Data Entered)*

In the present apparatus by use of an auxiliary gas loader; such ratings are presented for pressed charges at 70% and 88% TMD. Additional methods of obtaining a quantitative rating are also pointed out. Work on evaluating cast charges is still preliminary, but results are sufficient to indicate that castings are, in general, much less sensitive to DDT than pressed charges.

FOREWORD

The experimental work, documented in this report, was performed several years ago under tasks SF33-354-314/18462 and R000-01/03L-000, IR-159. Portions have been presented orally to NAVSEASYSCOM in 1974 and at a meeting on Safety and Performance Tests at ARRADCOM, Dover, N. J. in 1977. The present report summarizes the reported work on auxiliary gas loading of HEs as well as newer work on PBXs, and documents the results. They will be useful to those interested in understanding DDT and explosive sensitivity.

Approved by:

H. S. Hamm

for K. F. MUELLER, Head
Energetic Materials Division

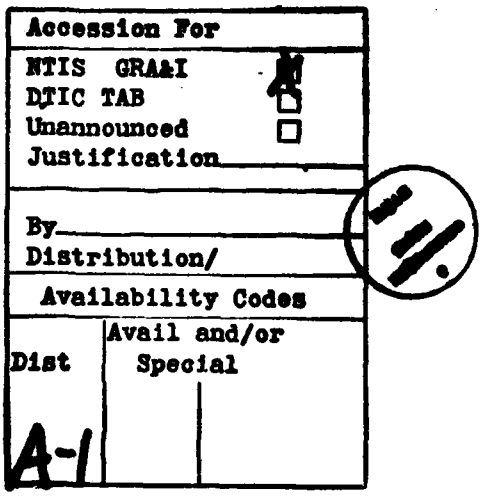

CONTENTS

	Page
INTRODUCTION	1
EXPERIMENTAL ARRANGEMENT AND PROCEDURE	3
EXPERIMENTAL RESULTS AND DISCUSSION	4
PRESSED EXPLOSIVES	4
TNT BASED CAST EXPLOSIVES	14
SELF-LOADED	14
GAS LOADED	18
CAST PLASTIC BONDED EXPLOSIVES	28
SELF-LOADED	28
GAS LOADED	28
GENERAL CONTROL PROBLEMS	32
SUMMARY AND CONCLUSIONS	33
REFERENCES	36
APPENDIX A--DETAILED DATA FOR DDT SHOTS	A-1

ILLUSTRATIONS

Figure		Page
1	DATA FOR 19.8 mm 94/6 RDX/WAX ON 1.24 g/cm^3 (68.9% TMD) RDX (SHOT 1011).	5
2	RELATIONSHIPS BETWEEN ℓ' and Δt_E. RELATIVE SENSITIVITIES TO DDT UNDER GAS LOADING.	8
3	DATA FOR 19.1 mm 88.1% TMD 94/6 RDX/WAX on 87.6% TMD COARSE TETRYL (SHOT 714).	10
4	SHOT 1414 ON CAST PENTOLITE CHARGE 25 mm DIA x 410 mm LENGTH.	17
5	DATA FOR 40.0 mm 95.0% TMD 94/6 RDX/WAX ON CAST PENTOLITE (SHOT 908).	21
6	DATA FOR 60 mm 95% TMD 94/6 RDX/WAX ON CAST 75/25 CYCLOTOL IN AN 18 INCH TUBE (SHOT 1409).	22
7	RELATIVE SENSITIVITY TO DDT OF THREE GAS LOADED CAST HE USING 95% TMD 94/6 RDX/WAX AS GAS LOADER.	23
8	RELATIONSHIP BETWEEN ℓ' AND $^I\Delta t_E$ FOR GAS LOADED CAST EXPLOSIVES.	25
9	TUBES RECOVERED FROM SHOTS OF SELF-LOADED PBXs.	30
10	DATA FOR 60 mm COLUMN OF 95% TMD 94/6 RDX/WAX ON PBXN 103 IN 18 INCH TUBE (SHOT 1316).	31
A-1	DATA FOR 20.0 mm 70.4% TMD 94/6 RDX/WAX ON 1.23 g/cm^3 (68.1% TMD) RDX (SHOT 708).	A-4
A-2	DATA FOR 20.1 mm 70.6% TMD 94/6 RDX/WAX ON 1.22 g/cm^3 (70% TMD) GROUND TETRYL(SHOT 1009).	A-5

ILLUSTRATIONS (CONT.)

Figure		Page
A-3	DISTANCE-TIME DATA FOR 19.1 mm 88.1% TMD 94/6 RDX/WAX ON 87.5% TMD 95/5 TNT/WAX (SHOT 716).	A-6
A-4	DATA FOR 9.5 mm 87.8% TMD 94/6 RDX/WAX ON 1.46 g/cm^3 (88.2% TMD) TNT (SHOT 702).	A-7
A-5	DATA FOR 28.6 mm 87.8% TMD 96/4 RDX/WAX ON 89.1% TMD TNT (SHOT 617).	A-8
A-6	DATA FOR 19 mm 94% TMD 94/6 RDX/WAX ON 93.9% TMD TNT (SHOT 715). . . .	A-9
A-7	DISTANCE-TIME DATA FOR 28.6 mm 93.7% TMD 94/6 RDX/WAX ON 93.6% TMD TNT (SHOT 814).	A-10
A-8	DATA FOR 28.6 mm 88% TMD 94/6 RDX/WAX ON 87.7% TMD EXPLOSIVE D (SHOT 616).	A-11
A-9	DATA FOR 38.1 mm 94% TMD 94/6 RDX/WAX ON 94.7% TMD EXPLOSIVE D (SHOT 903).	A-12
A-10	DATA FOR 60.3 mm 94.4% TMD 94/6 RDX/WAX ON 94.4% TMD EXPLOSIVE D (SHOT 1110).	A-13
A-11	SHOT 1318 ON CAST PENTOLITE (~97% TMD).	A-14
A-12	SHOT 1503 ON CAST PENTOLITE (~97% TMD).	A-15
A-13	SHOT 1413 ON CAST PENTOLITE IN CHARGES 25 mm DIA x 410 mm LENGTH.	A-16
A-14	SHOT 1508 ON CAST PENTOLITE.	A-17
A-15	SHOT 1209 ON CAST H-6 (CA. 97% TMD).	A-18
A-16	DATA FOR 40.0 mm 95.0% TMD 94/6 RDX/WAX ON CAST 75/25 CYCLOTOL (SHOT 1003).	A-19

ILLUSTRATIONS (CONT.)

Figure		Page
A-17	DATA FOR 50 mm 95% TMD 94/6 RDX/WAX ON CAST CYCLOTOL (CA. 99% TMD) IN AN 18 INCH TUBE (SHOT 1415).	A-20
A-18	DATA FOR 50 mm 95% TMD 94/6 RDX/WAX ON CAST COMP B IN AN 18 INCH TUBE (SHOT 1309).	A-21
A-19	DATA FOR 60 mm 96.7% TMD 94/6 RDX/WAX ON CAST COMP B IN AN 18 INCH TUBE (SHOT 1206).	A-22
A-20	DATA FOR 60 mm 96.7% TMD 94/6 RDX/WAX ON CAST TNT (SHOT 1102). . . .	A-23
A-21	DATA FOR 60 mm 96.7% TMD 94/6 RDX/WAX ON CAST TNT IN AN 18 INCH TUBE (SHOT 1105).	A-24
A-22	DATA FOR 50 mm 96.5% TMD RDX/WAX ON CAST CYCLOTOL 75/25 (CA. 96% TMD) IN 3 IN. DIA x 18 IN. LENGTH TUBE (SHOT 1716).	A-25
A-23	DATA FOR 50 mm 95% TMD 94/6 RDX/WAX ON CAST COMP B IN 3 IN. DIA x 18 IN. LENGTH TUBE (SHOT 1715).	A-26
A-24	DISTANCE-TIME DATA FOR 60 mm 95% TMD 94/6 RDX/WAX ON CAST PBXN 106 (SHOT 1704).	A-27

TABLES

Table		Page
1	EXPERIMENTAL RESULTS AT 70% TMD WITH 20 mm LOADER.	7
2	EXPERIMENTAL RESULTS AT 88% TMD WITH 19 mm LOADER.	9
3	EXPERIMENTAL RESULTS ON OTHER PRESSED CHARGES.	13
4	RESULTS ON SELF-LOADING OF CAST 50/50 PENTOLITE CHARGES.	15
5	RESULTS OF GAS LOADING OF CAST EXPLOSIVES IN REGULAR TUBE.	20
6	EFFECT OF DIAMETER ON GAS LOADED CAST HE	26
7	SHOTS ON SELF-LOADED PBXs.	29
A-1	DETAILED DATA FOR GAS LOADING OF PRESSED CHARGES.	A-28
A-2	DETAILED DATA FOR SELF-LOADING OF CAST 50/50 PENTOLITE IN STANDARD TUBE.	A-31
A-3	SELF-LOADING OF CAST H-6.	A-33
A-4	DETAILED DATA FOR GAS LOADING OF TNT BASED CAST CHARGES.	A-34
A-5	DETAILED DATA FOR GAS LOADING OF PBX EXPLOSIVES.	A-38

INTRODUCTION

The objective of this paper is to present all unreported or incompletely reported work on the auxiliary gas loading experiments in our study of deflagration to detonation transition (DDT). These experiments were primarily designed to elucidate the mechanism of DDT, but at the same time they also provide information about the sensitivity of an explosive to undergoing DDT.

In Refs. 1 and 2 we reported that the use of a rapidly burning, gas producing material (called the auxiliary gas loader): (1) confirmed the fundamental importance of a rapid increase in dp/dt in the ignition region to effect DDT, (2) confirmed the proposed mechanism of DDT for 91/9 RDX/wax mixtures, and (3) showed that the transition mechanism for gas loaded HE was the same as that for self-loaded HE save for the superposed more rapid burning of the loader. In the case of several HE which failed to exhibit DDT under self-loading in our apparatus, we demonstrated the existence of a critical column length of loader (ℓ_g^{crit}): if $\ell_g < \ell_g^{crit}$, no DDT; $\ell_g > \ell_g^{crit}$, DDT. Moreover, as $\ell_g > \ell_g^{crit}$ was increased, the predetonation column length of the test explosive decreased, as would be expected from increased gas loading and duration combined with the pressure sensitivity of the test explosive.

Since the publication of that report, we have frequently been asked to devise a method of assessing the tendency of HE to undergo DDT. It is far from a simple problem to obtain any sensitivity rating. That for DDT is particularly complex since the phenomena involved range from ignition and transient combustion all the way to a shock to detonation transition (SDT) which must terminate any successful DDT. Moreover, any quantitative

rating requires a positive result; failures cannot be placed on a rating scale. Finally, all results will inevitably be tied to the conditions of the experiment; those conditions may or (more generally) may not approximate the conditions of use.

There are many reasonable ways in which such a quantitative rating can be attempted. Some of them are:

1. Vary the confining tube (or its venting) to determine the critical confinement (venting) for DDT.
2. Vary the initial temperature to determine a critical value for DDT.
3. Determine the critical amount of admixed wax (RDX) to inhibit (effect) DDT.
4. Determine the critical amount of a non-detonating gas loader to effect DDT.

Each has advantages and disadvantages, but the last, or some variant of it, was most similar in method and procedures to work already in progress. Consequently, we incorporated the sensitivity problem into our studies. In other words, we used the same apparatus, and applied information available from previous work as the most expeditious way to rate sensitivity to DDT. To obtain positive results from insensitive materials, an auxiliary gas loader (94/6 RDX/wax), in a rapid burning but nondetonating column, is inserted between the igniter and the test explosive. The rapid pressure buildup that results, coupled with ignition and subsequent burning of the explosive, is sufficient to induce DDT in explosives such as porous TNT, Explosive D, and cast Composition B which do not show the transition in our apparatus under self-loading.[1,2,3] It is also the purpose of this paper to report sensitivity ratings obtained in this way, i.e. by varying the ignition system with an auxiliary gas loader.

EXPERIMENTAL ARRANGEMENT AND PROCEDURE

The experimental setup and procedures have been described in detail elsewhere.[1,2] In brief, a seamless steel tube (16.3 mm ID, 50.9 mm OD) with heavy end closures was used. The length of the B/KNO_3 ignitor column was 6.3 mm; the length of the standard explosive column was 295.4 mm. In the present work, the gas loader is inserted between the ignitor and the test explosive; the explosive column length is decreased accordingly. The DDT tube is instrumented with ionization probes (IP) and strain gages (SG) to monitor ionization fronts and strain, respectively.

Explosives were taken from commercial lots and satisfied the relevant military specifications. The same lots as those of the previous work were used; the weight mean particle sizes were: ammonium picrate (285μm), TNT (325μm), RDX (200μm) and tetryl (470 and 160μm). The carnauba wax (125μm) and the blending procedures were also those used previously.

The auxiliary gas loader used throughout is a mechanical mix of 94/6 RDX/wax. It will be referred to as the loader. It is used at the same %TMD as that of the acceptor for pressed charges, at 95% TMD for cast. All charges were examined by X-rays for voids.

The basic concept of these experiments is that the gas loader chosen reacts only in the burning mode, i.e., does not itself build up to either a shock or a full scale detonation capable of initiating the test materials. For this reason the loader has been examined for its behavior under self-loading. Over the range of 70 to 97% TMD, the predetonation column length ℓ varied from a minimum of 92 mm to a maximum of 135 mm.[4,5] In general, the loader length used (ℓ_g) was 55%ℓ or less.

The few variations in the general procedures, described above, will be described later in the appropriate experimental section.

EXPERIMENTAL RESULTS AND DISCUSSION

This section will be divided into three parts: PRESSED EXPLOSIVES, TNT BASED CAST EXPLOSIVES and CAST PLASTIC BONDED EXPLOSIVES.

PRESSED EXPLOSIVES

Detailed data for the gas loading of all pressed charges are given in Table A-1 of Appendix A. Only summary tables and representative figures will be presented in the body of the report.

Figure 1 shows a typical set of records for a pressed charge, in this case 68.9% TMD RDX with a 19.8 mm loader. In the figure, there is a mildly accelerating flame or IP front (~0.3 mm/μs) followed by the first detected compressive front (1.3 mm/μs) and the detonation front (6.85 mm/μs). Additional parameters that are measured from these data are the predetonation column length, $\ell' = \ell - \ell_g$, where ℓ is the x location of the onset of detonation, ℓ_g is length of loader column, and ℓ and ℓ_g are both measured from the igniter/loader interface. Various time intervals are also measured. Thus, Δt_D is relative time to detonation from ionization pin response at x = 28.7 mm. Similarly Δt_p is relative time to passage of the compression wave at the same pin location. Finally

$$\Delta t_E = \Delta t_D - \Delta t_p$$

would represent the relative time to detonation after the compression wave had passed the location x = 28.7 mm.

In using the above formula to compute Δt_E, it is necessary to have a common zero on the time scales. For example, if a short extrapolation is made of the IP curve to x = 29 mm, the new zero time value must also be

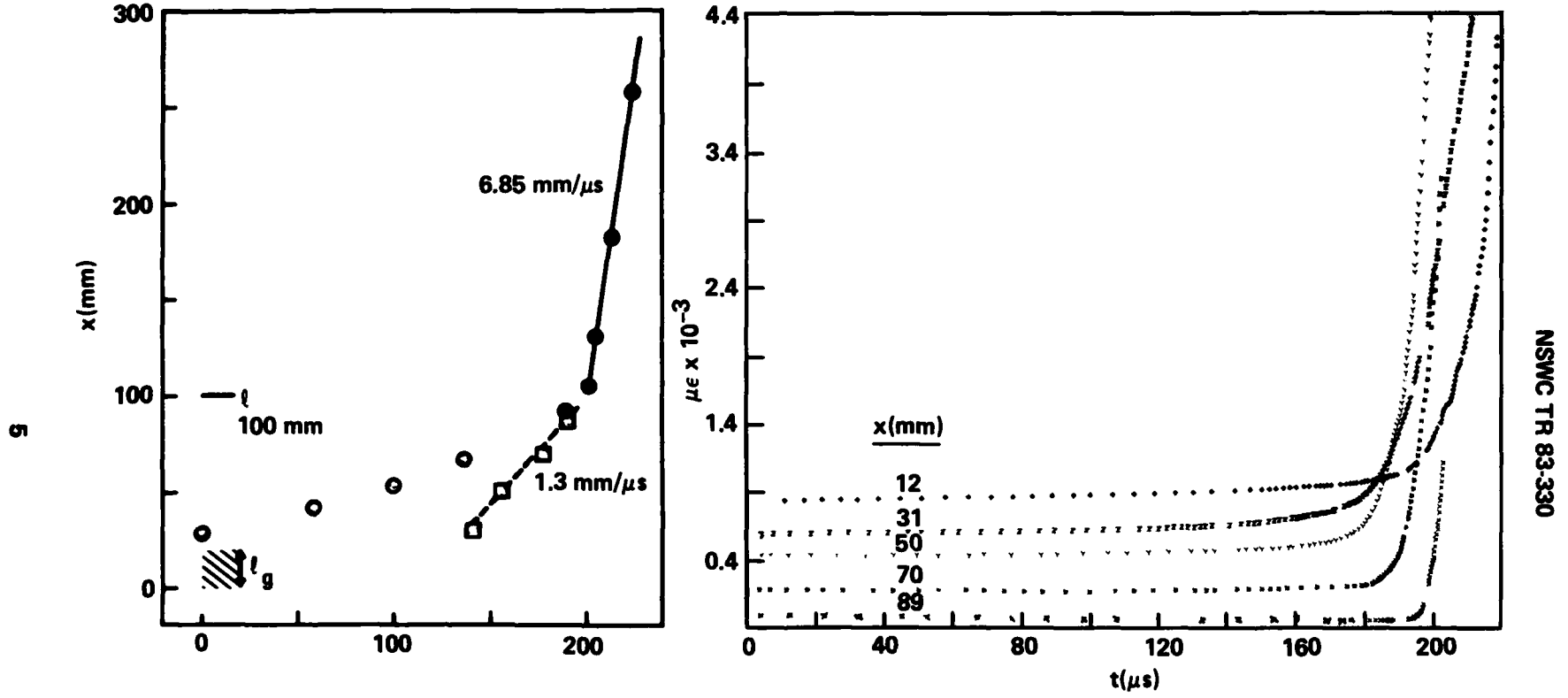

a. DISTANCE-TIME (O NOL PROBES, ● COMMERCIAL PROBES, □ SG EXCURSION TIME.)

b. STRAIN-TIME DATA [EACH CURVE, EXCEPT THE LOWEST, HAS BEEN RAISED 200 με (OR AN INTEGRAL MULTIPLE THEREOF) FOR BETTER DISPLAY]

FIGURE 1. DATA FOR 19.8 mm 94/6 RDX/WAX ON 1.24 g/cm^3 (68.9% TMD) RDX (SHOT 1011)

used in determining $^{29}\Delta t_p$. Instead of using the formula, the time interval between $^{29}\Delta t_p$ and the onset of detonation can be measured directly on whatever time scale discharge of the triggering probe produces.

Figure 1b shows the strain gage locations and records for this shot. It is from this figure that the data for the compressive wave, i.e., times of pressure excursions, are obtained.

Table 1 contains the summary data from five different charges at 70% theoretical maximum density (TMD) subjected to the same length of auxiliary gas loader (ℓ_g~20 mm, 70% TMD). The charges vary in sensitivity to DDT from those which exhibit transition under self-loading (e.g., 70% TMD RDX) to those that do not (70% TMD TNT and Expl D). It is evident from the tabulation that the predetonation column length (ℓ') does not correlate well with Δt_D or Δt_p, but seems to show the same trend as does Δt_E (time to detonation relative to time of passage of the compression wave at x~28.7 mm). Figure 2a confirms the fact that either ℓ' or Δt_E gives the same sensitivity rating for these five 70% TMD charges (four explosives). The TNT and ground tetryl (160 μs) values do not appear to be significantly different.

Table 2 contains the summary data for 88% TMD charges subjected to the same gas loader (ℓ_g~19 mm, 88% TMD) and Figure 3 shows a typical record for DDT under gas loading of an 88% TMD charge of 470 μm tetryl. Although the elements of this figure are the same as those of Figure 1, the arrangement is somewhat different. In particular, for the four shots from which strain gage records were obtained, the compressive front paralleled the IP front from the discharge of the third ionization probe on to the transition point (see Figure 3a). Moreover, in three out of the other four shots, the pressure front preceded the IP front by 8, 6, and 7 μs (Shots 714, 510, and 608, respectively). It followed in the 70% TMD charges, but in both cases it originated in the gas loader region. To obtain an estimate of Δt_E for Shot 716 (no SG record), it was assumed that the pressure front preceded the IP front by the average (7μs) and paralleled the line connecting the 3rd and 4th (x,t) pairs.

TABLE 1. EXPERIMENTAL RESULTS AT 70% TMD WITH 20 mm LOADER

	Test Material[a]			Gas Loader				Relative Times, μs		
Shot No.[c]	Mat.	ρ_0 g/cm^3	%TMD	ρ_0 g/cm^3	%TMD	ℓ_g (mm)	ℓ' (mm)	Δt_D	Δt_p	Δt_ℓ
708	RDX	1.229	68.1	1.210	70.4	20.0	73	188	147	41
1011	RDX	1.244	68.9	1.214	70.6	19.8	80	291	249	42
1009	Ground Tet.	1.215	70.0	1.215	70.6	20.1	110	209	170	39
410	TNT	1.214	73.4	1.208	70.2	19.7	127	176	135	41
409	D	1.210	70.3	1.212	70.5	19.6	153	167	126	41

a Tet. is tetryl with nominal average particle size of 180μ. It is the production tetryl (Type B) which has been ball milled for one hour. D is Explosive D or ammonium picrate.

b Δt_D is relative time to detonation from discharge of first probe. That probe was at x = 28.7 mm except for Shot 1011 where it was at 28.4 mm.
Δt_p is relative time at which the compression front passed the probe at 28.7 mm.
$\Delta t_\ell = \Delta t_D - \Delta t_p$ = time interval, compression front at x = 28.7 mm to onset of detonation.

c Detailed records for Shots 409 and 410 are in BRL Ii those for 708 and 1009 are in the Appendix, and those for 1011 are in Fig. 1.

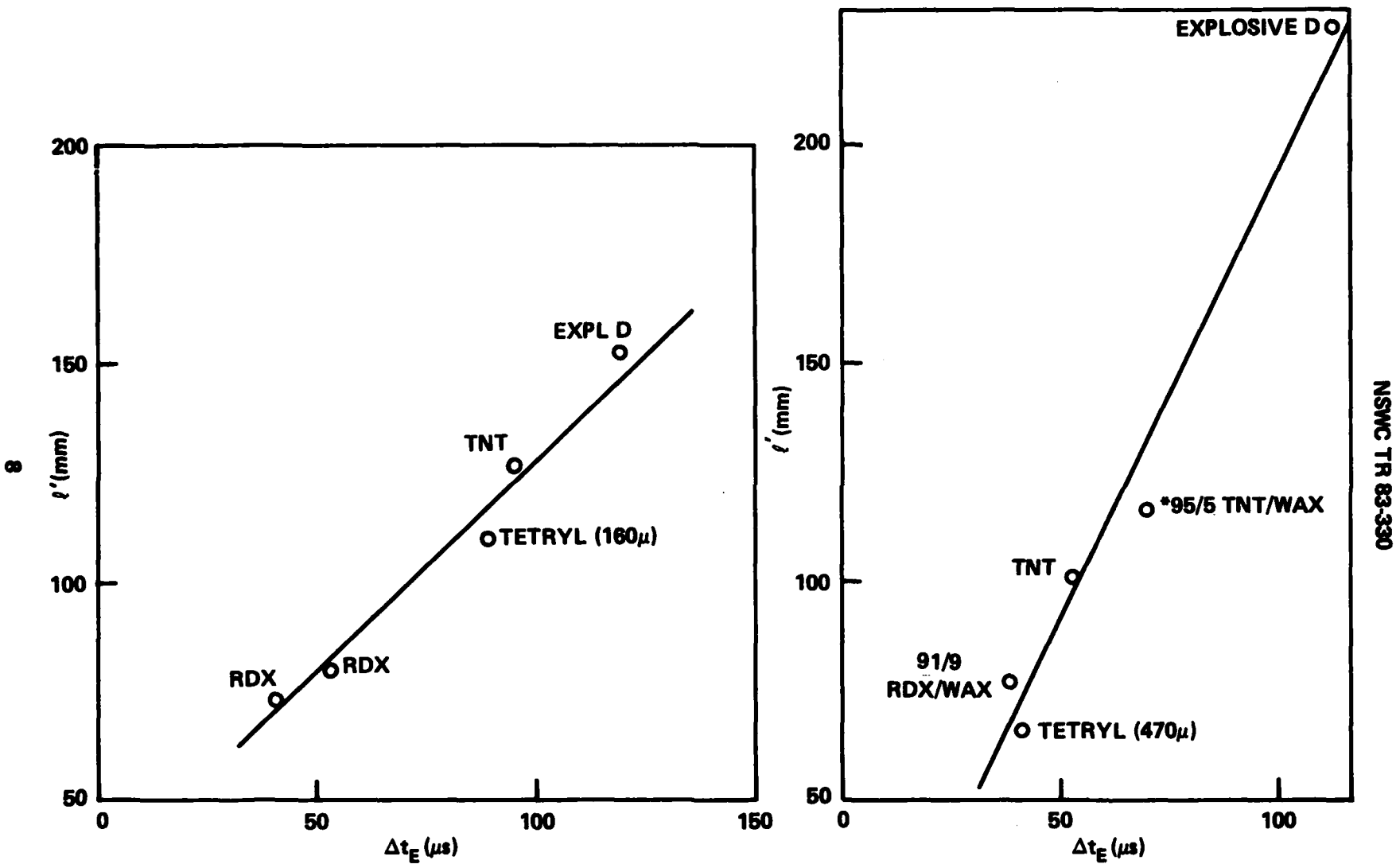

FIGURE 2. RELATIONSHIPS BETWEEN ℓ' AND Δt_E. RELATIVE SENSITIVITIES TO DDT UNDER GAS LOADING

TABLE 2. EXPERIMENTAL RESULTS AT 88% TMD WITH 19 mm LOADER

	Test Material[a]			Gas Loader				Relative Times (μs)[b]	
Shot No.[c]	Mat.	ρ_o g/cm^3	%TMD	ρ_o g/cm^3	%TMD	ℓ_g(mm)	ℓ' (mm)	Δt_D	Δt_ϵ
714	Tet.	1.543	87.6	1.515	88.1	19.1	66	46.5	41
701	A	1.477	87.9	1.515	88.1	19.1	77.5±3.5	47.5	38.5
510	TNT	1.467	88.7	1.516	88.1	19.1	101	61.0	59
716	95/5	1.398	87.5	1.515	88.1	19.1	116	78.0	78[d]
608	D	1.513	88.0	1.513	88.0	19.1	226	111.5	112.5

a Tet. is production tetryl (470μ); A is a mechanical mix of 91/9 RDX/wax; 95/5 is a mechanical mix of TNT/wax, and D is Explosive D.

b Δt_D is relative time to detonation from discharge of first probe at $x \sim 29$ mm; in the 700 series, this required a short extrapolation. Δt_ϵ is the time interval, arrival of compression front at $x \sim 29$ mm to onset of detonation; this also requires a small extrapolation.

c Detailed records for Shots 701, 510, and 608 are in Refs. 1 and 2; those for 714 are Fig. 3; and those for 716 are Fig. A-3.

d In this shot, the SG records were lost. See text for method of estimating Δt_ϵ.

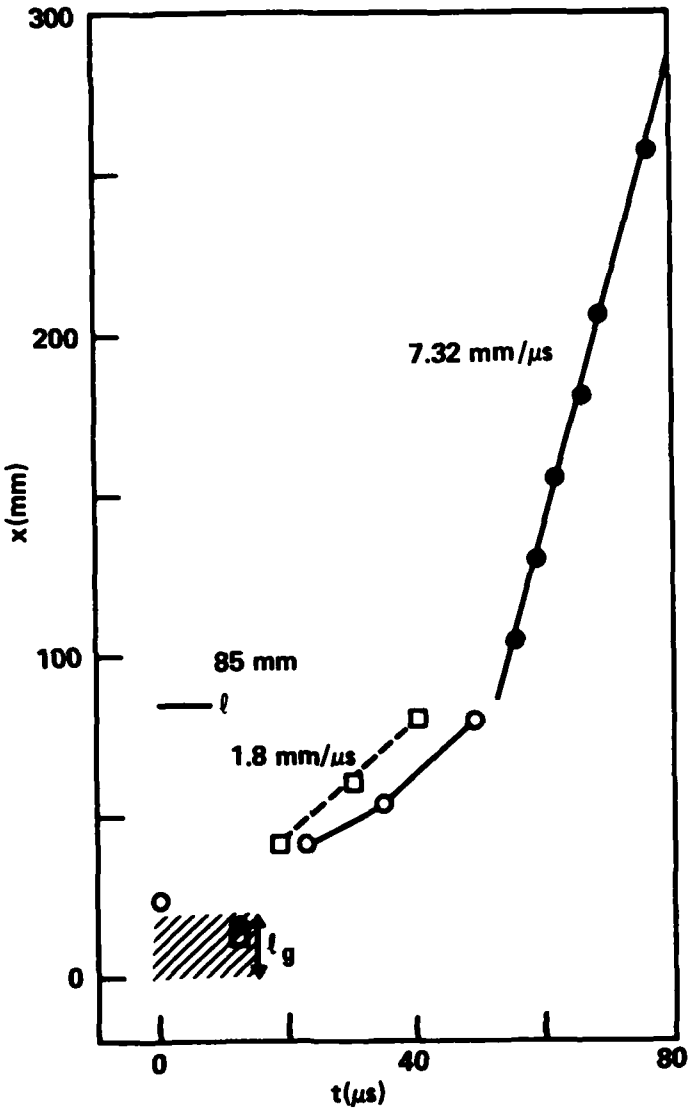

a. DISTANCE-TIME DATA. (LEGEND OF FIG. 1a, ^ INDICATES DATA FROM GAS LOADER REGION.)

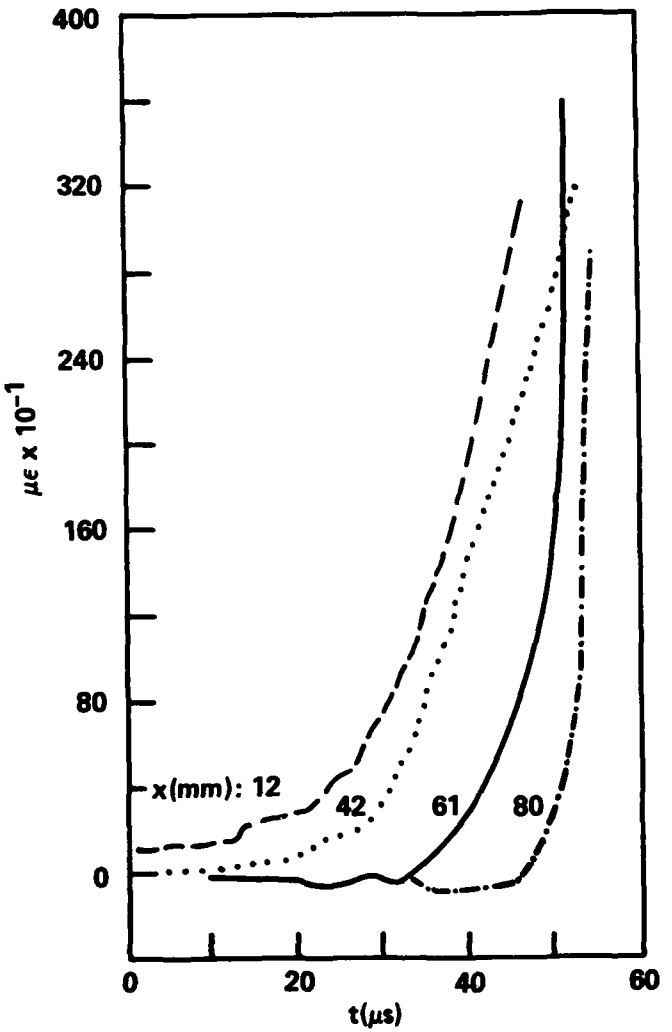

b. STRAIN-TIME DATA

FIGURE 3. DATA FOR 19.1 mm 88.1% TMD 94/6 RDX/WAX ON 87.6% TMD COARSE TETRYL (SHOT 714)

The data of Table 2 are plotted ℓ' vs Δt_E in Figure 2b. Again either ℓ' or Δt_E will rate the explosives' sensitivity the same way although 91/9 RDX/wax and 470 μm-tetryl are not significantly different,* Only Expl D (ammonium picrate) and TNT appear in both parts a and b of Figure 2. Their quantitative rating at 70% TMD seems to differ from that at 88% TMD. This is not surprising since we have found in waxed RDX,[4,5,6,7] waxed HMX,[4,5] tetryl,[8,9,10] and picric acid[8,9,10] (presumeably, in general) that a change in porosity affects both ℓ (or ℓ') and Δt_E, but in different manners. Hence a change in %TMD will affect the ℓ' versus Δt_C relationship; surprisingly, it remains linear. However, the linearity might disappear if a greater number of HEs were examined.

Thus Figure 2 gives us two different scales of sensitivity for two different degrees of compaction of the charges. To be sure, Expl D is less sensitive than TNT on both, but not by the same amount. How the two scales are related is unknown. We could have avoided using either ℓ' or Δt_E by determining the critical loader length, ℓ_g^{crit} for each charge. The rating would then be given by the critical values, each of which would require two or more shots for a determination. However, this would not suffice to compare charges of two different degrees of compaction. To do this we must abandon the experimental design of the same degree of compaction of loader and test explosive. Instead, the more highly compacted loader is used for both charges. (This is based on the assumption that sensitivity to DDT decreases with decreasing permeability and active surface area as it does for Explosive D[1]). Then the ℓ_g^{crit} values should serve to rate charges of various compactions as long as the range in sensitivity is not too great.

Table 3 summarizes the data obtained on the remaining pressed charges tested. They are arranged in four groupings within which ℓ_g has been varied. In view of this, all data (Δt_D and Δt_E as well as ℓ') have been measured from the loader/explosive interface; the superscript "I" indicates this for the relative times. Only one grouping has enough data to bracket ℓ_g^{crit} and that is the first. To induce a transition to metastable detonation (see Tables 3 and A-1) of 88% TMD TNT, ℓ_g^{crit} is less than 9.5 mm of 88% TMD 94/6 RDX/wax; to induce transition to steady state detonation, $9.5 < \ell_g^{crit} \leq 19.1$ mm. However, these values only apply to 88% TMD loader, and are therefore inadequate for a quantitative evaluation of sensitivities at higher degrees of compaction. We learn more qualitatively about sensitivity and more rapidly with the indices of ℓ' and Δt_E.

It is evident from the data of Table 3 that gas loading affects ℓ' and $^I\Delta t_E$ the same way, i.e., increasing ℓ_g decreases both ℓ' and $^I\Delta t_E$. This confirms the results of Refs. 1 and 2 as does the fact that TNT is more sensitive than Expl D to DDT at any given %TMD. The data for 88% TMD TNT suggest that ℓ' stays constant at $\ell_g \geq 19.1$ mm. This seems improbable in view of the results found on 70% TMD Expl D[1] (ℓ' and $^{29}\Delta t_E$ were 153 mm and 107 μs for ℓ_g = 19.6 mm and 125 mm and 94 μs for ℓ_g = 29.8 mm.) The next question is whether Shot 510 or 617 is more likely to be misrepresentative. In view of the fact that the data of Shot 510 seemed consistent with the data of several other 88% TMD explosives, the data of Shot 617 are suspect. Consequently, the values in parentheses for Shot 617 are for linear extrapolation of the ℓ' vs ℓ_g and $^I\Delta t_E$ vs ℓ_g curves defined by the two shorter loaders. Of course, this approximation assumes that transition to metastable detonation and to steady state detonation lie on the same curve. That may not be so, but the extrapolated values show the expected trend and are consistent with that found for 70% TMD Expl D[1].

TABLE 3. EXPERIMENTAL RESULTS ON OTHER PRESSED CHARGES

	Test Material			Gas Loader				Relative Times* (μs)	
Shot No.	HE	ρ_o g/cm^3	%TMD	ρ_o g/cm^3	%TMD	ℓ_g (mm)	ℓ' (mm)	$I_{\Delta t_D}$	$I_{\Delta t_E}$
702	TNT	1.458	88.2	1.510	87.8	9.5	130.5[a]	91.5[a]	74[a]
510	TNT	1.467	88.7	1.516	88.1	19.1	101	71	59
617	TNT	1.473	89.1	1.510	87.8	28.6	104(72)[c]	78.5	63(44)[c]
715	TNT	1.553	93.9	1.616	94.0	19.1	221	93	106
814	TNT	1.548	93.6	1.611	93.7	28.6	106.4	79	64.5[b]
608	Expl D	1.513	88.0	1.513	88.0	19.1	226	121	120
616	Expl D	1.508	87.7	1.50	87.2	28.6	175	84	84
903	Expl D	1.629	94.7	1.616	94.0	38.1	F	F	F
1110	Expl D	1.624	94.4	1.624	94.4	60.3	F	F	F

Shots 510 and 608 reported in Refs.1 and 2. Remaining records are in the Appendix, Figs. A-4-A-10.

*Time relative to loader/HE interface. Both curves (IP and SG excursions) extrapolated.

a Metastable detonation at 4.9 mm/μs.

b SG records lost. Parallelism of Shot 617 assumed.

c Values in parentheses are straight line extrapolations of first two ℓ' vs ℓ_g and $I_{\Delta t_E}$ vs ℓ_g pairs.

We can conclude that at ℓ_g = 19 mm, increasing the %TMD from 88 to 94% for TNT and Expl D results in a marked increase in ℓ' and $I_{\Delta t_E}$ for both HE (94% TMD Expl D failed to transit with ℓ_g = 60 mm). The same conclusion can be drawn for ℓ_g = 28.6 mm provided the extrapolated values are accepted for Shot 617. This trend would certainly be expected with the loss of voids and the approach to TMD. However, if the values of 70% TMD TNT are added to the series of ℓ_g ~ 19 mm, a reversal between 70 and 88% TMD occurs. This might be attributed to the different effects of compaction on the two variables (already discussed) or to error in one of the two measurements.

TNT BASED CAST EXPLOSIVES

Self-Loaded

In the case of cast explosives, we examined the behavior under self-loading prior to using a gas loader. Cast 50/50 pentolite was chosen for this purpose because we had already established that it exhibited DDT and that cast Comp B and cast TNT did not under experimental conditions similar to our regular configuration.[3]

Thirteen charges of pentolite were examined: seven in a regular tube (16 mm dia) and six in a larger tube (25 mm dia.). Detailed data for five of these shots are given in Table A-2; Table 4 is a summary table of all the shots. As those data show, two shots failed, and one showed transition to a metastable rather than a steady-state detonation. Positive results from the remaining ten indicate no detectable difference between two different pentolite batches (X731 and X887) and between the presence or absence of an end closure on these charges. In addition, the castings in the regular tube behaved far more reproducibly than those in the large tube. For example, the predetonation column length ℓ varied from 176 to 194 mm (Av. 185) in the former, and from 118 to 285 mm (Av. 191) in the latter. The greater variability of pentolite cast in the larger tubes might well arise from the resultant change in the cooling schedule during solidification. So too might the unusually long delay in ignition observed in Shot 1508 (see Appendix).

TABLE 4. RESULTS ON SELF-LOADING OF CAST 50/50 PENTOLITE CHARGES

Shot No.	Pentolite Lot	ℓ(mm) Tube	ℓ(mm) IP[a]	Chosen	Bottom Closure	$41_{\Delta t_D}$ μs
		Regular Tube				
407	X731	181	168-206		No	
413	X731	194	156-194		No	
414	X731	189	168-194		No	
1318	X887	185	168-188		Yes	280
1503	X887	232[b]	214-239		Yes	
1601	X887	176	-		No	
1604	X898	>295[c]	-		Yes	
		Av. 185[b]	175-204			
		25.4 mm ID 72 mm OD Tube		Chosen		
1413	X887	118[d]	156-181	181	Yes	127
1414	X887	118[d]	118-143	137	Yes	85
1508	X887	200	<220		Yes	-
1519	X887	285[d]	-		No	
1520	X887	>295[c]	-		No	
1603	X887	234	-		Yes	
		Av. 191	199-209[e]	207[e]		

a. IP data can only define region between successive probes containing onset. b. Metastable detonation (2.2 mm/μs) omitted from average. c. Negative result omitted from average.
d. Charge length of 410 mm instead of standard 295 mm. e. ℓ from tube used when IP range not obtained.

In Table 4, the value of ℓ from tube fragment markings and from the interval between probes, within which onset of detonation occurred, are both given when available. This was done because there are, atypically, apparent disagreements between the two (Shots 1413 and 1414). From the distance-time plot of these shots (Figure A-13 and Figure 4), it is evident that the most probable values of ℓ are 181 mm (see Appendix) and 136* mm, respectively.

Figure 4 is typical of DDT in cast pentolite under self-loading. The first event is formation of an ignition driven (IP) front. It is followed by a front, outlined by the response of SGs, arising in the ignitor region and, in this case, already at shock velocity. This front typically merges with the detonation portion of the IP curves. Hence onset occurred close to x = 136 mm in this shot. The DDT mechanism seems quite similar to that found for porous charges.[6,7]

In Figure 4 as in many other distance-time illustrations, there is more than one point for the pressure excursion at several SG locations. An excursion is a sharp change in slope, generally an increase. But in the case of cast pentolite, tube stretching caused by strong chemical reaction or strong axial shock fronts or both result in formation of minima in the SG records. The exact point to read, e.g., the minimum or level just preceding it, is in doubt. We have recorded the readings for all reasonable possibilities.

For this shot the driving reaction has been sufficiently vigorous to overboost the pentolite; thus the detonation front travels about 50 mm at 9.8 mm/μs before it settles to a steady state value of 7.2 mm/μs.

*This value was obtained from the time of the last SG excursion which fell on the extrapolated detonation curve. However, the time difference between this point and that for the SG 19 mm away was about one μs. Such a small difference is undoubtedly caused in part by error in reading the curves, but it also indicates the possibility that detonation onset might have been 118 ± 3 mm.

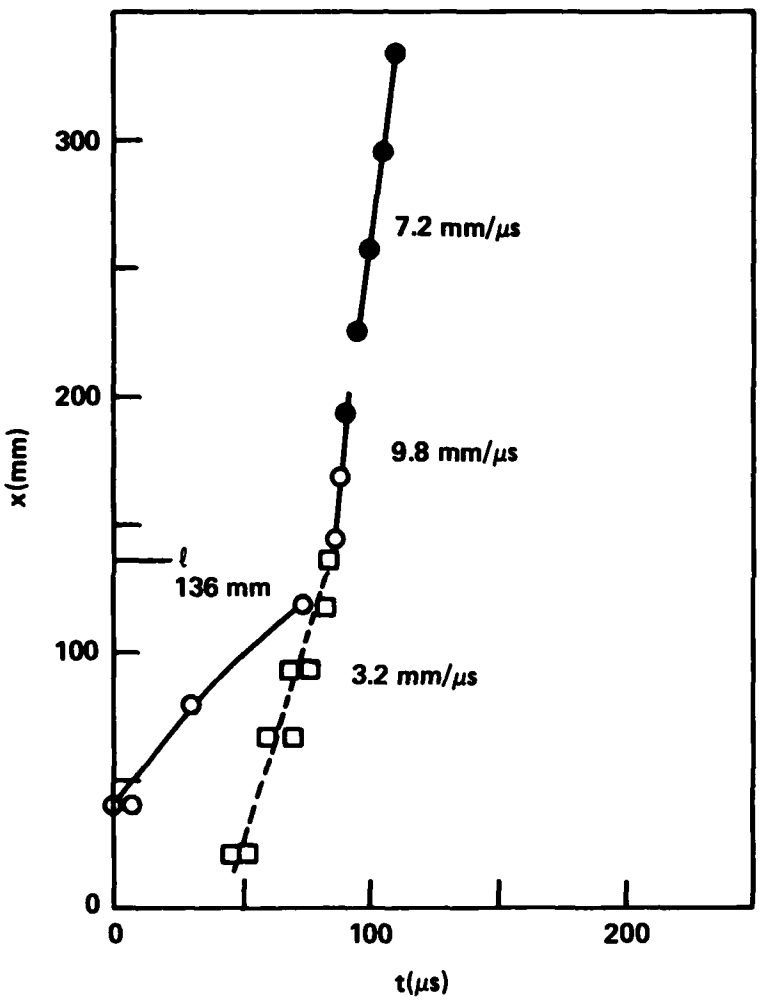

a. DISTANCE-TIME DATA (LEGEND OF FIG. 1a.)

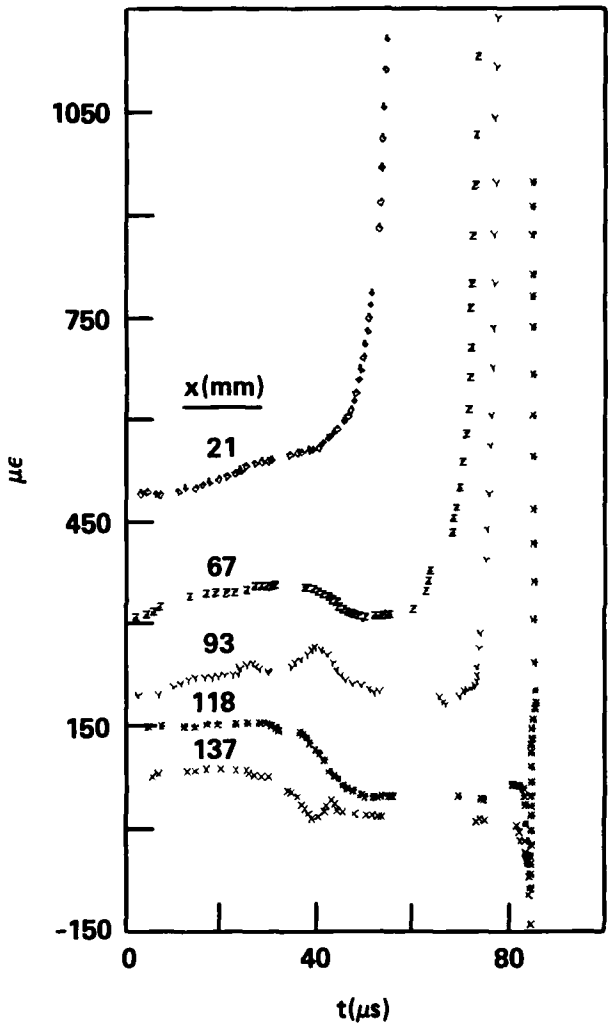

b. STRAIN-TIME DATA (LEGEND OF FIG. 1b WITH INCREMENT OF 75 με).

FIGURE 4. SHOT 1414 ON CAST PENTOLITE CHARGE 25 mm DIA. x 410 mm LENGTH

The difference between the most probable average values of ℓ, 185 mm and 207 mm for regular and large tubes, respectively, amounts to 12%. In view of the scatter of data in the large charges, 12% is probably the order of magnitude of the experimental error; it is certainly a lesser order than the 56% increase in tube size. Thus the values for the regular and larger tube do not differ significantly. We conclude, therefore, that DDT phenomena, under self-loading of cast pentolite, do not scale.

The only other cast HE of this group tested by self-loading was cast H-6. It failed to transit to detonation. The data appear in Table A-3; their plots in Figure A-15.

Gas Loaded

Table A-4 contains the data obtained from gas loading of TNT based cast explosives. Since loader and test material cannot both be cast into the tube to form known compositions on either side of a planar interface, it was decided to use high density (ca 95% TMD) pressed 94/6 RDX/wax as the loader. The test explosive is cast into the tube with a metal spacer in the gas loader position. When the test material has hardened and the tube has been conditioned at 25°C, the loader can be inserted into the cavity provided by the spacer. The isostatically pressed loader is machined into a cylinder of the desired size (16.2 mm dia). The curved surface of the cylinder is then covered with a thin layer of an uncured polyurethane (PU) mixture. The loader cylinder is then "slipfit" into the metal tube (ID 16.3 mm) with care to avoid trapping any PU at the loader/explosive interface; PU at the ignitor end of the cylinder is avoided by glueing the gas loader and ignitor together before applying the PU. Cure time at room temperature for this PU is 24 hours. After that interval, the annular space between the gas loader and the metal tube is filled with solid; this eliminates any possible "flashdown" from the ignitor toward the test explosive.

Preliminary tests showed that our usual column length of 295 mm (loader plus test HE) was inadequate to produce a transition in cast Comp B (60/40/1, RDX/TNT/wax). Consequently, a column length of 410 mm (tube length of 457 mm or 18 in.) has been used for most of the shots on cast HE. Even so, Comp B is the least sensitive cast HE on this sensitivity scale. TNT failed to transit and is, therefore, off-scale.

Table 5 is a summary table of the results obtained in the regular (i.e. 16 mm ID) tube. Figure 5 illustrates the DDT behavior of gas loaded pentolite (Shot 908) in contrast to self-loaded (Figure 4). In the case of auxiliary loading, the SG records also show minima, and the first SG front follows the IP front. However, the SG front overtakes the IP front about 20 μs later and thereafter precedes it. Transition occurs at 119 mm and 42.5 μs (referred to IP at 42 mm). The value $\ell' = 119 - 40 = 79$ mm is that comparable to ℓ under self-loading; i.e., it is the distance the disturbance has run to the onset of detonation in the acceptor. The average predetonation column length ℓ in the regular tube under self-loading was 185 mm; the average time to detonation $^{42}\Delta t_D$ (4 tubes) was 230 μs and was not very reproducible. The 40 mm of 95% TMD 96/4 RDX/wax has considerably reduced both predetonation column length and relative time to detonation for cast pentolite.

Figure 6 illustrates DDT for cast cyclotol 75/25 with 60 mm of the loader. As in the case of pentolite, the SG front precedes the IP front, and the SGs show minima which deepen as the front progresses. Both of these phenomena were observed in all loaded cast HE - even those that failed to transit (see Appendix).

Finally, Figure 7 shows the trend ℓ' vs ℓ_g for the three cast HE which exhibited DDT; it is the usual decrease of ℓ' with increase of ℓ_g. It is quite evident that in order of decreasing sensitivity the castings are pentolite, cyclotol, and Comp B. A quantitative ordering can be obtained by using a 50 or 60 mm loader length and measuring ℓ', or by determining ℓ_g^{crit} in each case. Negative results were obtained with a 60 mm loader on cast TNT. Evidently the experiment must be further modified to obtain a scale covering this less sensitive casting.

TABLE 5. RESULTS OF GAS LOADING OF CAST EXPLOSIVES IN REGULAR TUBE

Shot No.	HE	Tube[a] Length	ℓ_g[b] mm	ℓ mm	ℓ' mm	$^{35}\Delta t_D$[c] µs	$I_{\Delta t_E}$[c] µs
908	50/50 Pentolite	343	40	118.9	79	38	31
1003	75/25 Cyclotol	343	40	284	244	<108	<103
1415	75/25 Cyclotol	457	50	262	212	103	85
1409	75/25 Cyclotol	457	60	229	169	76	62
1309	Comp B.	457	50	361.4	311	213	135
1206	Comp B	457	60	313	253	144	106
1102	TNT	343	60	F	F	F	-
1105	TNT	457	60	F	F	F	-

[a]All tubes 16.3 mm ID, 50.8 mm OD

[b]Gas loader is 95% TMD 94/6 RDX/wax

[c]Most values extrapolated; I represents loader/HE interface.

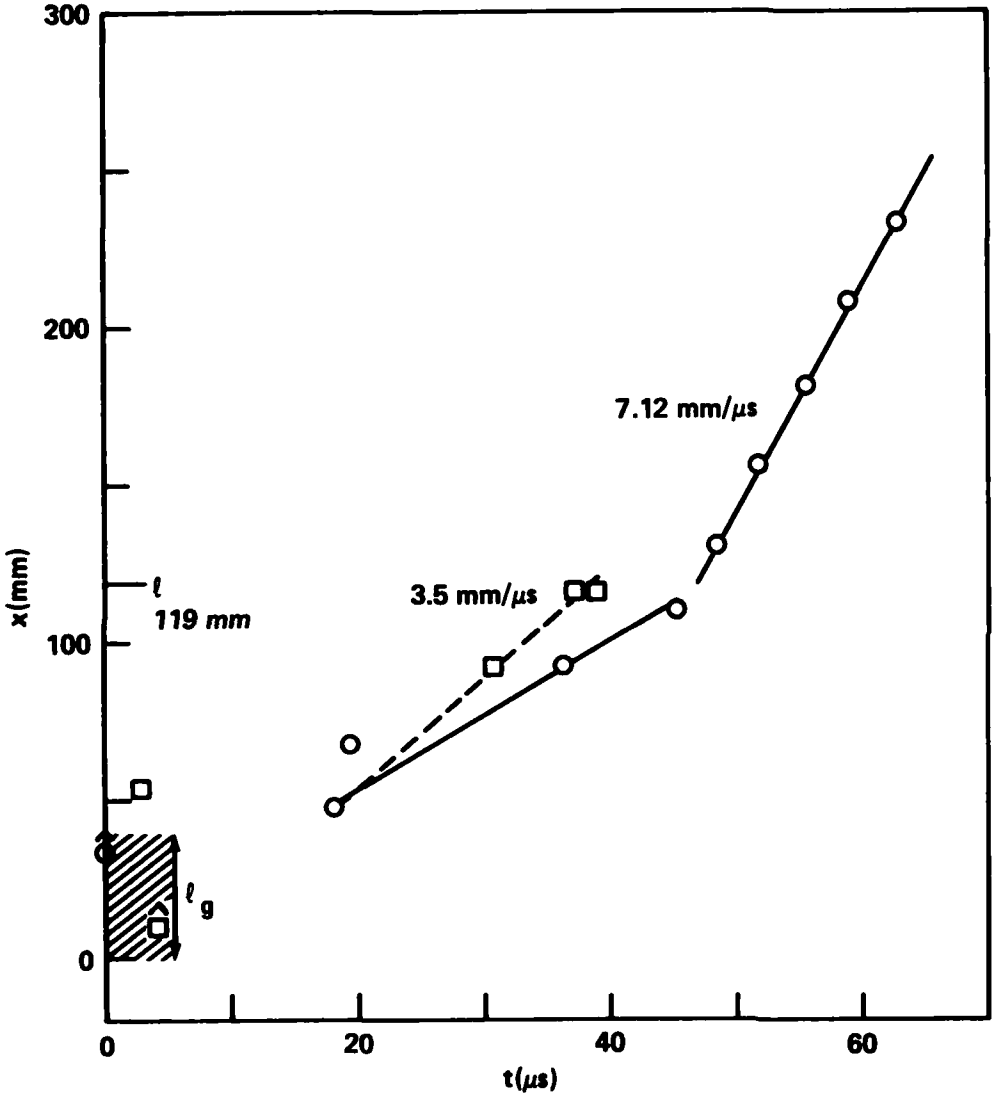

a. DISTANCE-TIME (LEGEND OF FIGURE 3a).

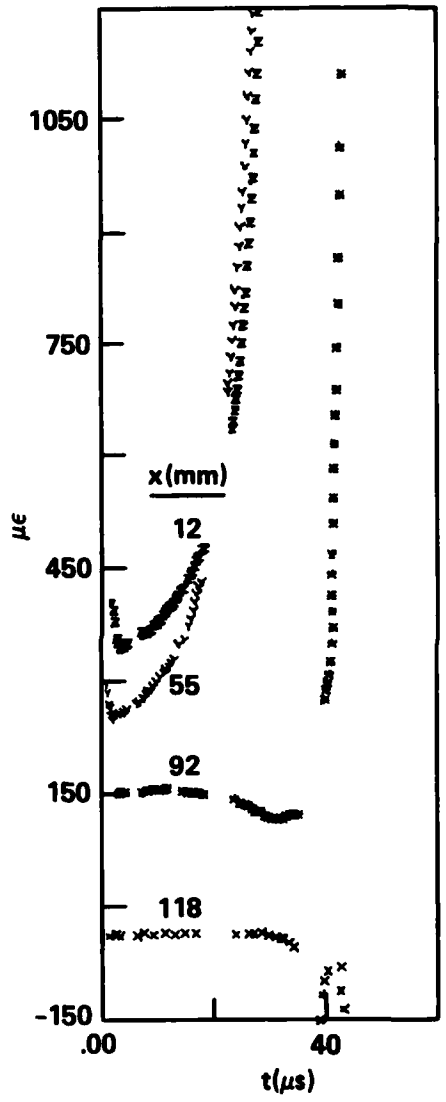

b. STRAIN-TIME DATA (LEGEND OF FIGURE 4b).

FIGURE 5. DATA FOR 40.0 mm 95.0% TMD 94/6 RDX/WAX ON CAST PENTOLITE (SHOT 908)

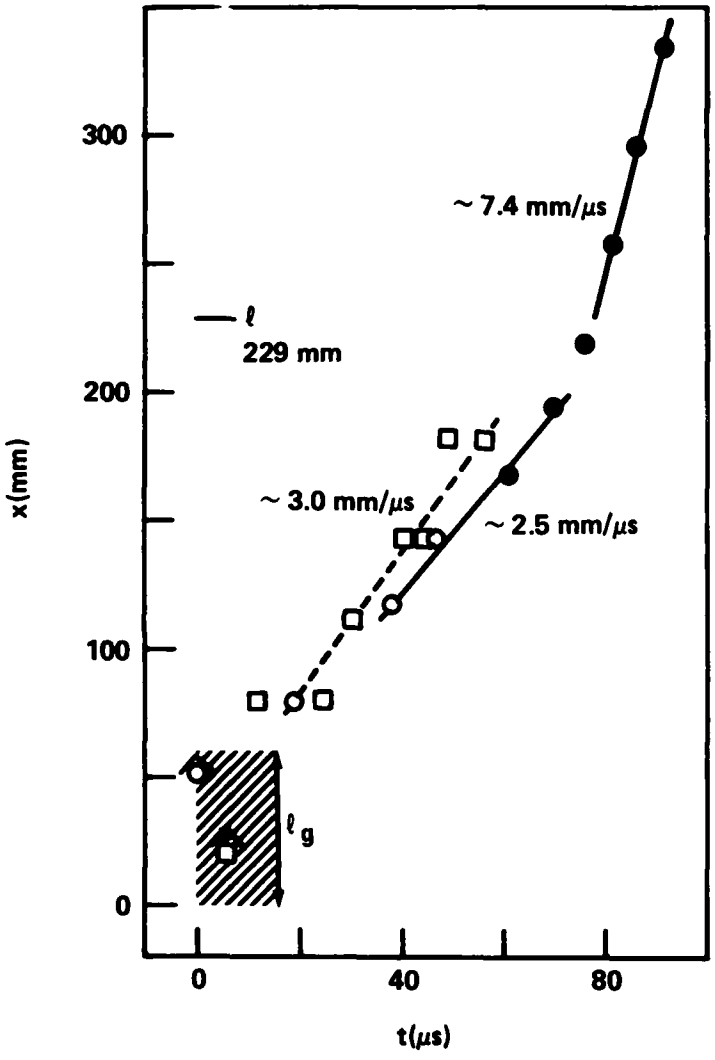

a. DISTANCE-TIME DATA (LEGEND OF FIGURE 3a).

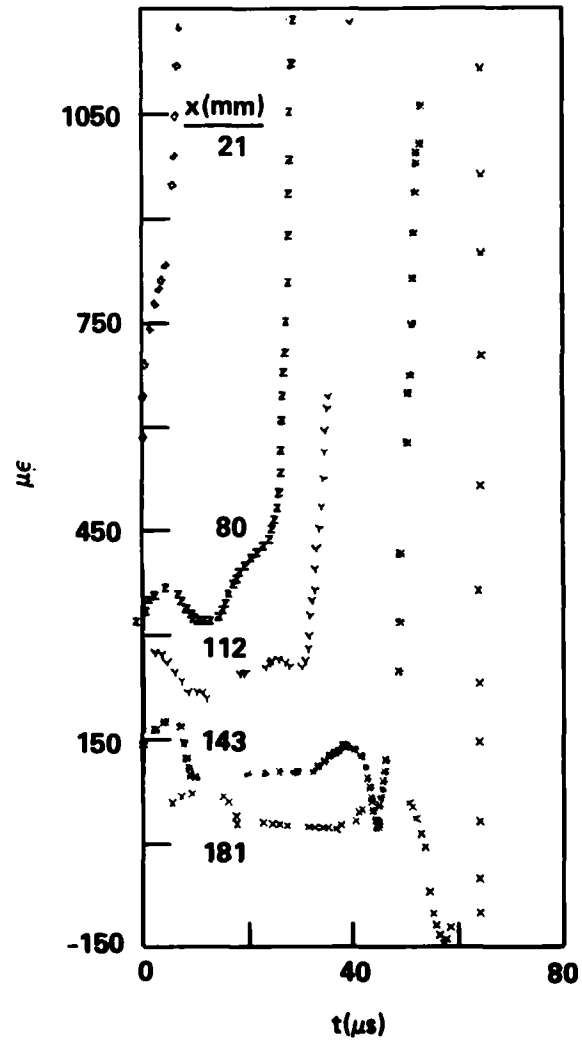

b. STRAIN-TIME DATA (LEGEND OF FIGURE 4b).

FIGURE 6. DATA FOR 60 mm 95% TMD 94/6 RDX/WAX ON CAST 75/25 CYCLOTOL IN AN 18 INCH TUBE (SHOT 1409)

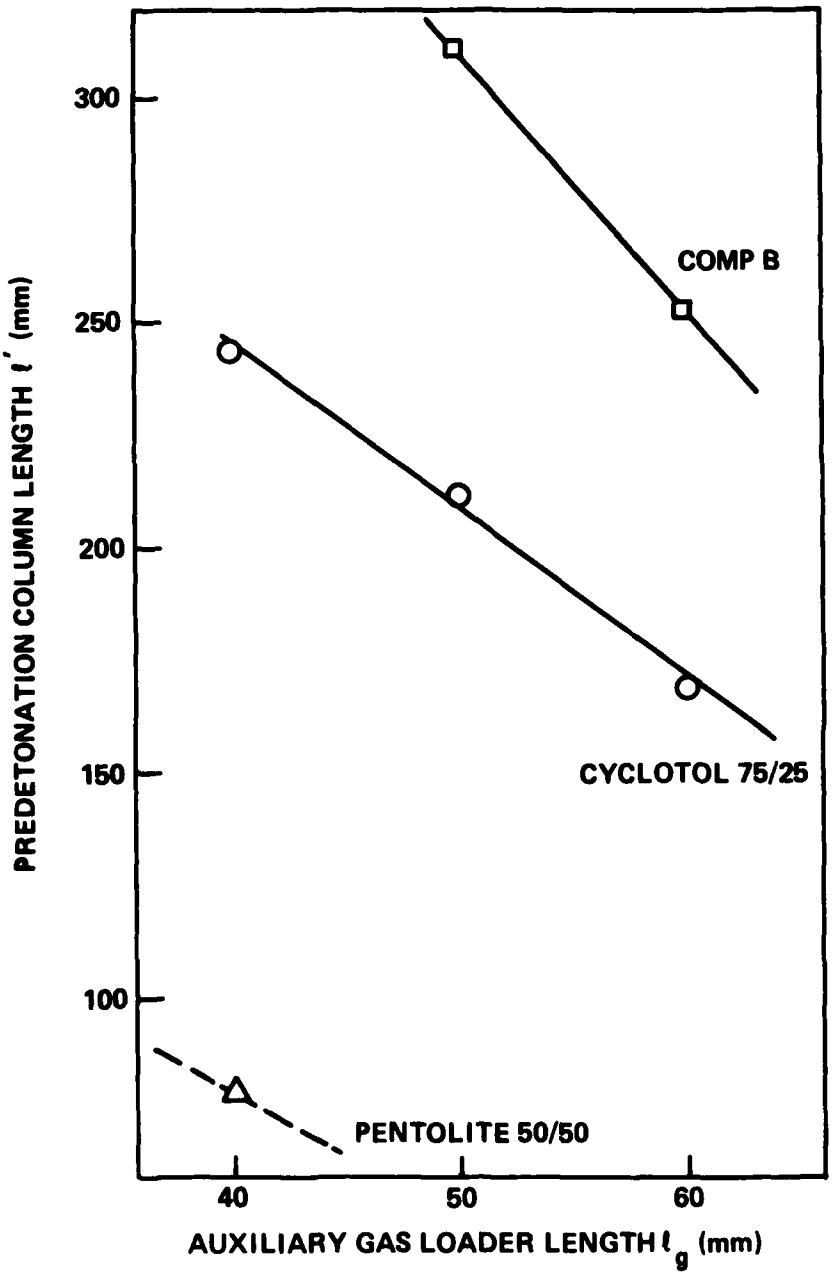

FIGURE 7. RELATIVE SENSITIVITY TO DDT OF THREE GAS LOADED CAST HE USING 95% TMD 94/6 RDX/WAX AS GAS LOADER

A comparison of ℓ' vs Δt_E was made for pressed explosives with a constant loader length. In that case the time was relative to the discharge time of an IP beyond the end of the loader. In order to make a similar comparison for cast explosives with different loader lengths, Δt_E has been determined relative to the time the SG curve reaches the interface between the loader and test explosive. It is designated ${}^{I}\Delta t_E$ in Table 5 and was obtained by extrapolating the SG curve back to that interface. As Fig. 8 shows, there is evidently a correlation with ℓ' of the time interval between passage of the SG wave and the onset of detonation (${}^{I}\Delta t_E$). Data for Comp B and cyclotol 75/25 (5 points) fall on a straight line. The single point for pentolite falls below the extrapolation of that line. That could result from (1) experimental error, (2) curvature of the line to go through the origin, (3) a different curve for RDX/TNT combinations from that for PETN/TNT, or some combination of the three. (The slope of the Figure 8 curve, ~1.8 mm/μs, gives a reasonable plastic wave velocity for these TNT based explosives.)

In Table 6, data are given for 75/25 cyclotol and Comp B tested at two diameters: 16.2 and 25.4 mm. Unfortunately, the length of the larger tube was not scaled up with the diameter because the self-loaded pentolite indicated that the phenomena did not scale. With a 50 mm gas loader, however, the gas loading appears to dominate the DDT and in the case of 75/25 cyclotol, both ℓ' and ${}^{I}\Delta t_E$ seem to scale with the ID. In the case of Comp B, the result is inconclusive because the larger diameter tube was too short. The 16.2 mm dia tube exhibited DDT at ℓ' = 311 mm. If it scales as did the cyclotol, in the larger diameter ℓ' should be $311 \times \frac{25.4}{16.2}$ = 488 mm or ℓ = 538 mm. If the tube had been scaled in effective length, a positive result might have been obtained, but with an effective tube length of only 410 mm, a failure would be predicted and was observed. Should further testing show that gas loading scales, that result would imply that there exists some critical combination of values in the p vs t and dp/dt vs t curves beyond which the DDT process would scale. In other words, without the slow processes of ignition and low pressure combustion, DDT might scale.

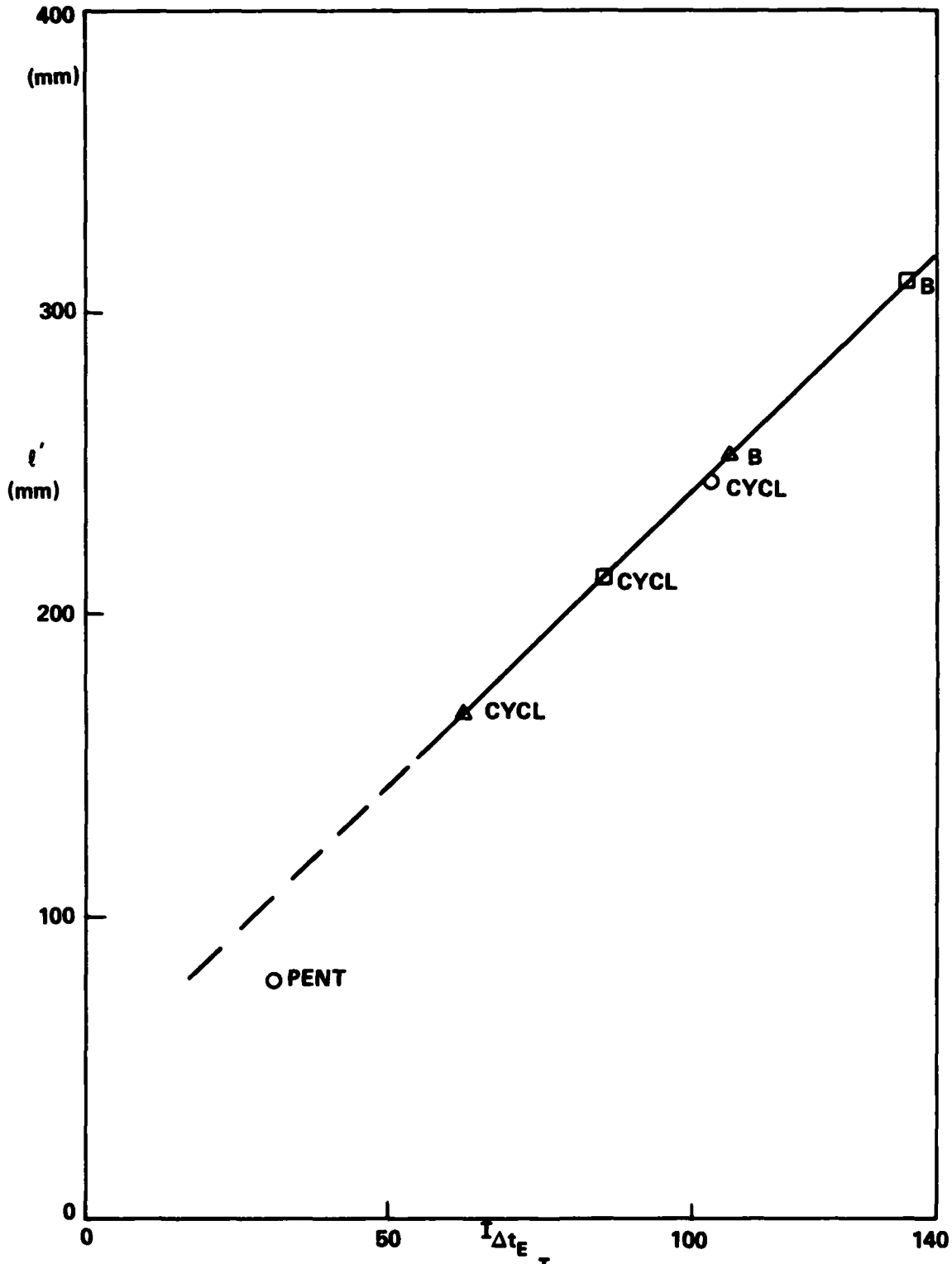

FIGURE 8. RELATIONSHIP BETWEEN ℓ' AND $I_{\Delta t_E}$ FOR GAS LOADED CAST EXPLOSIVES (O ℓ_g = 40 mm, □ ℓ_g = 50 mm, Δ ℓ_g = 60 mm)

TABLE 6. EFFECT OF DIAMETER ON GAS LOADED CAST HE

Shot No.	HE	ℓ_g mm	ID* mm	ℓ' mm	ℓ'/ID	$I_{\Delta t_E}$	Fig.
1415	75/25 cyclotol	50	16.2	212	13.1	85	A17
1716	75/25 cyclotol	50	25.4	315	12.4	128 $I_{\Delta t_E} \times \frac{16.2}{24.5} = 82$	A22
1309	Comp B	50	16.2	311	19.2	135	A18
1715	Comp B	50	25.4	F	F	F	A23

*All tubes were 18 in. long, i.e. provided 410 mm for gas loader plus test HE.

The present results, compared to those for pressed charges, make it very clear that good castings will be far less sensitive to DDT than pressed charges. Thus TNT at 94% TMD showed a transition with 19 mm TMD loader at 94% TMD (Table 3) and cast TNT (98% TMD) failed to transit under 60 mm 95% TMD loader or over three times the amount of 96/4 RDX/wax. Both pressed and cast pentolite 50/50 at 97% TMD are more shock sensitive than pressed 91/9 RDX/wax at 83-96% TMD.[12] But cast pentolite requires a gas loader of 40 mm of 95% TMD before its predetonation column length is reduced to that of 88% TMD 91/9 RDX/wax produced under a 19 mm loader. Since cast pentolite is more shock sensitive than 88% TMD 91/9 RDX/wax, there must be another factor that makes it less sensitive to DDT. An obvious factor differentiating cast and pressed HE is the available reactive surface area. Hence with all other factors the same, pressed charges would be expected to exhibit DDT more easily than cast because they have more burning surface and thus produce more gas products and greater pressure buildup in less time.

These results do not guarantee that a shell filled with any cast HE will be less sensitive than a press filled charge. The sensitivity to DDT will be determined by both chemical and physical factors. In the latter, the more important are permeability (near zero in the original casting) and the surface available for burning; that can be minimized in a casting only by avoiding cracks and annular spacings resulting from large volume changes during cooling or setting of the charge.

CAST PLASTIC BONDED EXPLOSIVES

Self-Loaded

Only two cast plastic bonded explosives were tested under self-loading, and this was done in the large tubes (25.4 mm ID and 410 mm HE column). Two charges of PBXW 108I and one of AFX 108 failed to transit under these conditions. Moreover both IP and SG records were very poor or missing. The end results of these shots will be qualitatively described, but the fragmentary data will not be tabulated. Table 7 describes these shots and Figure 9 shows the tubes recovered after them.

Both PBXW 108I and AFX 108 had to be vacuum loaded into the confining tube. Because the loading apparatus could not handle the large steel tubes, we used a thin walled (0.71 mm) steel tube. This tube was subsequently potted in the larger tube with polyurethane; thus any annular space for "flashdown" of hot combustion gases from the ignition area was avoided. Dimensions of the completed composite were 24.1 mm I.D., 76.2 mm O.D., ratio of 0.316. X-rays were obtained prior to the potting and had far better definition than those taken in the thick walled tube.

Gas Loaded

Table A-5 contains the detailed data for gas loaded PBXN 103 (Fig. 10) and PBXN 106 (Fig. A-24). Both failed to show a transition as did a repeat shot on PBXN 106 (Shot 1707) the data of which have not been displayed; they seemed very erratic, possibly because of an odd breakup of the confining tube. In Shot 1704 (Fig. A-24), the tube split longitudinally and the IP data gave a reasonable trend, but in Shot 1707 the tube burst was very asymmetric; the IP data, erratic.

The gas loaded (ℓ_g = 60 mm) PBXN 103 produced IP and SG records very like those of gas loaded Comp B (ℓ_g = 50 mm, Fig. A-18 and ℓ_g = 60 mm, Fig. A-19) in that IP data and SG excursions mapped out about the same front,

TABLE 7. SHOTS ON SELF-LOADED PBXs

Shot No.	HE	
1806	PBXW108	SG front preceded IP front which did not appear until about 400μs after triggering. Both fronts had velocity of order of magnitude of 2 mm/μs. Tube showed pressure burst - see Figure 9. No dent in bottom bolt - some unburned HE in bombproof.
1807	PBXW108	SG front steeper than in previous shot and preceded IP front which appeared about 300μs after triggering and had a velocity less than one mm/μs. In this shot, the end closure was blown off before tube ruptured - see Figure 9. No unburned HE.
1808	AFX108	The probe records for this shot were better than those above; they started about 200μs after triggering and showed an IP front velocity of 2.1 mm/μs. However, the pressure records were extremely poor and almost obliterated by noise. The tube showed an unsymmetrical pressure burst. See Figure 9.

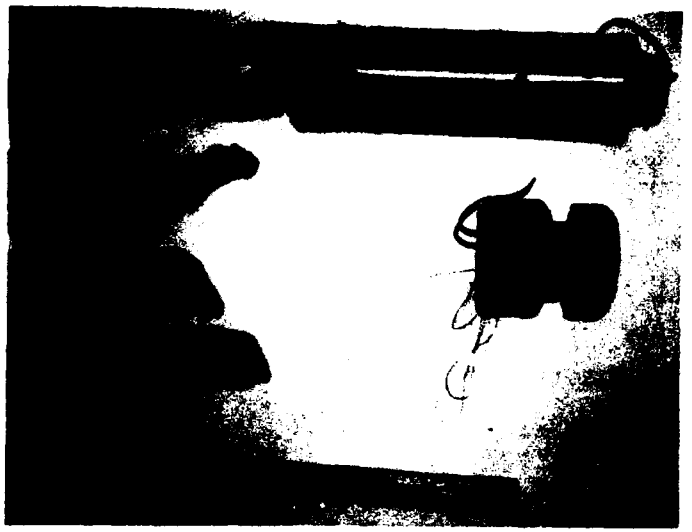

SHOT 1806
PBXW 108

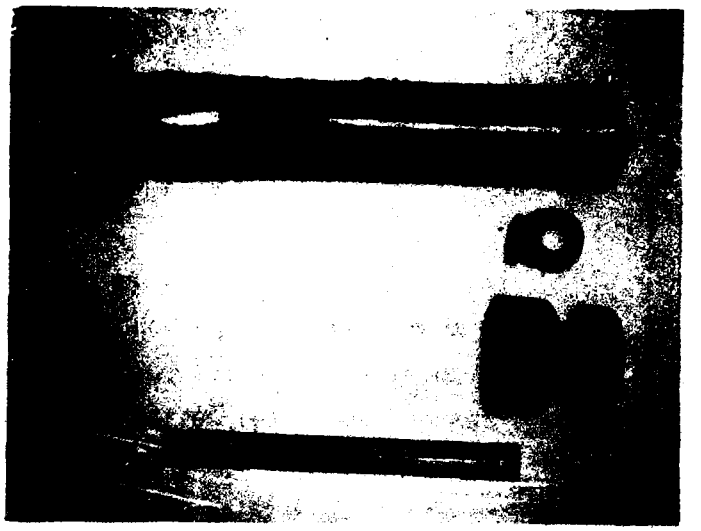

SHOT 1807
PBXW 108

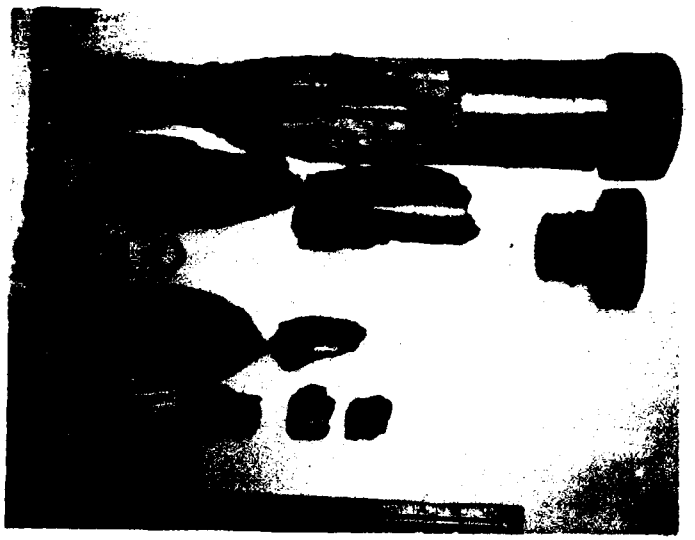

SHOT 1808
AFX 108

FIGURE 9. TUBES RECOVERED FROM SHOTS OF SELF-LOADED PBXs (IGNITOR END AT LEFT)

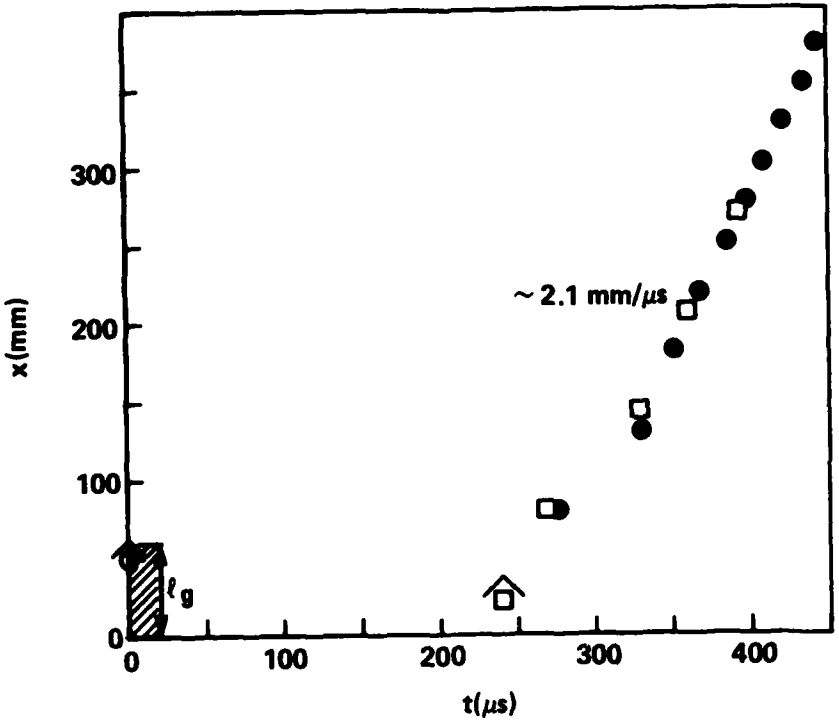

a. DISTANCE-TIME DATA (LEGEND OF FIG. 1a)

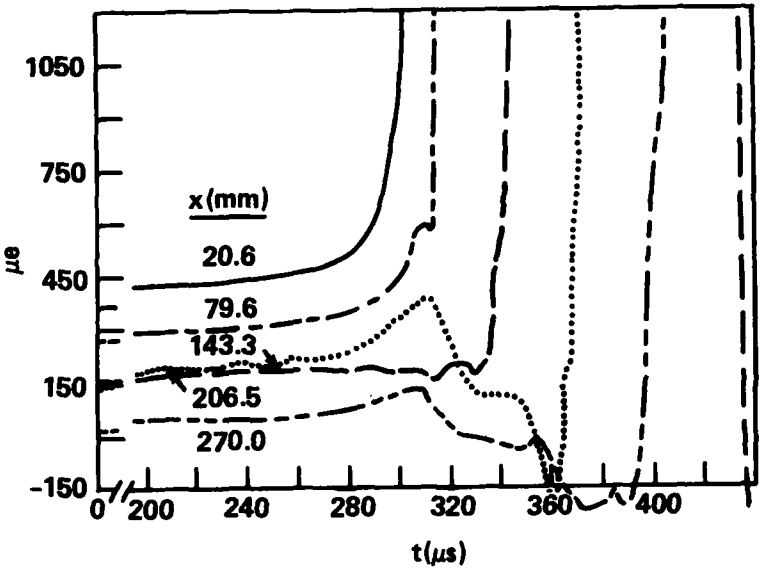

b. STRAIN-TIME DATA (LEGEND OF FIG. 4b)

FIGURE 10. DATA FOR 60 mm COLUMN OF 95% TMD 94/6 RDX/WAX ON PBXN 103 IN 18 INCH TUBE (SHOT 1316)

and minima appeared at the second strain gage station and increased in depth with increasing x. The growing reaction indicated by these minima appeared about 200μs later than that for Comp B, and the IP front velocity was 2.1 mm/μs rather than the 2.4 - 2.8 mm/μs of Comp B. The PBXN 103 records are also similar to those of TNT, which also failed to transit under gas loading (Figs. A-20 and A-21). The SG minima for TNT appeared later than those for Comp B but earlier than those for PBXN 103. However, once they appeared, the depths of the minima from PBXN 103 increased much more rapidly than those from TNT. This suggests that the reaction is harder to start in PBXN 103, but, once started, it seems to grow as rapidly as that in Comp B and more rapidly than that in TNT. From the present results we suggest that the loading most resistant to DDT is a cast material of negligible volume change on solidification and sufficiently rubbery to avoid cracking under rough handling; its explosive components should, of course, be relatively insensitive.

GENERAL CONTROL PROBLEMS

The transitional portions of the DDT process are neither equilibrium nor steady-state behaviors; they are therefore difficult to reproduce. Moreover, the physical factors (e.g. initial particle size, permeability, etc.) have a very large effect on the results. Consequently, we X-ray each charge before instrumenting it. To be sure, this is not an extremely sensitive test, but we can be sure that if it detects cracks, density gradients or other heterogeneities, the charge should not be fired.

From the past experience with pressed charges, we estimate the scatter of the data in any given investigation of trends to be of the order of magnitude of ±10%. This is also the size suggested by the apparent reversals in sensitivity of 88% TMD tetryl vs 88% TMD 91/9 RDX/wax, according to whether ℓ' or Δt_E is used for rating. (See Table 2). The difference between these two HEs at 88% TMD is considered experimentally insignificant. Similarly, at 70% TMD the difference between TNT and ground tetryl seems insignificant. (See Table 1).

We have not yet run enough tests on cast HE to estimate the scatter, but the large role played by the physical form of the charge is still very evident. Thus in an attempt to increase the range to include less sensitive materials, we tried increasing the charge diameter (ID/OD of the confining tube was kept constant). But this increased the solidification time of the charge which, of course, affected its crystal size. The results from the series of cast pentolite charges certainly indicate a scatter larger than that for pressed charges if the confining tube is 25 mm dia. (See Table 4).

It should be emphasized again that the present results reflect the present experiment. It is carried out under very high confinement and charge support. Many uses of both explosives and propellants are under little or no confinement and with little physical support. In fact, some damaging effects result from a charge breakup which is largely avoided in the present experiment. Hence the present results offer guidance to sensitivity to DDT, but their rating is not necessarily that which will be found in applications.

Finally, any test development of this method should explore the effect of varying test conditions: length, diameter, finish, and yield strength and confinement (ID/OD) of tube. In addition, an investigation should be made of variations in charge preparation: (1) pressing by increments into the tube vs isostatic pressing, machining and potting of the charge and (2) change in rate of cooling of cast charges with tube diameter.

SUMMARY AND CONCLUSIONS

Five explosives, pressed to 70% TMD, with a 20 mm loader (also at 70% TMD) showed a linear correlation between their predetonation column length (ℓ') and Δt_E (time to detonation relative to time of passage of the compression wave at x ~ 29 mm). Under these conditions, the rating in order of decreasing sensitivity to DDT was RDX, (ground tetryl and TNT), and Explosive D.

Five explosives pressed to 88% TMD with a 19 mm loader (also at 88% TMD) also showed a linear (but different) correlation between ℓ' and Δt_E. The order in this case was: (coarse tetryl and 91/9 RDX/wax), TNT, 95/5 TNT/wax, and Expl D.

This work produced two quantitative but different sensitivity scales, one for each of the two degrees of compaction. Except for the enhancement of pressure and pressure buildup in the early stages caused by the gas loader, all the pressed HE examined seemed to follow the same mechanism each exhibited under self-loading. Those which did not show DDT under self-loading, seemed to follow the transitional mechanism first described for 91/9 RDX/wax.[6,7]

In examining TNT based, cast explosives, 50/50 pentolite and H-6 were first studied under self-loading. H-6 failed to transit but pentolite seemed to follow a DDT mechanism similar to that of pressed HE. The events were, in order, passage of an ignition (or IP) front followed by a SG front which originated in the ignitor region of the tube and merged with the detonation front outlined by the downstream IPs. All castings exhibited minima formation in the strain-time curves and progressive growth of the minima according to records from the downstream SGs; this was also true of those cast HE which failed to transit under gas loading, e.g., cast TNT. (It is to be expected that stress waves in solids, as recorded by the external SGs, will differ from the internal gas pressures of the very porous charges.)

Gas loading was carried out on cast pentolite, cyclotol 75/25, Comp B and TNT. The first three could be rated quantitatively with linear ℓ' vs ℓ_g curves. In order of decreasing sensitivity they were pentolite, cyclotol, and Comp B. TNT failed to transit with a 60 mm loader and therefore was off-scale.

The gas loading experiment was scaled up from 16 mm ID to 25 mm ID (at constant ID/OD ratio) for cyclotol and Comp B. The experiment seemed to scale although earlier work on self-loading of pentolite did not scale.

However, only a few shots were made and scatter of the data from the larger tubes was much greater than that obtained from the regular tubes. This larger scatter may indicate the importance of cooling rate, during casting, in affecting charge reactivity.

Comparison of results of pressed charges with cast charges led to much firmer conclusions. Good castings are far less sensitive to DDT than pressed charges of the same HE at approximately the same density. This is attributed chiefly to the greater amount of internal burning surface to be expected from pressed charges.

PBXW 108I (2 shots) and AFX 108 failed to transit under self-loading in the large tubes (25 mm ID and 410 mm HE column). Gas loaded PBXN 106 (2 shots) and PBXN 103 failed to transit with ℓ_g = 60 mm although the records in the latter case were quite similar to those of Comp B.

REFERENCES

1. Price, D., and Bernecker, R. R., "Sensitivity of Porous Explosives to Transition from Deflagration to Detonation," Combustion and Flame, Vol. 25, 1975, pp. 91-100.

2. Bernecker, R. R., and Price, D., Sensitivity of Explosives to Transition from Deflagration to Detonation, NOLTR 74-186, Feb 1975.

3. Price, D., and Wehner, J. F., "The Transition from Burning to Detonation in Cast Explosives," Combustion and Flame, Vol. 9, 1965, pp. 73-80.

4. Price, D., and Bernecker, R. R., "Effect of Wax on the Deflagration to Detonation of Porous Explosives," Proceedings of Symposium on Behavior of Dense Media under High Dynamic Pressure, (Paris: C.E.A., 1978) pp. 149-159.

5. Price, D., and Bernecker, R. R., DDT Behavior of Waxed Mixtures of RDX, HMX, and Tetryl, NSWC/WOL TR 77-96, Oct 1977.

6. Bernecker, R. R., and Price, D., "Studies in Transition from Deflagration to Detonation in Granular Explosive," Combustion and Flame, Vol. 22, 1974, pp. 111-117, 119-129, and 161-170.

7. Bernecker, R. R., and Price, D., Transitions from Deflagration to Detonation in Granular Explosives, NOLTR 72-202, Dec 1972.

REFERENCES (CONT.)

8. Bernecker, R. R., and Price, D., "Burning to Detonation Transition in Picric Acid," 17th Symposium (International) on Combustion (Pittsburgh: Combustion Institute, 1979), pp. 55-61.

9. Price, D., Bernecker, R. R., Erkman, J. O., and Clairmont, Jr., A. R., DDT Behavior of Tetryl and Picric Acid, NSWC/WOL TR 76-31, May 1976.

10. Price, D., and Bernecker, R. R., DDT Behavior of Ground Tetryl and Picric Acid, NSWC/WOL TR 77-175, Jan 1978.

11. Bernecker, R. R., Price, D., Erkman, J. O., and Clairmont, Jr., A. R., "Deflagration to Detonation Transition Behavior of Tetryl," 6th Symposium (International) on Detonation, ONR ACR-221 (Washington, D. C.: U. S. Gov. Print. Office, 1978) pp. 426-435.

12. Price, D., Clairmont, Jr., A. R., and Erkman, J. O., The NOL Large Scale Gap Test. III Compilation of Unclassified Data and Supplementary Information for Interpretation of Results, NOLTR 74-40, Mar 1974.

APPENDIX A

DETAILED DATA FOR DDT SHOTS

Tables A-1 to A-5 contain all the detailed data for previously unreported shots on gas loading of pressed charges (Table A-1), self-loading of cast charges (Tables A-2 and A-3), and gas loading of cast charges (Tables A-4 and A-5). Figs. A-1 through A-24 display data for those shots not illustrated in the main text.

In Figure A-2, the gas loading of tetryl, the SG records are consistent with the mechanism described for tetryl.[A-1] Only mild pressure rises appear on the first three SG records. On the 88.4 and 107.8 mm gages, however, the mild rise is followed by a very sharp, exponential-like rise as the onset of detonation (ℓ' = 110 mm) is approached. The plateaus are like those observed in the gas loading of porous charges and are associated with compaction. The rearward traveling wave could be shock, retonation, or a disturbance traveling through the confining tube.

In Figure A-4, [ℓ]** indicates a predetonation run length to a metastable detonation (D = 4.9 mm/μs) as compared to the steady state value of 7.0 mm/μs shown in Figure A-5.

Figure A-10 shows two apparent fronts for the pressure excursions. This results from the difficulty in selecting the location when SG records show well developed minima, as is the case here with 94% TMD Expl D under a 60 mm column of gas loader. (Minima began to develop in gas loaded 88% TMD Expl D e.g., Figure A-8. Subsequent records show that such minima are characteristic of cast HE. It may be that stress propagation from gas loading is similar in low porosity pressed charges to that in cast HE.) From the seven possible locations of pressure excursions selected from Figure A-10b, four

[A-1] Bernecker, R. R., Price, D., Erkman, J. O., and Clairmont, Jr., A. R., "Deflagration to Detonation Transition Behavior of Tetryl," 6th Symposium (International) on Detonation, ONR ACR-221 (Washington, D. C.: U. S. Gov. Print. Office, 1978) pp. 426-435.

could be chosen to draw a front nearly parallel to the IP front, similar to that found in Figure 9a (95% TMD Expl D under 38 mm gas loader).

Figure A-11 and subsequent ones are for cast HE. Figures A-11 to A-14 and Figure 4 of the text show data for self-loaded cast pentolite. All show minima in the SG records and pressure excursions originating in the ignitor region after the IP front has passed. The compression front outlined by them seems to follow the buildup process 30 - 100 μs prior to the onset of detonation; thereafter, the detonation front.

As mentioned in the text, there was a discrepancy in determining ℓ for Shot 1413 (Figure A-13) and Shot 1414 (Figure 4), i.e. tube marking data and IP data appeared to differ. The "more probable" value in these cases was selected on the basis of the SG curve patterns. Thus Figure A-13b showed very late development of minima in the SG curves; there was only one prominent minimum and that in the last curve from the SG at x = 181 mm. Moreover the time at that minimum was 125 μs as compared to 127 μs at 181 mm in Figure the x-t diagram. This point should fall on the detonation portion of the IP curve as shown in Fig. A-13 and is therefore the preferred value in the range 156-181 mm for the adjacent IPs. Again, from the SG records, Fig. 4b shows a very prompt appearance and progressive strengthening of the minima. The last gage, at 137 mm, has its minimum at 85 μs and falls on the slightly extrapolated IP curve in the over-boosted detonation region. Hence in the IP range of 118-143 mm, the preferred value is 137 mm. Why the tube markings show different values in these two cases has not been determined.

Figure A-14 shows an unusually long time between triggering of the scopes and evidence of reaction - probably another example of the difficulty of exactly reproducing cast charges.

Self-loaded H-6 (Figure A-15) has SG records showing a strong, late disturbance (ca. 640 μs) traveling at 6.6 mm/μs from the first to the second gage, but it has disappeared by the third SG at 232 mm and no transition occurred.

Records for gas loaded cyclotol (Figures A-16b and A-17b) showed early development of minima in the SG records and also a transition. In Figure A-17b there is an inversion in the 80 and 131 mm records which can be caused by a base-line shift or a SG malfunction. The two possible pressure fronts of Figure A-17a might be a result of this shift since both Figure 5a and Figure A-16a show only one.

Figure A-18is for a 50 mm column of loader on a 410 mm column of Comp B. Figure A-18b shows inversions in the SG records at early times but pressure excursions falling on the IP curve at later times. DDT did occur in this case but only after a run at 2.8 mm/μs on the last 4 IPs before the last. FigureA-19 for the 60 mm loader, however, has SG records of a more usual type.

Figures A-20 and A-21 for gas loaded cast TNT again show development of minima in SG records although transition does not occur. These shots are duplicates except for tube length. Both show a pressure front nearly parallel and preceding the IP front, and the same final IP front velocity of about 2.3-2.4 mm/μs. Events in the longer tube are about 20μs later and 10 mm further down tube than analogous ones of Figure A-20a.

Figure A-23is of data for cast Comp B with a 50 mm loader. As in some other castings, the SG excursions start near the ignitor in the gas loader and the pressure front continues uninterrupted into the Comp B. However the buildup in IP front velocity is small and slow; despite the 410 mm length of charge, the reaction fails to transit.

By contrast Figure A-24 for PBXN 106 shows a lack of continuity in the front produced by the pressure excursions in the gas loaded PBX. However, the SG front in the explosive seemed to parallel or coincide with the IP front; the latter reached the same velocity (2.3 mm/μs) it attained in the Comp B at a somewhat earlier time. It too failed to transit. (In this shot the SG excursions were read directly from the original Polaroid records which were not completely read and plotted.)

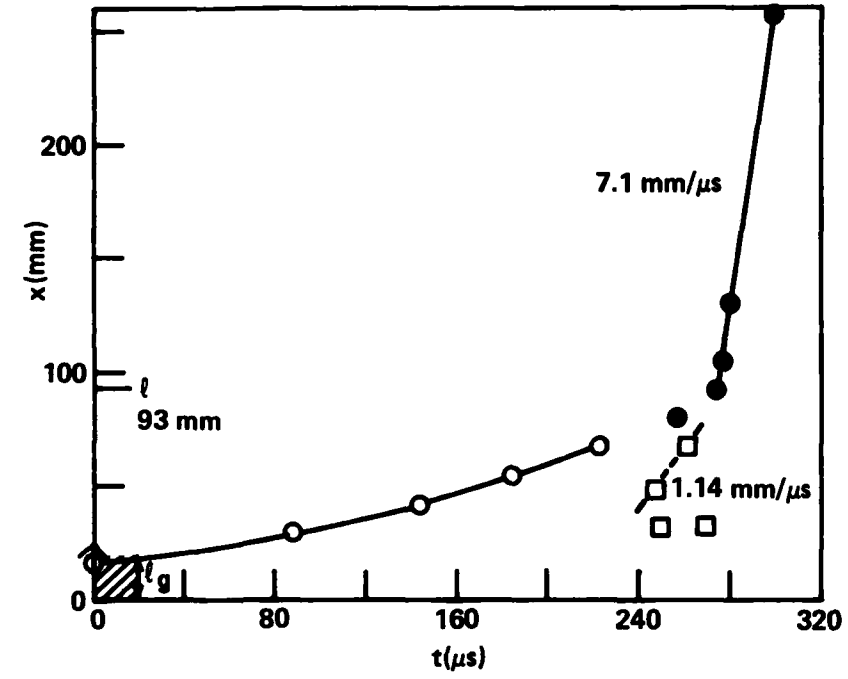

a. DISTANCE-TIME DATA (LEGEND OF FIGURE 1a).

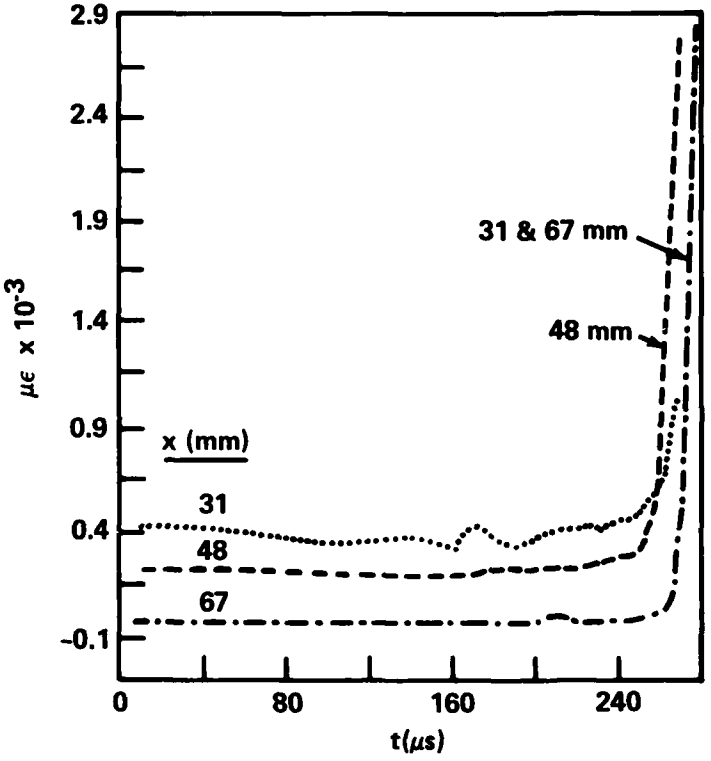

b. STRAIN-TIME DATA (LEGEND OF FIGURE 1b).

FIGURE A-1. DATA FOR 20.0 mm 70.4% TMD 94/6 RDX/WAX ON 1.23 g/cm^3 (68.1% TMD) RDX (SHOT 708)

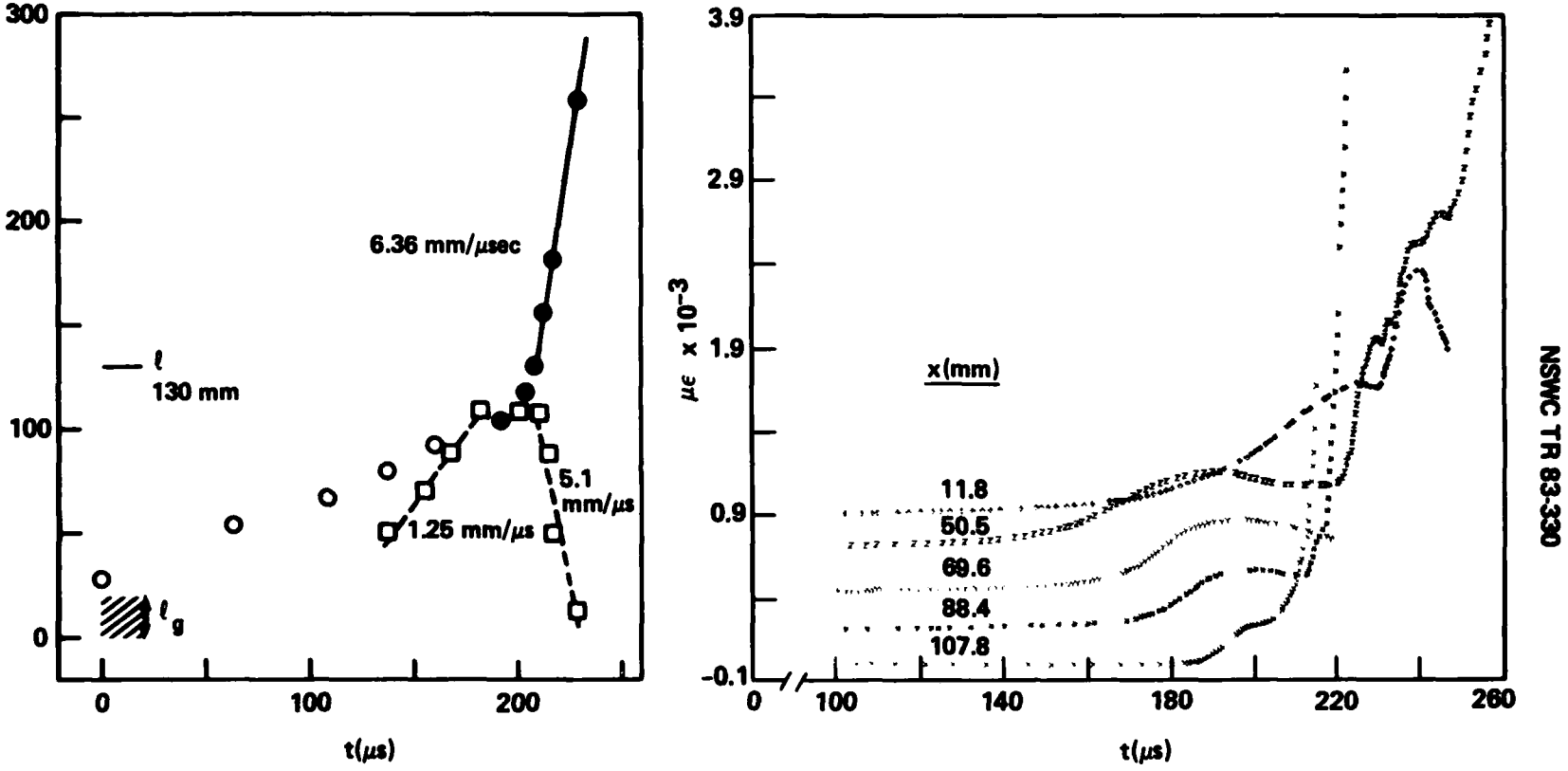

a. DISTANCE-TIME DATA (LEGEND OF FIGURE 1a).

b. STRAIN-TIME DATA (LEGEND OF FIGURE 1b).

FIGURE A-2. DATA FOR 20.1 mm 70.6% TMD 94/6 RDX/WAX ON 1.22 g/cm^3 (70% TMD) GROUND TETRYL (SHOT 1009)

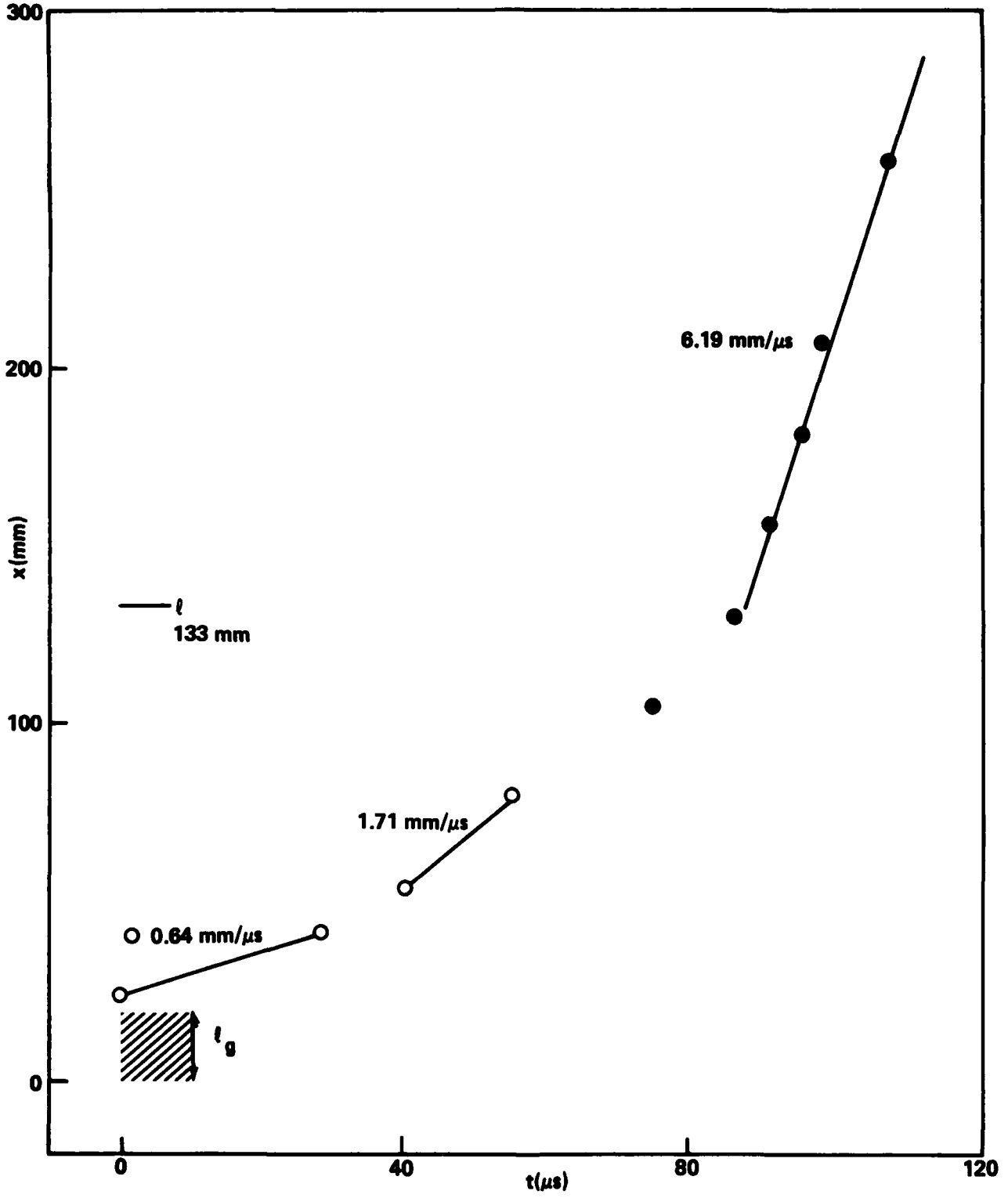

FIGURE A-3. DISTANCE-TIME DATA FOR 19.1 mm 88.1% TMD 94/6 RDX/WAX ON 87.5% TMD 95/5 TNT/WAX (SHOT 716) (LEGEND OF FIGURE 1a)

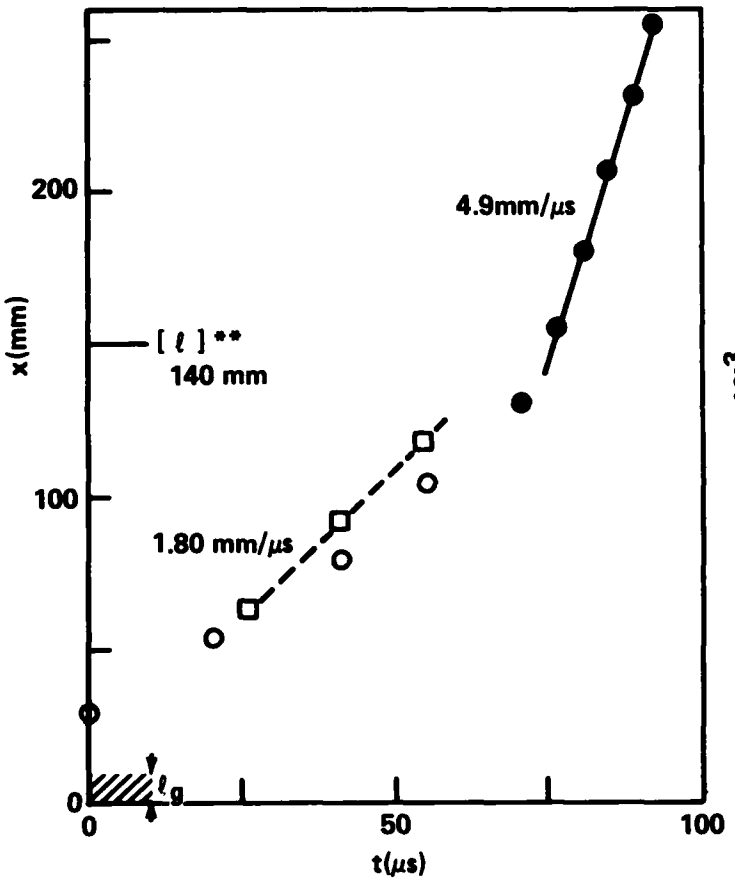

a. DISTANCE-TIME DATA (LEGEND OF FIGURE 1a).

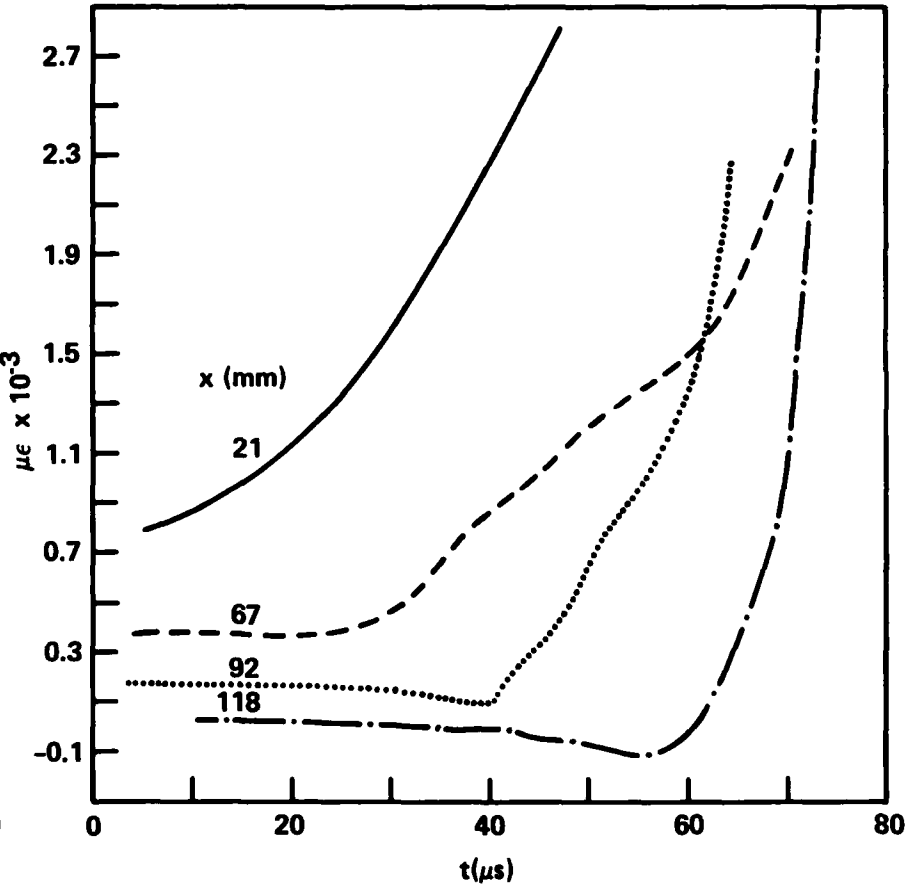

b. STRAIN-TIME DATA (LEGEND OF FIGURE 1b).

FIGURE A-4. DATA FOR 9.5 mm 87.8% TMD 94/6 RDX/WAX ON 1.46 g/cm^3 (88.2% TMD) TNT (SHOT 702)

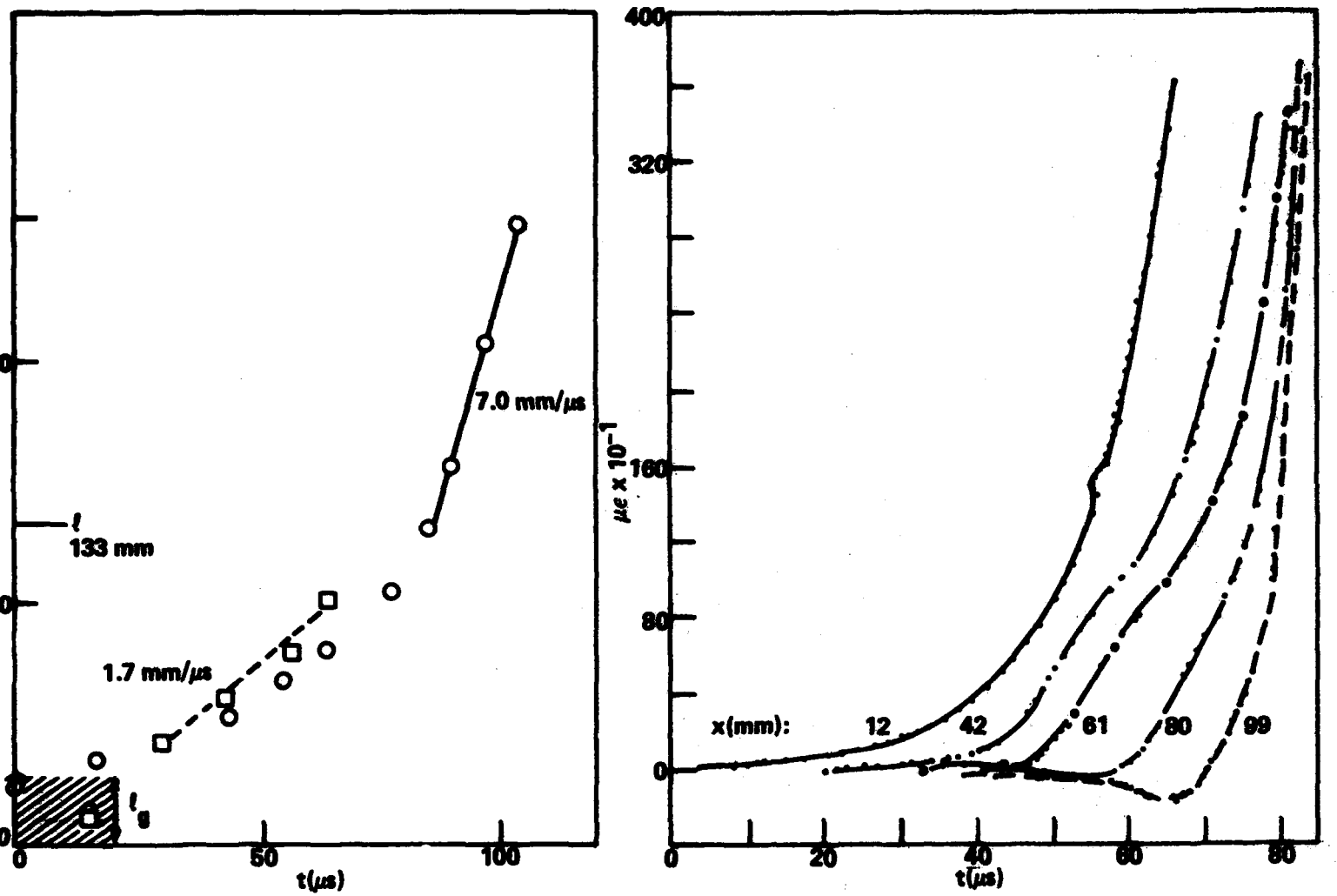

a. DISTANCE-TIME DATA (LEGEND OF FIGURE 1a).

b. STRAIN-TIME DATA

FIGURE A-5. DATA FOR 28.6 mm 87.8% TMD 96/4 RDX/WAX ON 89.1% TMD TNT (SHOT 617)

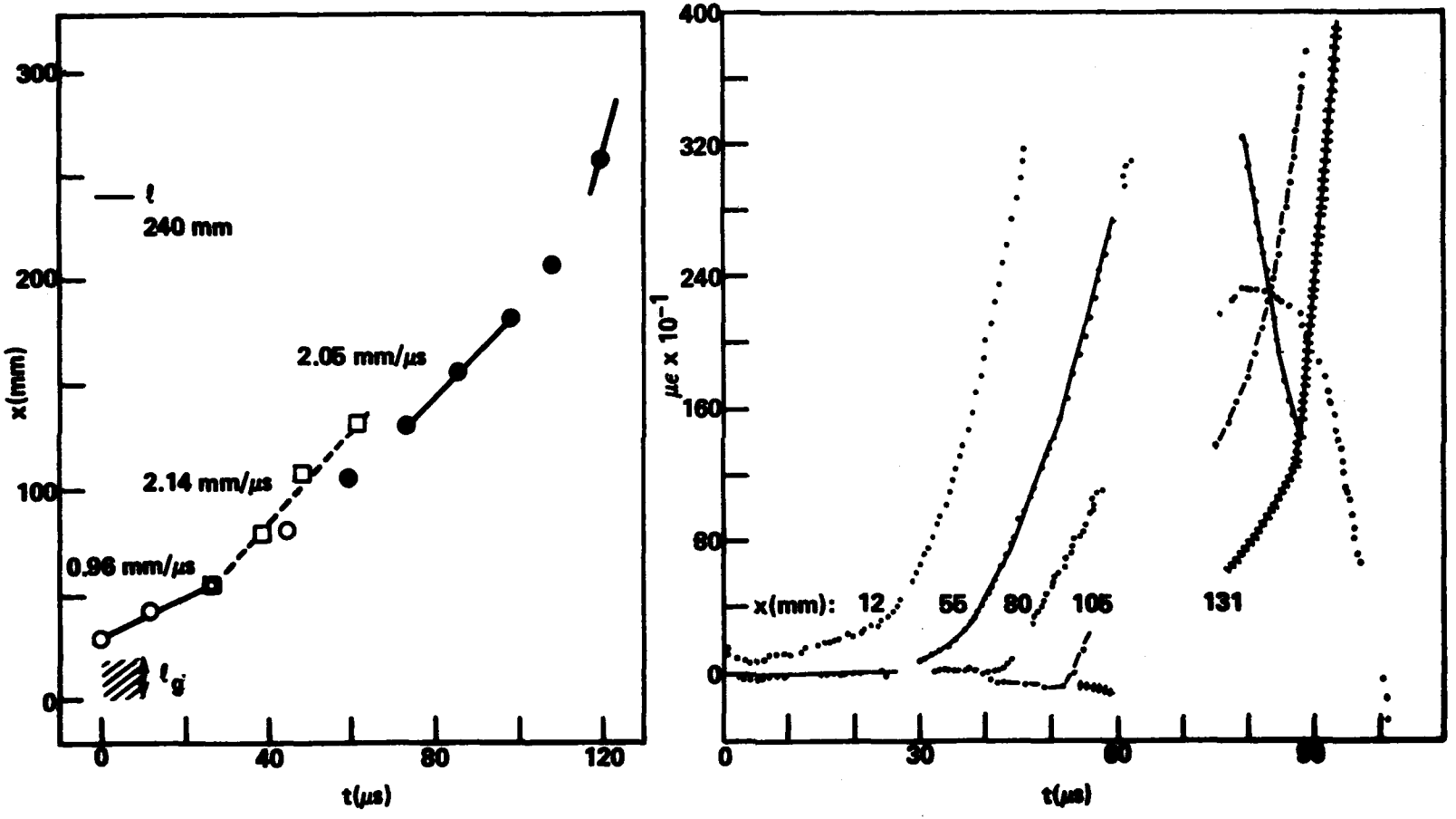

a. DISTANCE-TIME DATA (LEGEND OF FIGURE 1a).

b. STRAIN-TIME DATA.

FIGURE A-6. DATA FOR 19 mm 94% TMD 94/6 RDX/WAX ON 93.9% TMD TNT (SHOT 716)

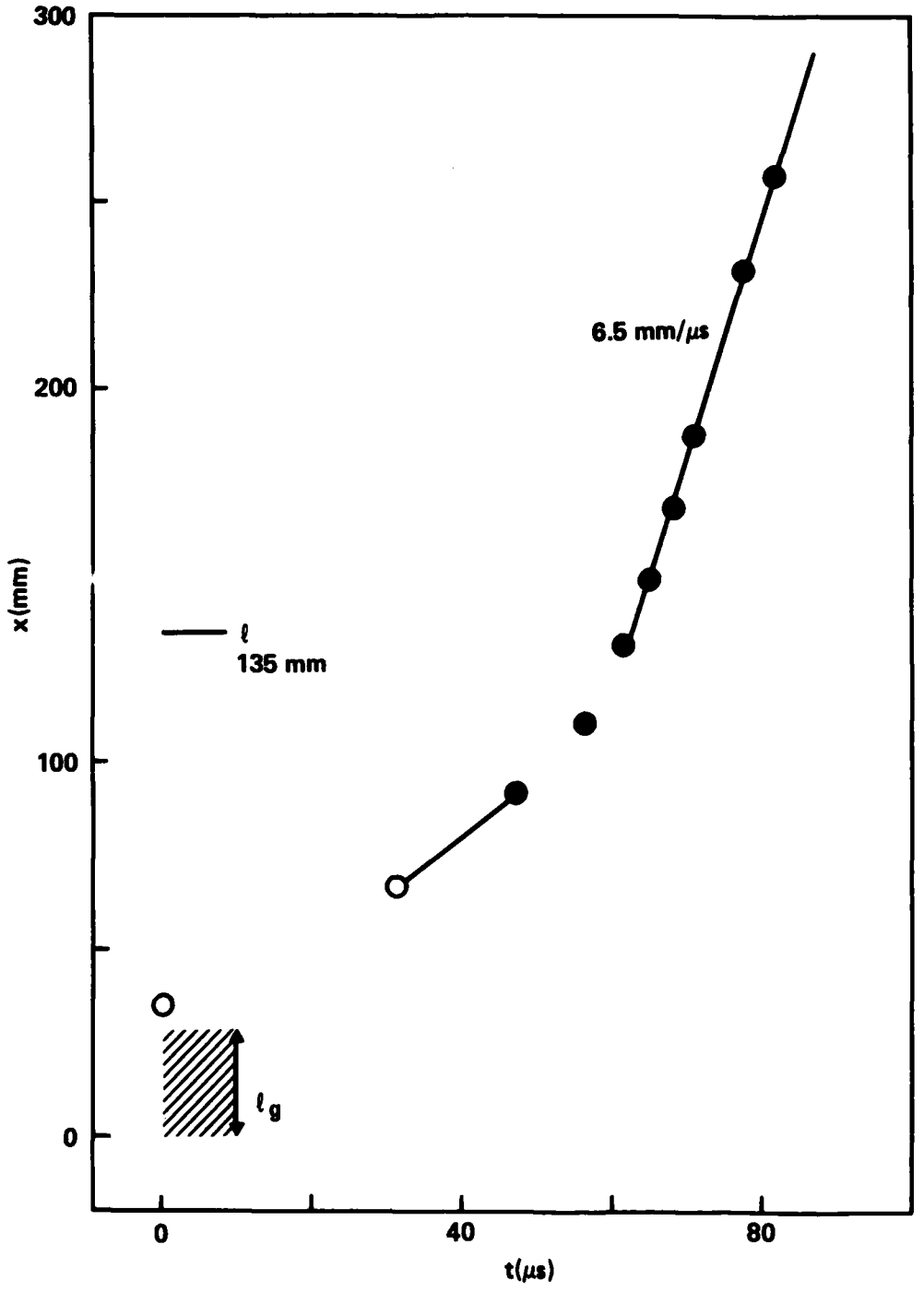

FIGURE A-7. DISTANCE-TIME DATA FOR 28.6 mm 93.7% TMD 94/6 RDX/WAX ON 93.6% TMD TNT (SHOT 814) (LEGEND OF FIGURE 1a)

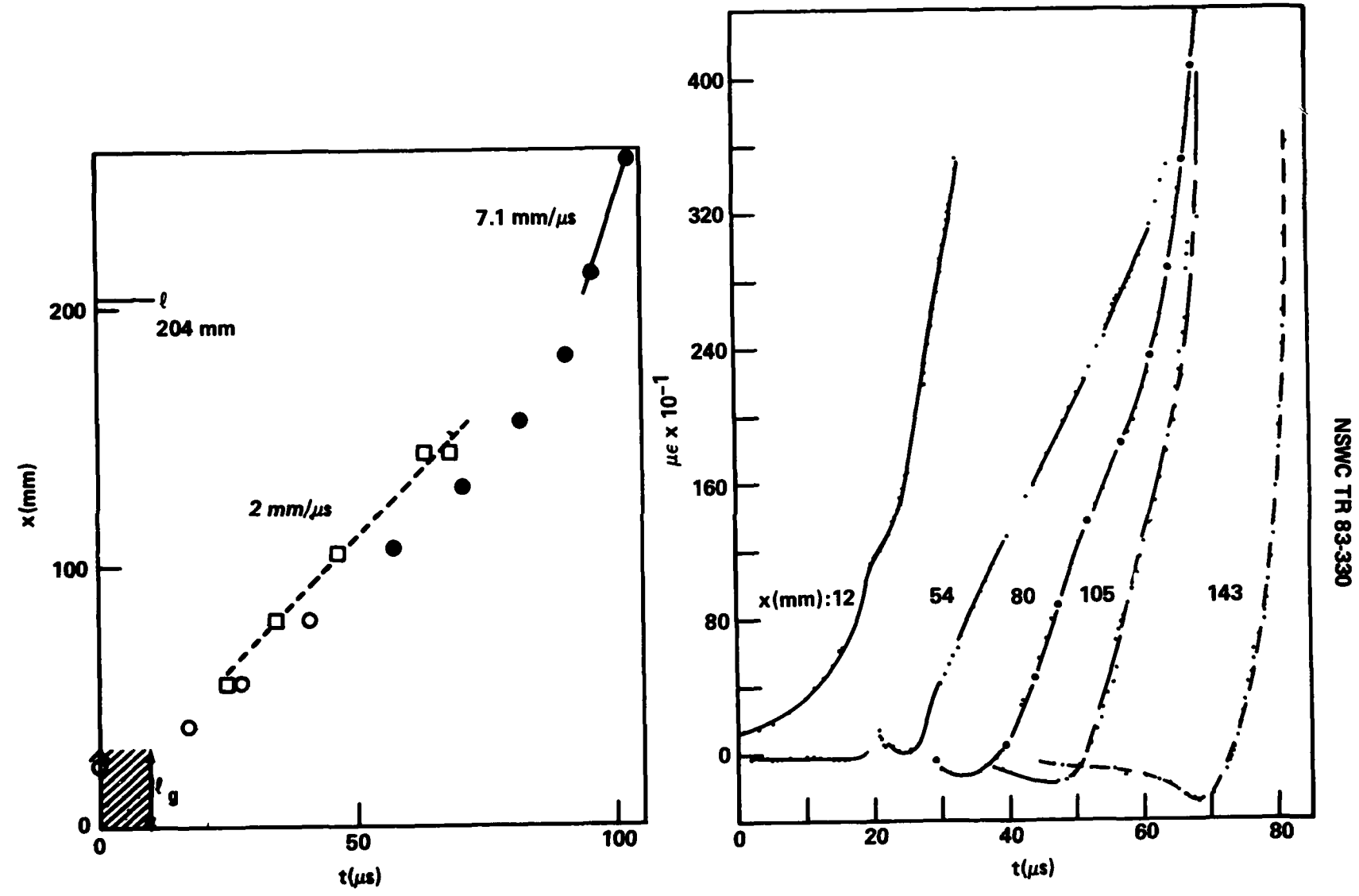

a. DISTANCE-TIME DATA (LEGEND OF FIGURE 3a).

b. STRAIN-TIME DATA

FIGURE A-8. DATA FOR 28.6 mm 88% TMD 94/6 RDX/WAX ON 87.7% TMD EXPLOSIVE D (SHOT 616)

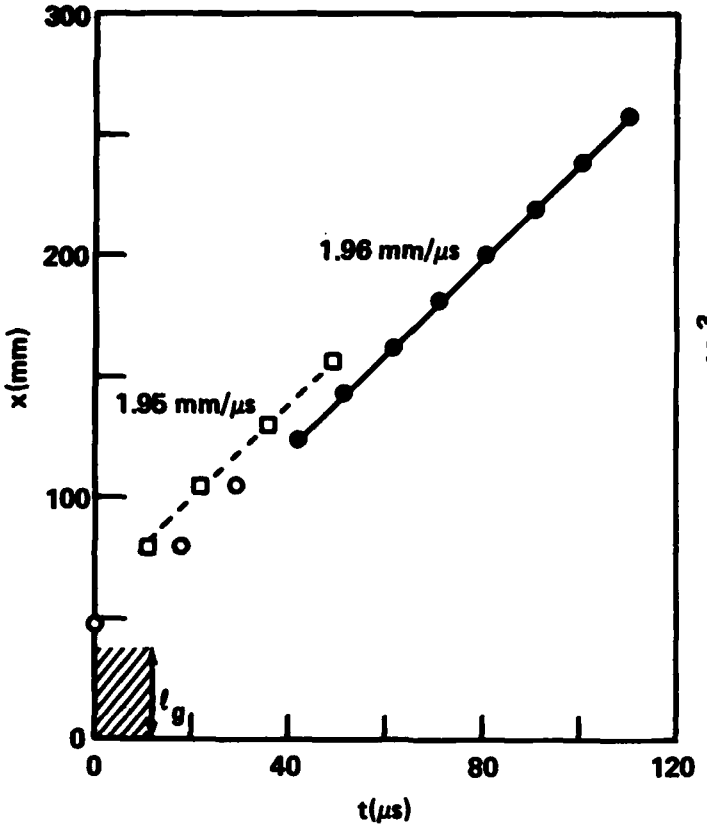

a. DISTANCE-TIME DATA (LEGFND OF FIGURE 1a).

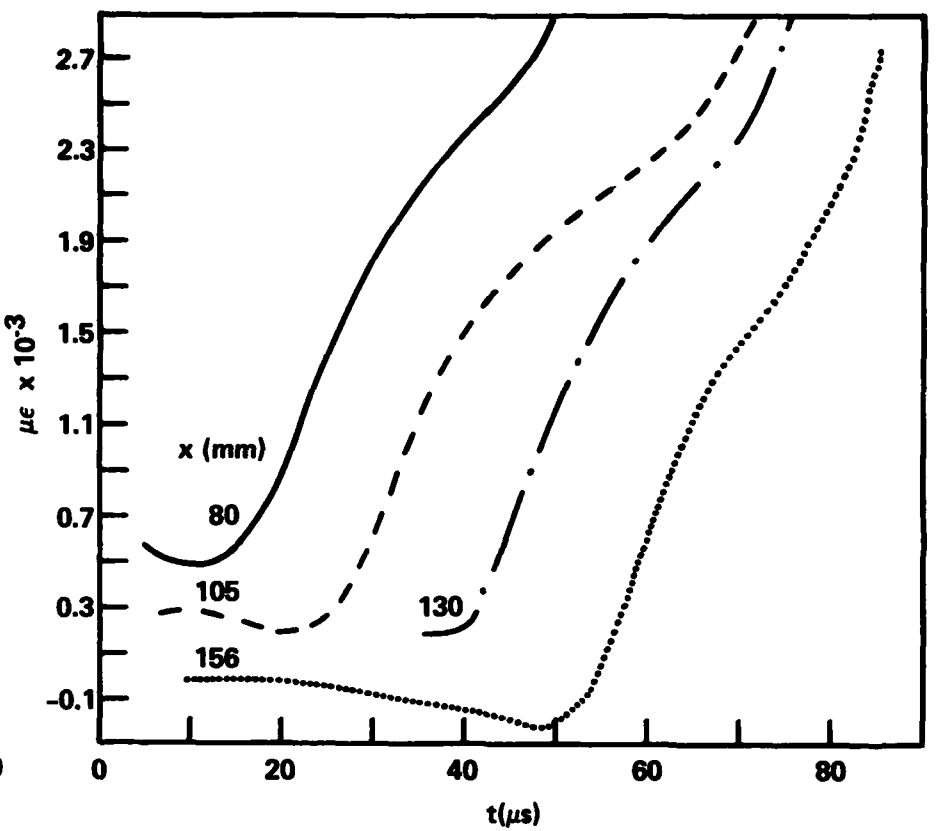

b. STRAIN-TIME DATA (LEGEND OF FIGURE 1b).

FIGURE A-9. DATA FOR 38.1 mm 94% TMD 94/6 RDX/WAX ON 94.7% TMD EXPLOSIVE D (SHOT 903)

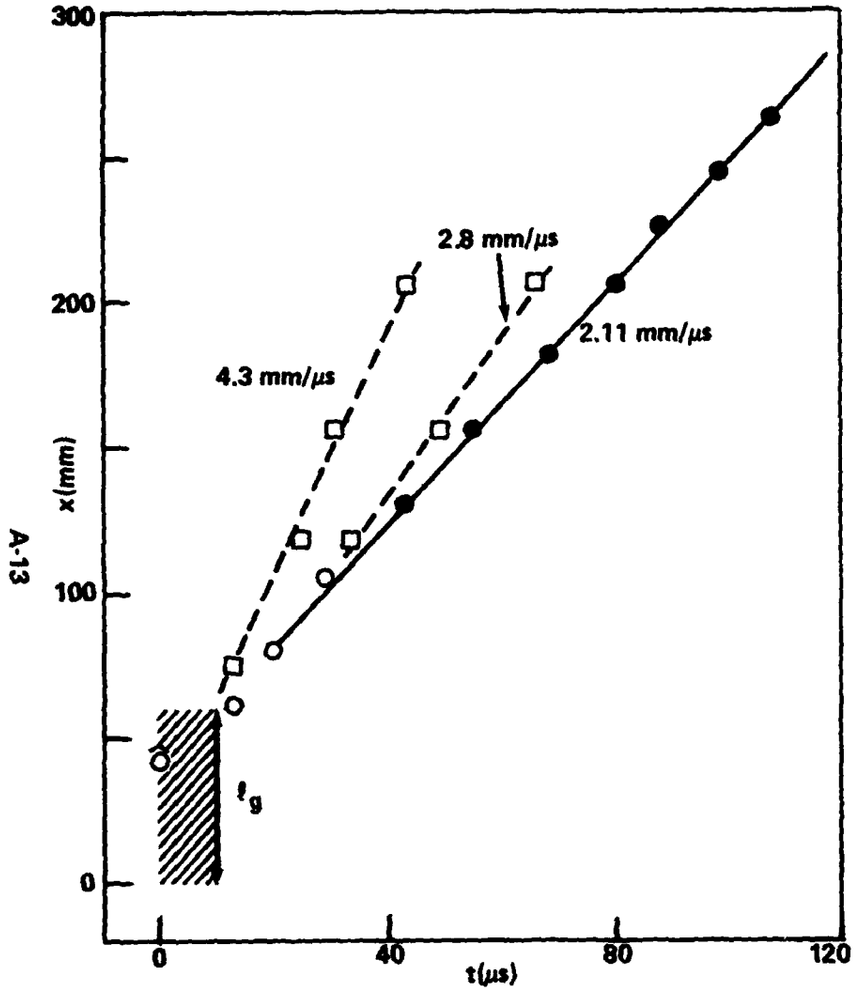

a. DISTANCE-TIME DATA (LEGEND OF FIGURE 3a).

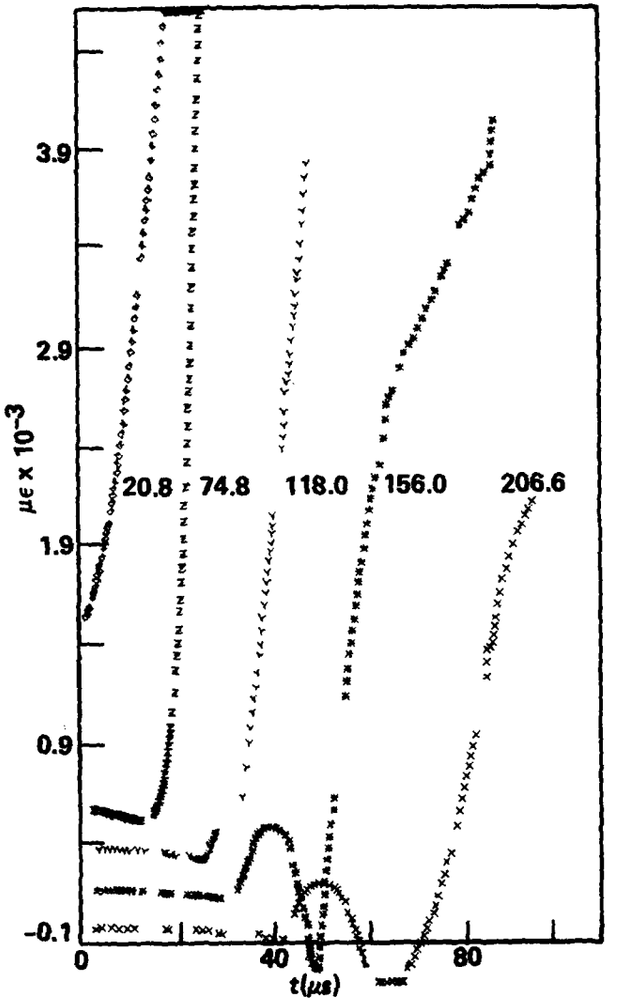

b. STRAIN-TIME DATA (LEGEND OF FIGURE 1b).

FIGURE A-10. DATA FOR 60.3 mm 94.4% TMD 94/6 RDX/WAX ON 94.4% TMD EXPLOSIVE D (SHOT 1110)

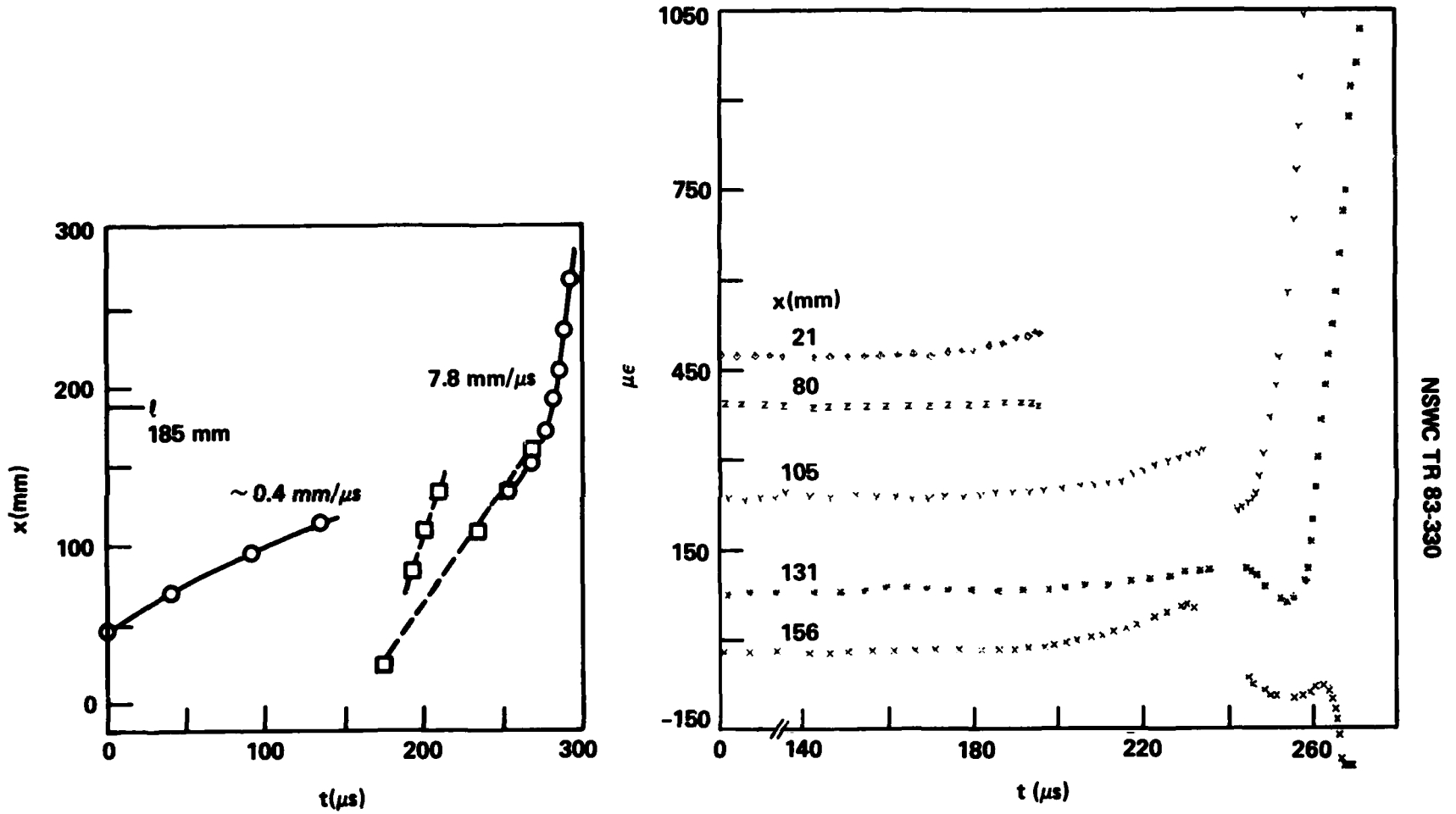

a. DISTANCE-TIME DATA (LEGEND OF FIGURE 1a).

b. STRAIN-TIME DATA (LEGEND OF FIGURE 4b).

FIGURE A-11. SHOT 1318 ON CAST PENTOLITE (~ 97% TMD)

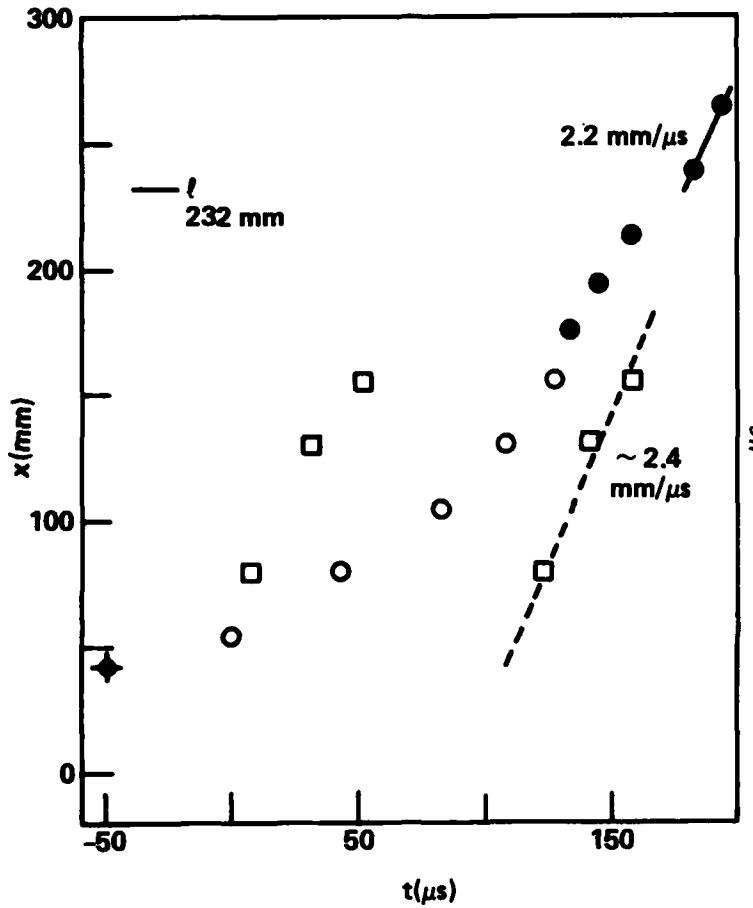

a. DISTANCE-TIME DATA (LEGEND OF FIGURE 1a, ✦ CONDUCTIVITY PROBE)

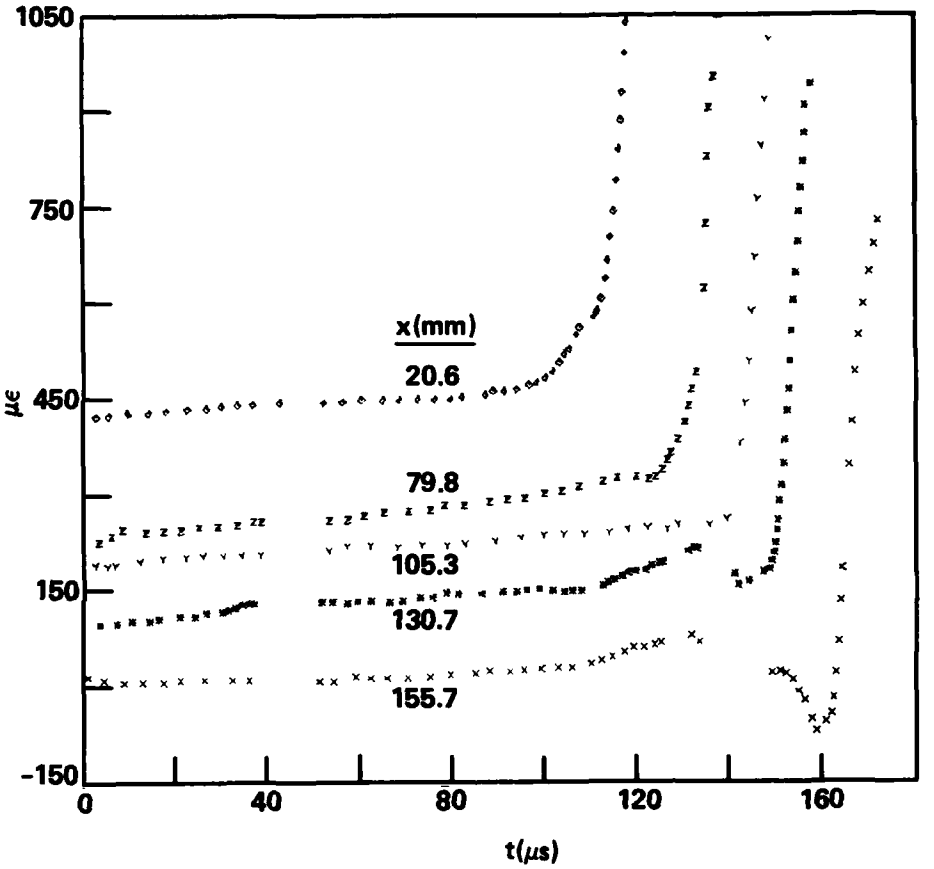

b. STRAIN-TIME DATA (LEGEND OF FIGURE 4b).

FIGURE A-12. SHOT 1503 ON CAST PENTOLITE (~ 97% TMD)

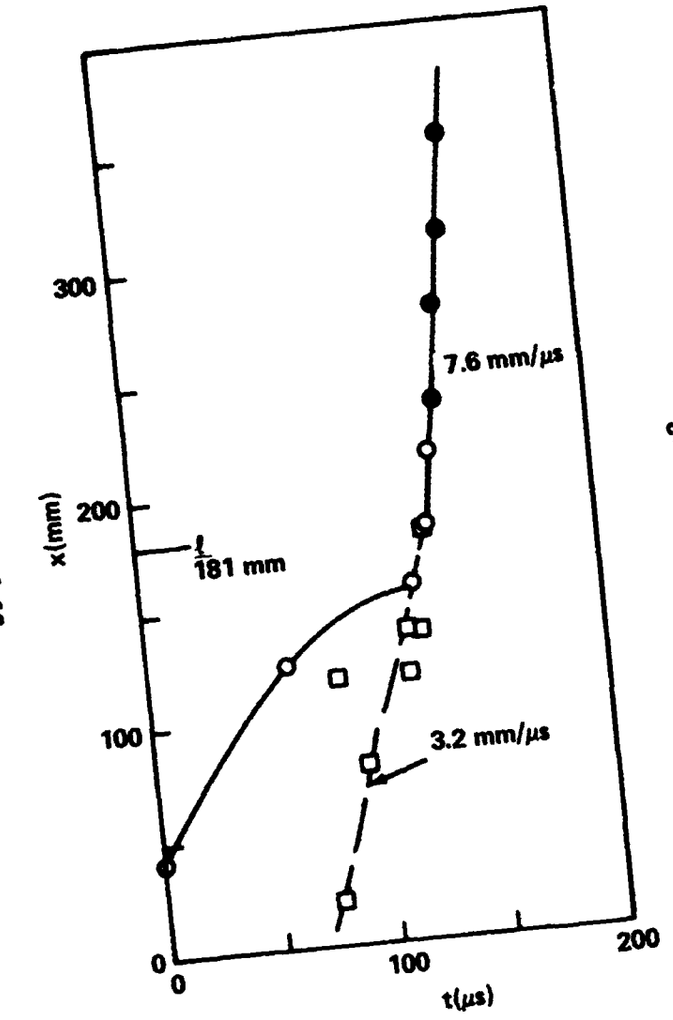

a. DISTANCE-TIME DATA (LEGEND OF FIGURE 1a).

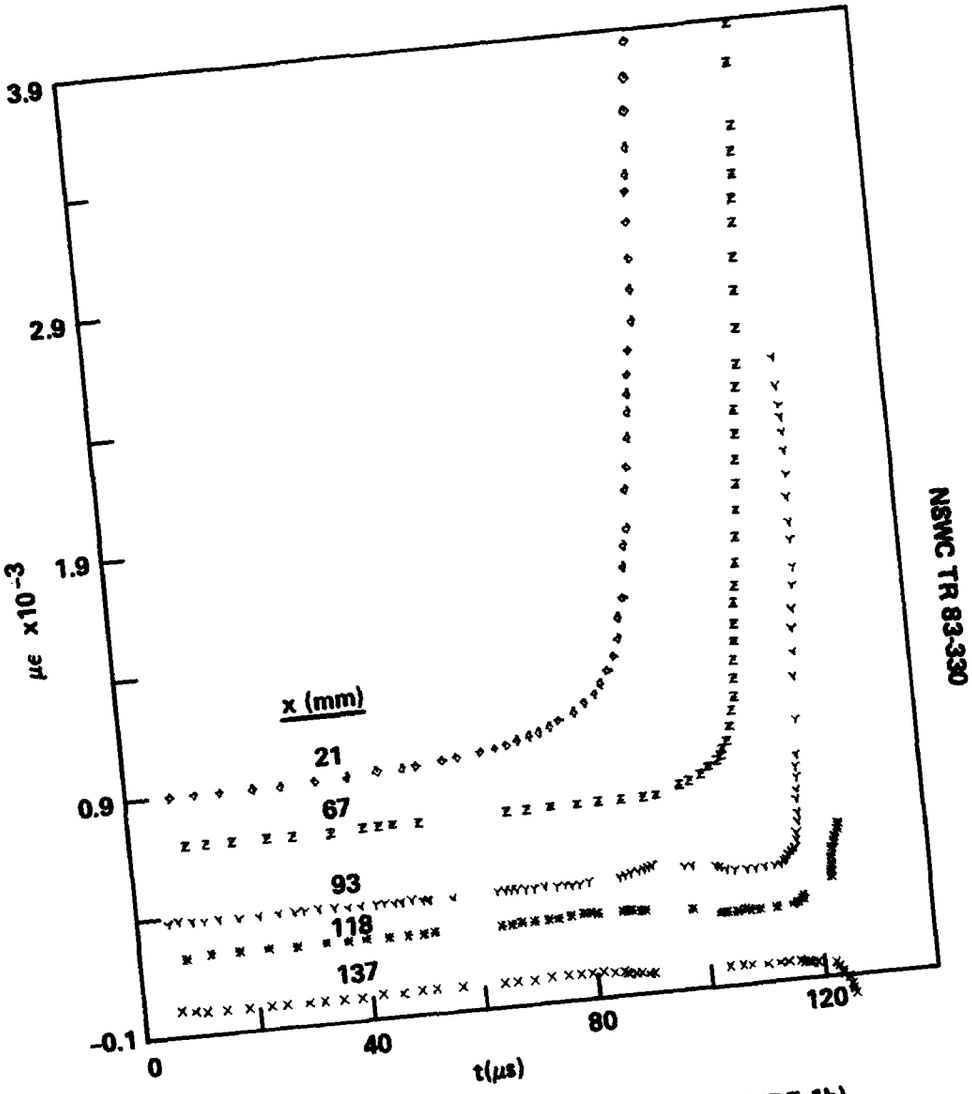

b. STRAIN-TIME DATA (LEGEND OF FIGURE 1b).

FIGURE A-13. SHOT 1413 ON CAST PENTOLITE IN CHARGES 25 mm DIA. x 410 mm LENGTH

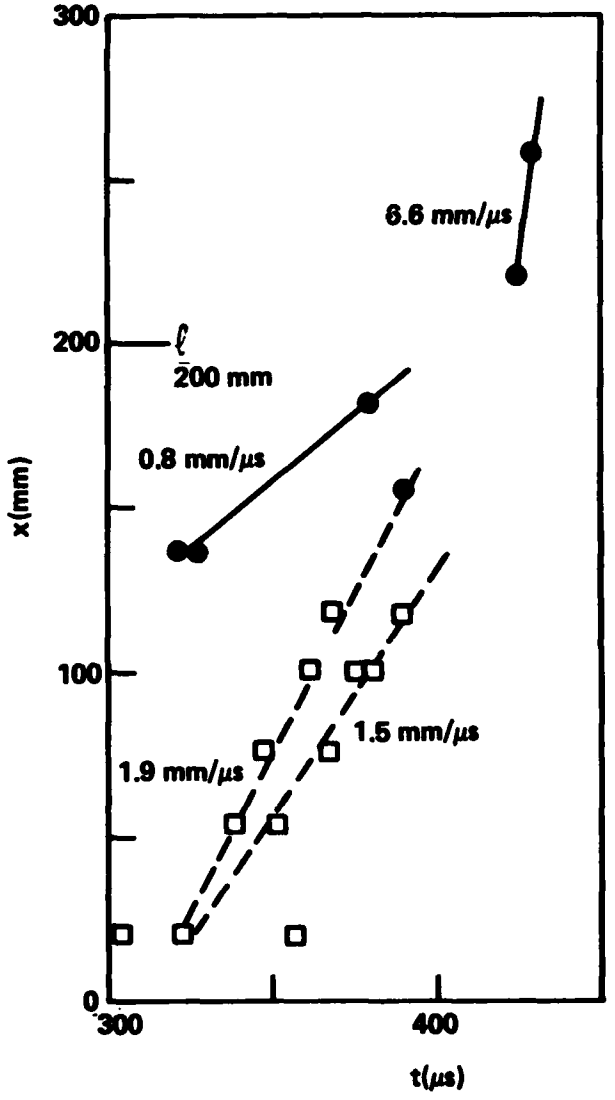

a. DISTANCE-TIME DATA (LEGEND OF FIGURE 1a).

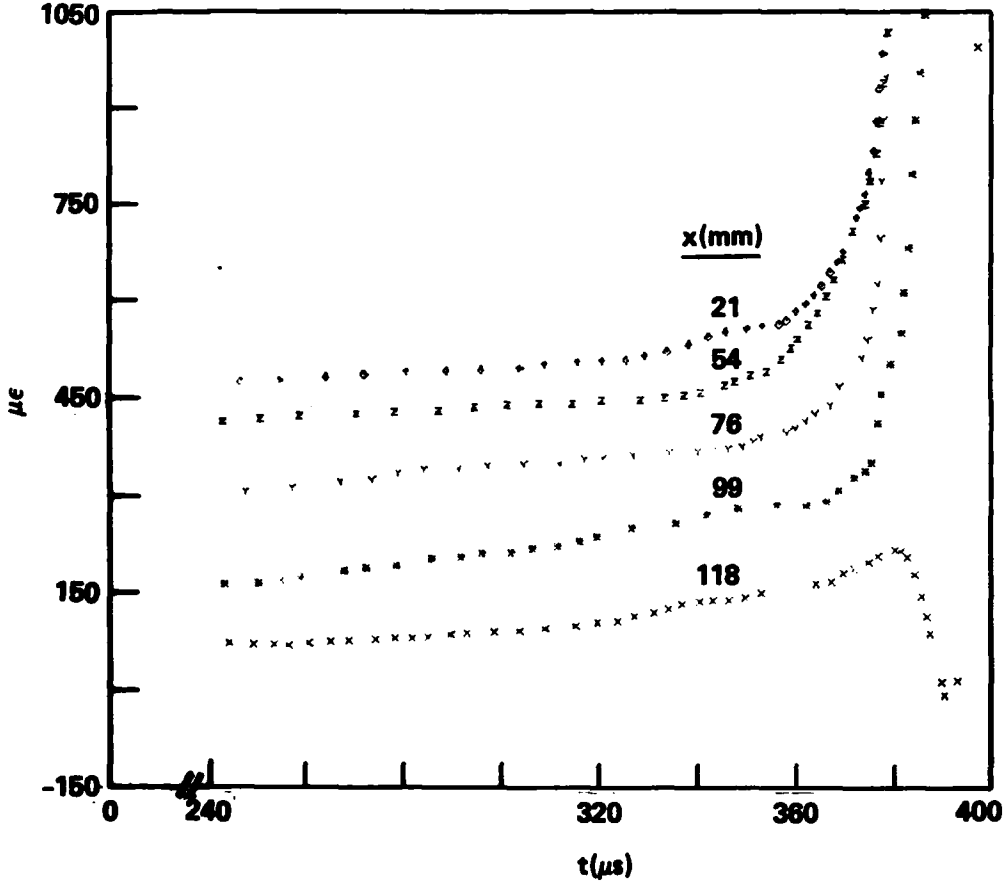

b. STRAIN-TIME DATA (LEGEND OF FIGURE 4b)

FIGURE A-14. SHOT 1508 ON CAST PENTOLITE

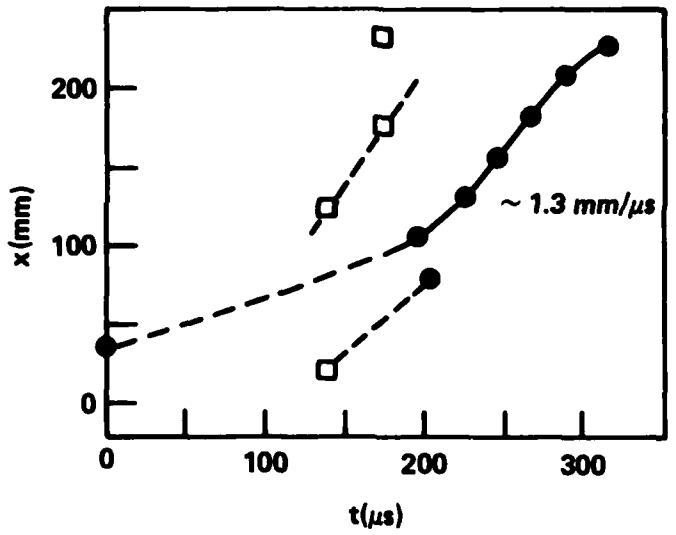

a. DISTANCE-TIME DATA (LEGEND OF FIGURE 1a).

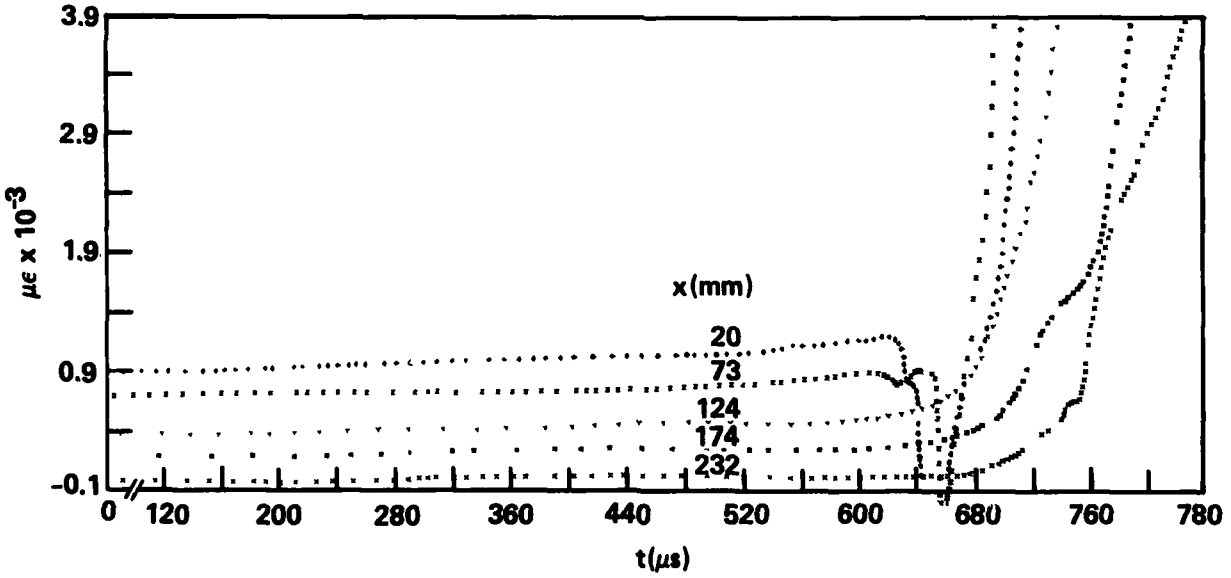

b. STRAIN-TIME DATA (LEGEND OF FIGURE 1b).

FIGURE A-15. SHOT 1209 ON CAST H-6 (CA. 97% TMD) (LEGEND OF FIGURE 1a)

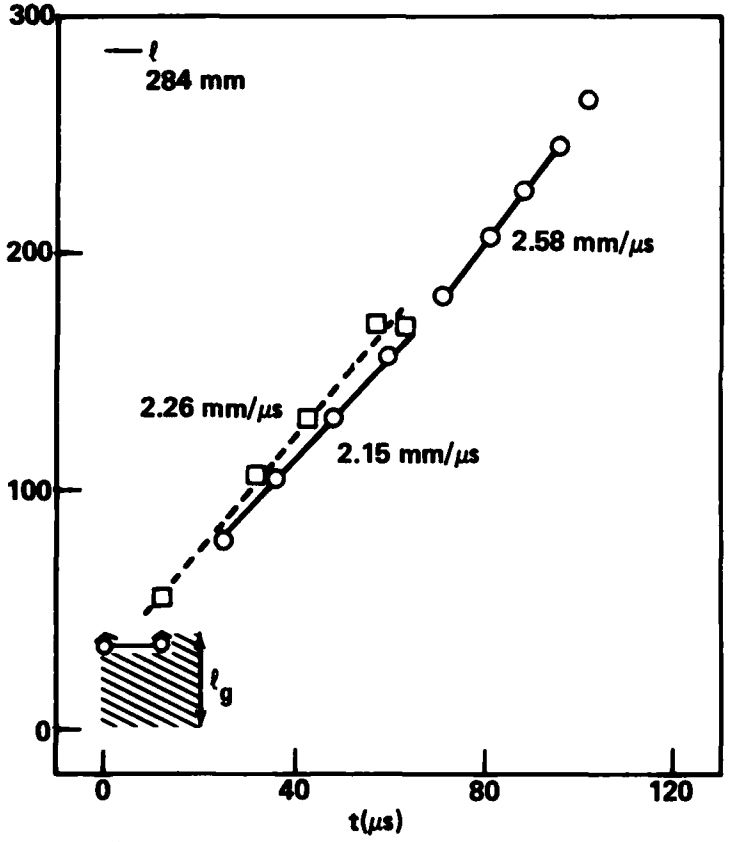

a. DISTANCE-TIME DATA (LEGEND OF FIGURE 3a).

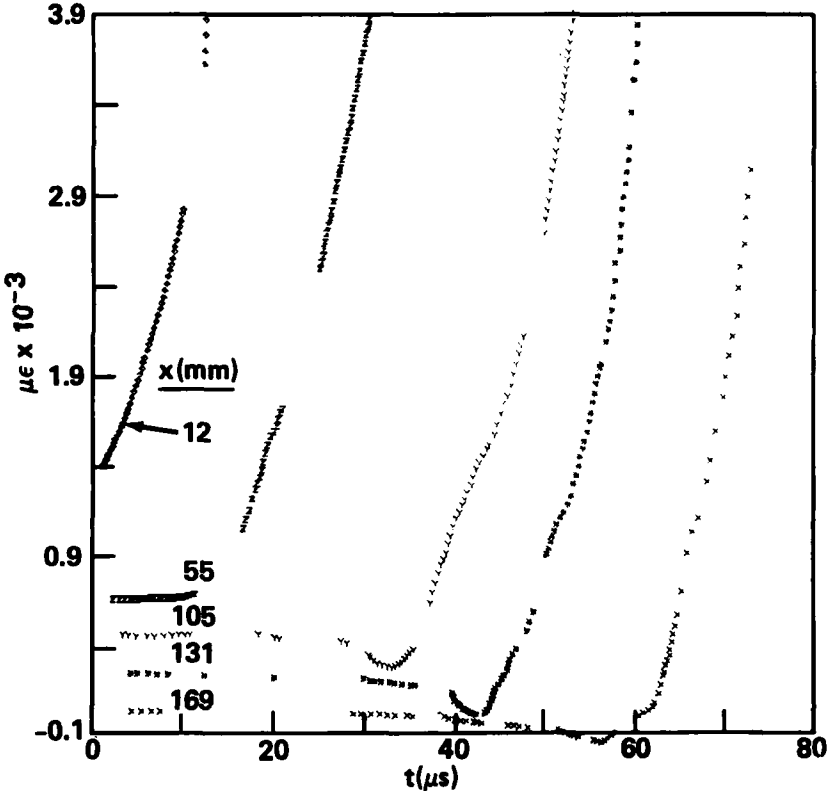

b. STRAIN-TIME DATA (LEGEND OF FIGURE 1b).

FIGURE A-16. DATA FOR 40.0 mm 95.0% TMD 94/6 RDX/WAX ON CAST 75/25 CYCLOTOL (SHOT 1003)

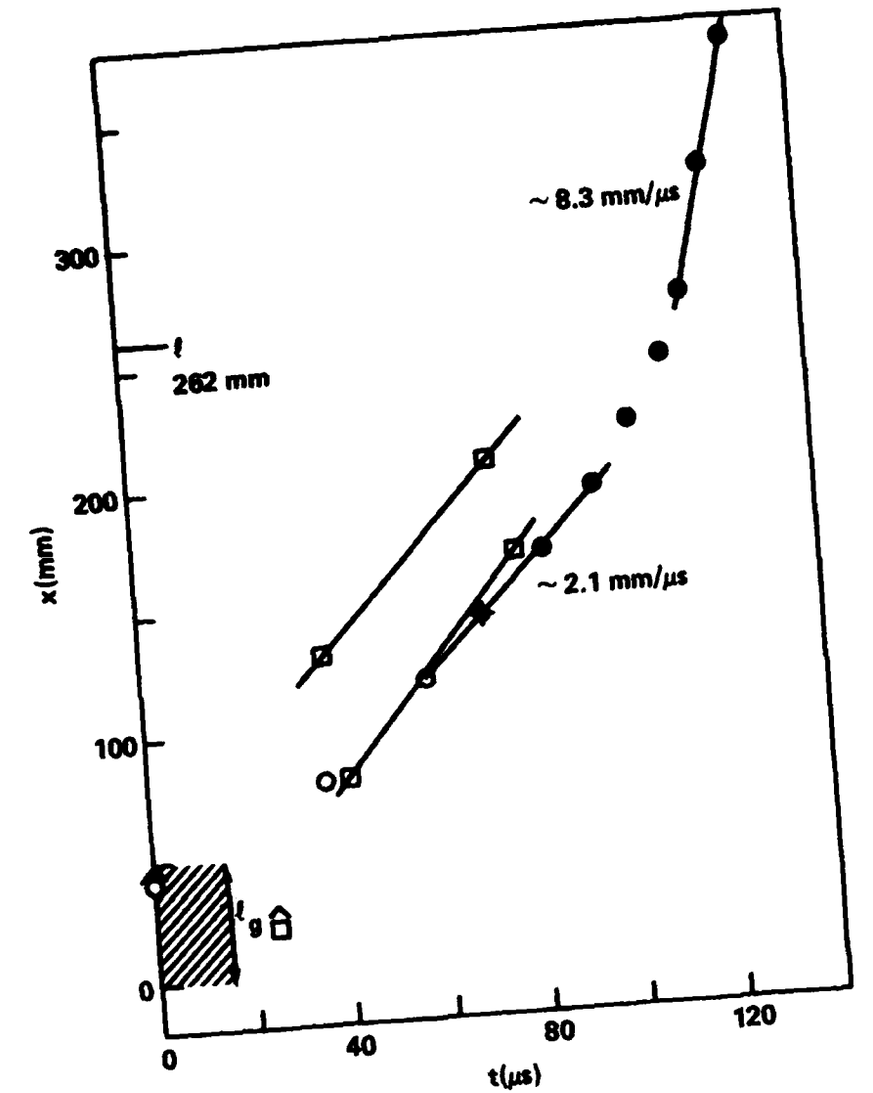

a. DISTANCE-TIME DATA (LEGEND OF FIGURE 3a, ◆ CONDUCTIVITY PROBE).

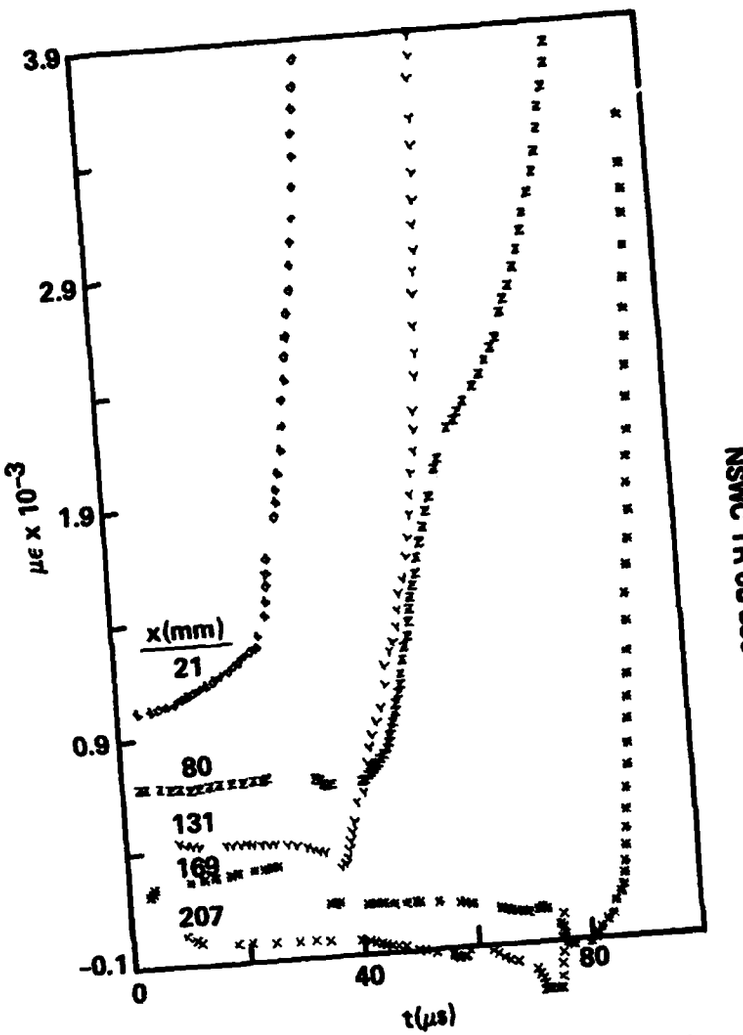

b. STRAIN-TIME DATA (LEGEND OF FIGURE 1b).

FIGURE A–17. DATA FOR 50 mm 95% TMD 94/6 RDX/WAX ON CAST CYCLOTOL (CA. 99% TMD) IN AN 18 INCH TUBE (SHOT 1415)

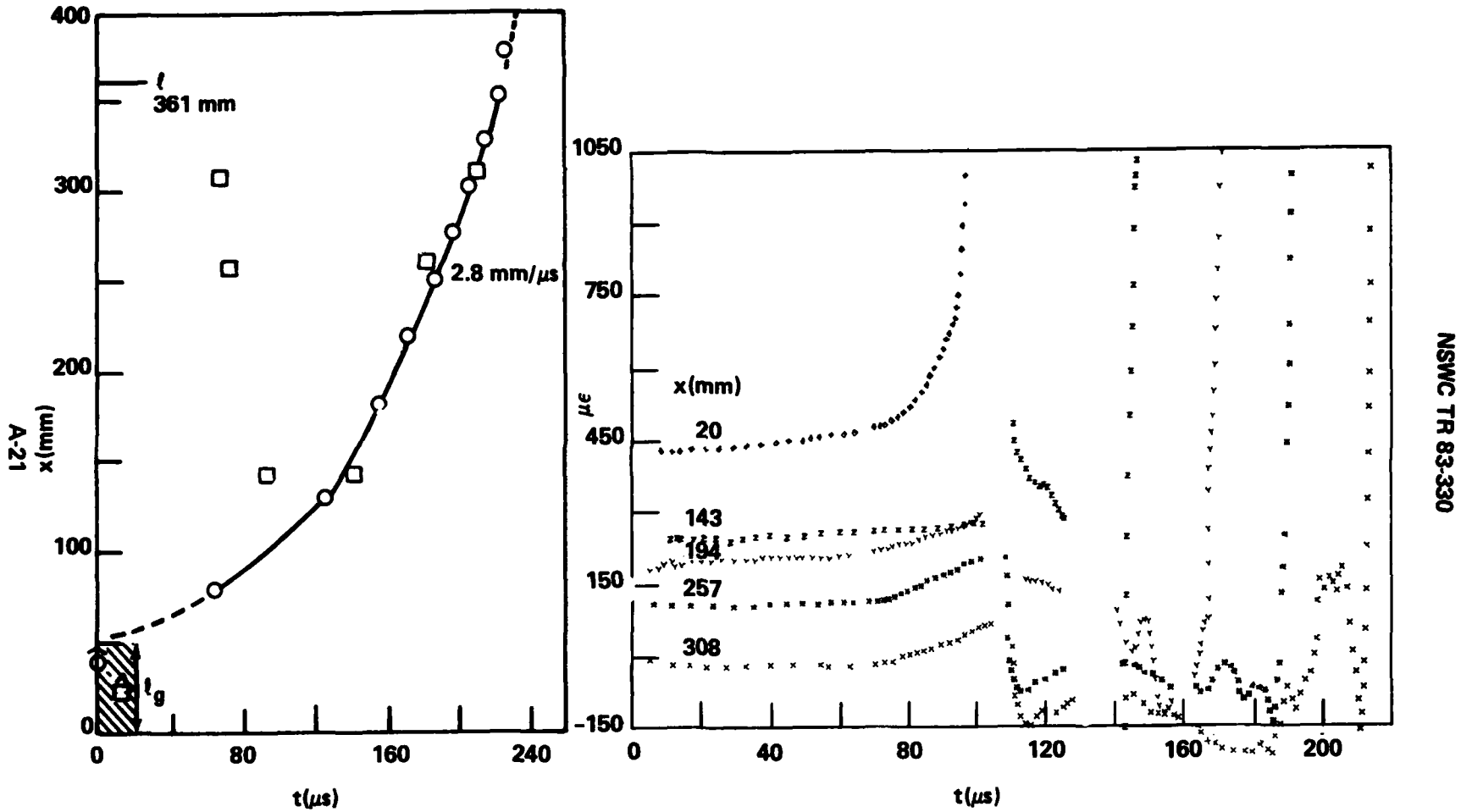

a. DISTANCE-TIME DATA (LEGEND OF FIGURE 3a).

b. STRAIN-TIME DATA (LEGEND OF FIGURE 4b).

FIGURE A-18. DATA FOR 50 mm 95% TMD 94/6 RDX/WAX ON CAST COMP B IN AN 18 INCH TUBE (SHOT 1309)

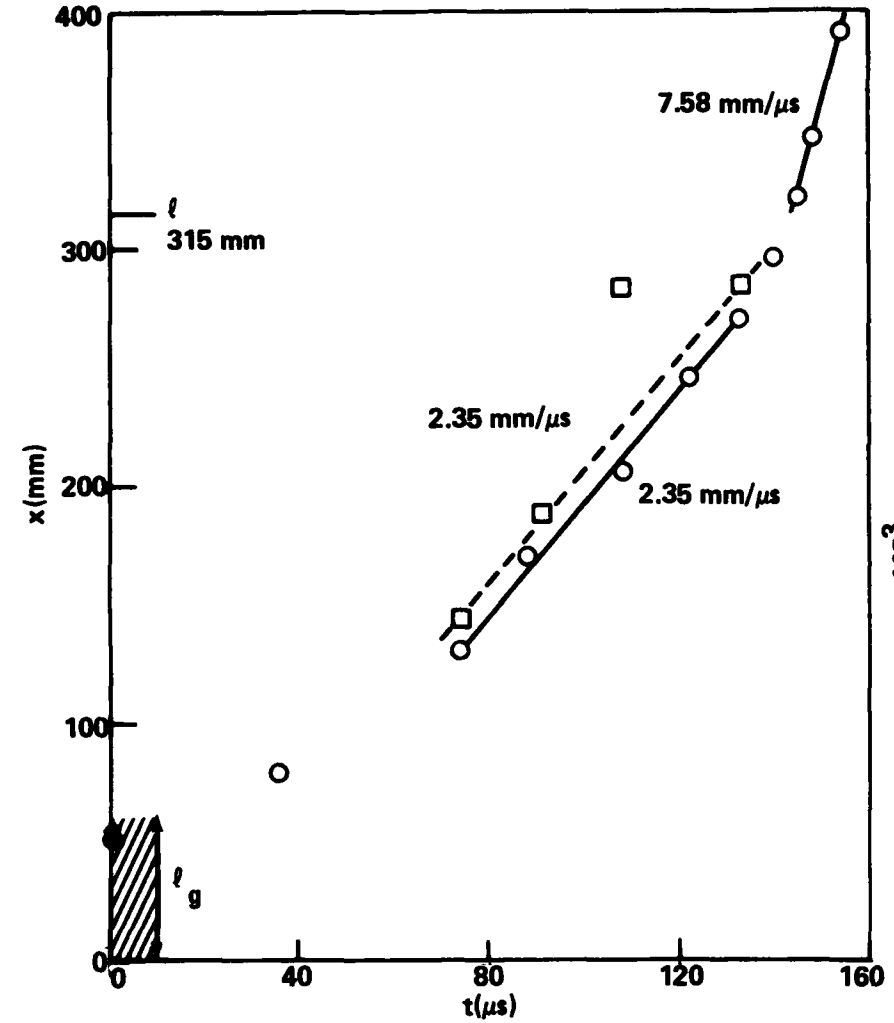

a. DISTANCE-TIME DATA (LEGEND OF FIGURE 3a).

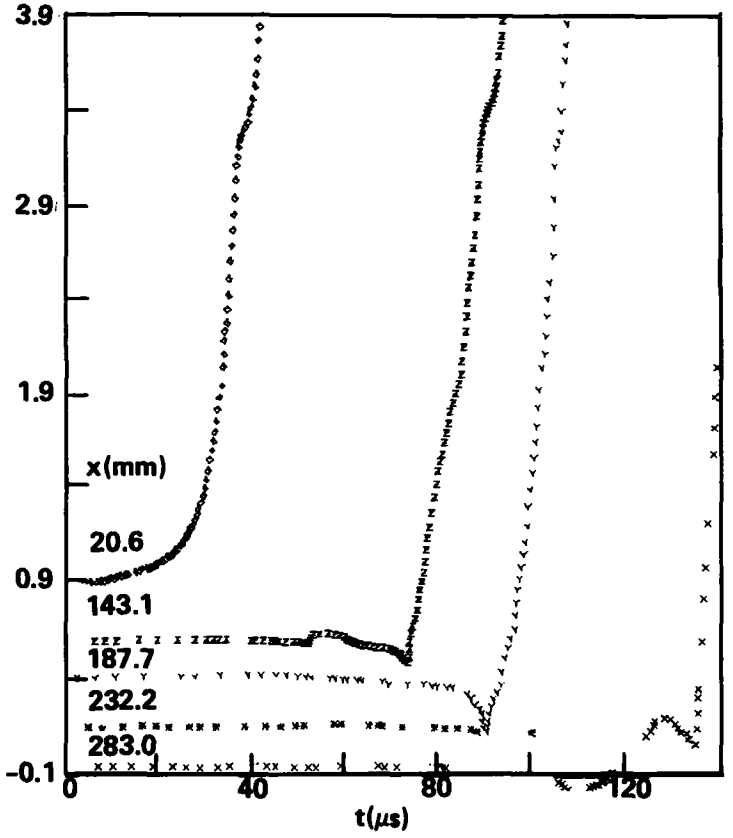

b. STRAIN-TIME DATA (LEGEND OF FIGURE 1b)

FIGURE A-19. DATA FOR 60.0 mm 96.7% TMD 94/6 RDX/WAX ON CAST COMP B IN AN 18 INCH TUBE (SHOT 1206)

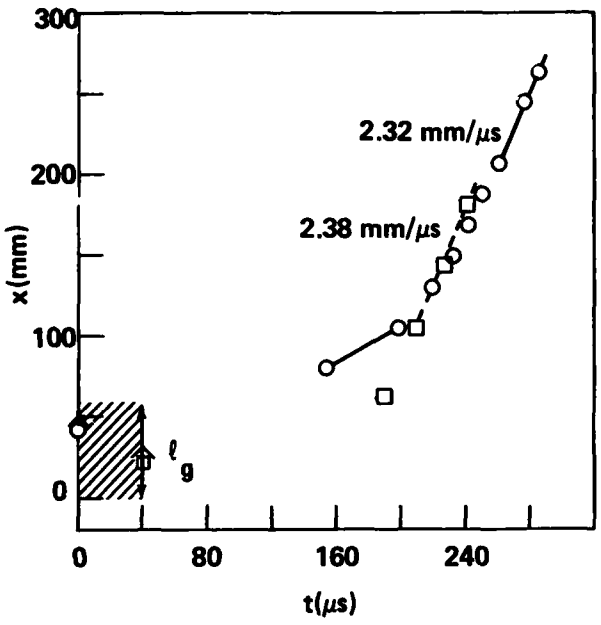

a. DISTANCE-TIME DATA (LEGEND OF FIGURE 3a).

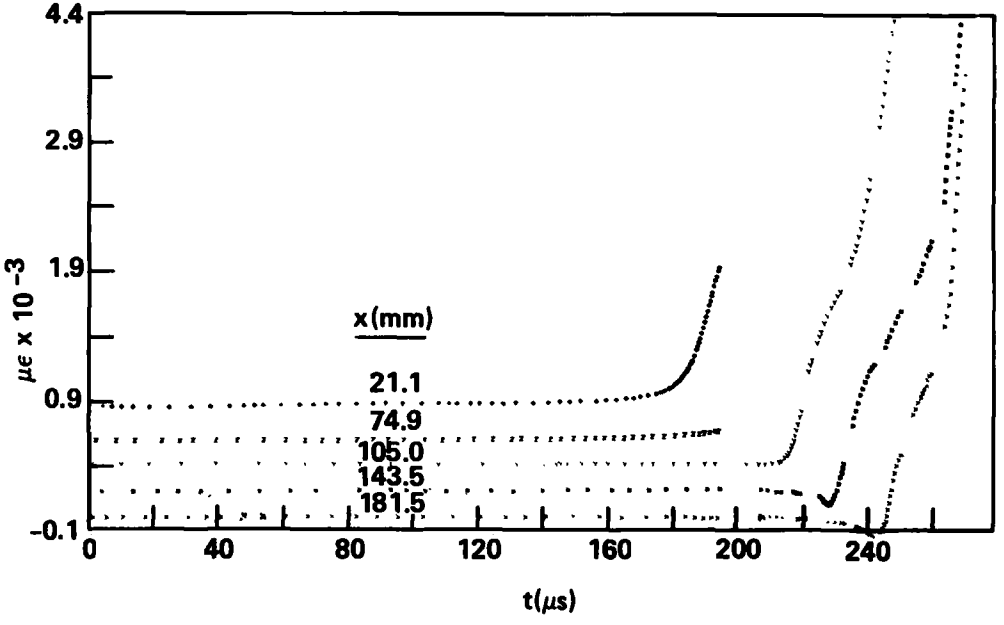

b. STRAIN-TIME DATA (LEGEND OF FIGURE 1b).

FIGURE A-20. DATA FOR 60.0 mm 96.7 % TMD 94/6 RDX/WAX ON CAST TNT (SHOT 1102)

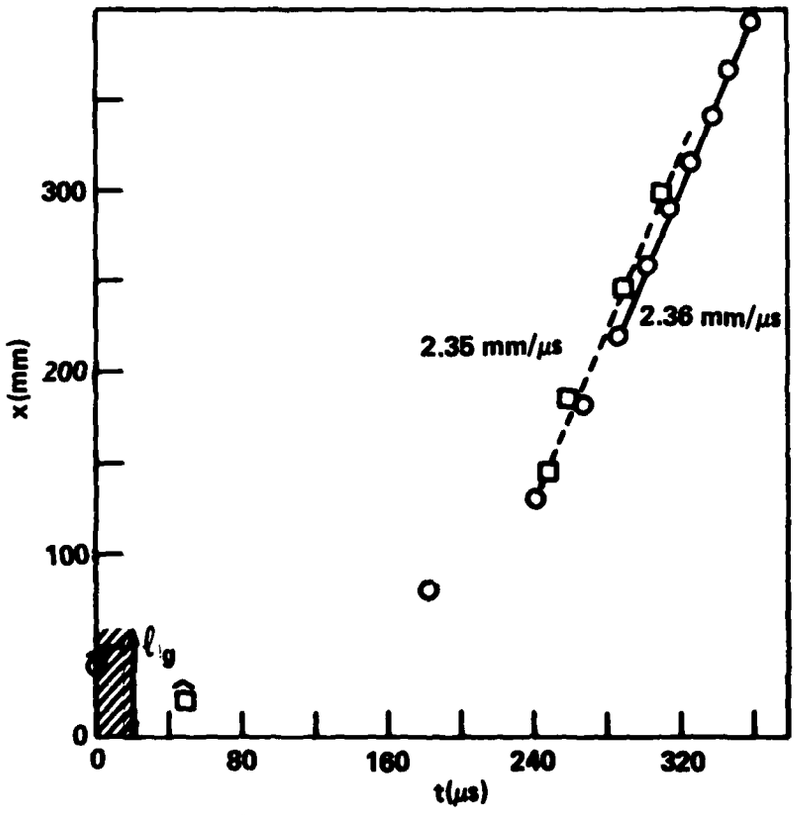

a. DISTANCE-TIME DATA (LEGEND OF FIGURE 3a).

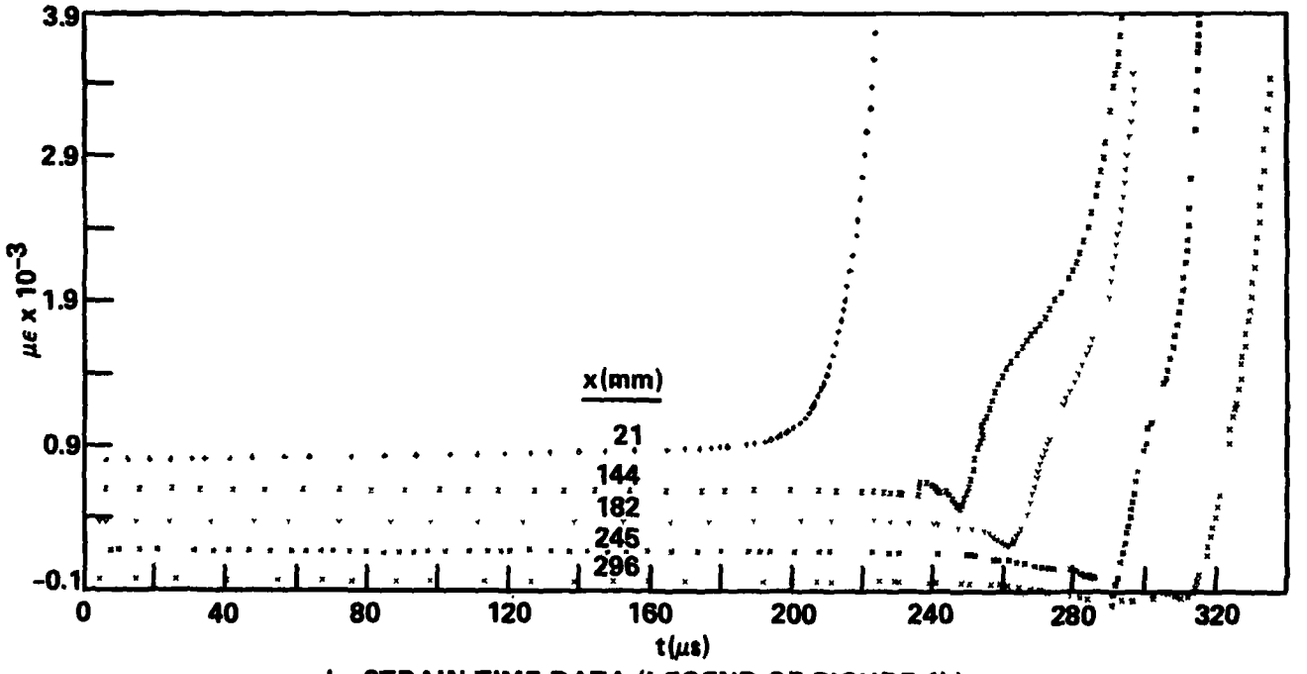

b. STRAIN-TIME DATA (LEGEND OF FIGURE 1b).

FIGURE A-21. DATA FOR 60.0 mm 96.7% TMD 94/6 RDX/WAX ON CAST TNT IN AN 18 INCH TUBE (SHOT 1105)

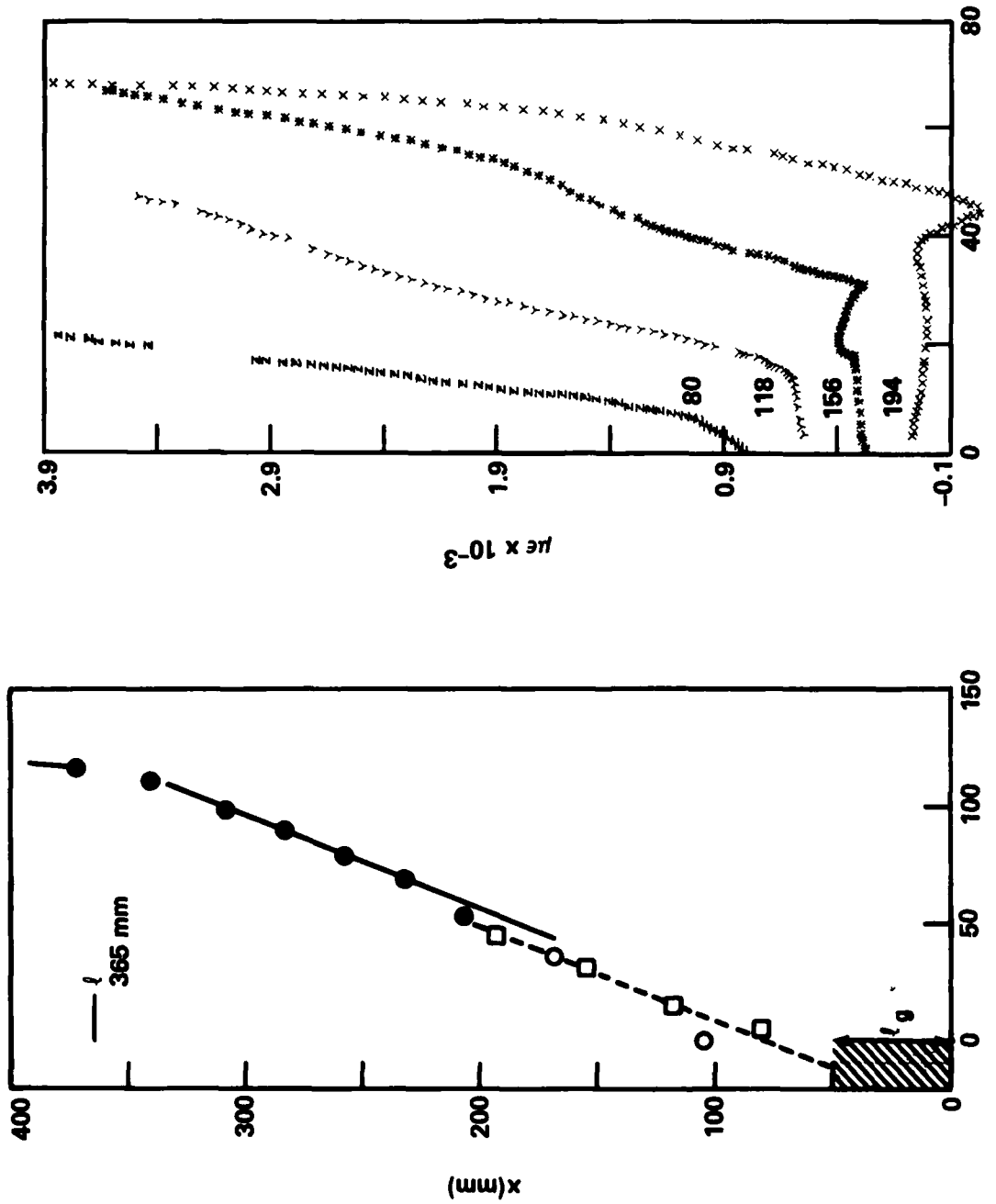

a. DISTANCE-TIME DATA (LEGEND OF FIGURE 1a). b. STRAIN-TIME DATA (LEGEND OF FIGURE 1b).

FIGURE A-22. DATA FOR 50 mm 96.5% TMD 94/6 RDX/WAX ON CAST CYCLOTOL 75/25 (CA. 96% TMD) IN 3 IN. DIA. x 18 IN. LENGTH TUBE (SHOT 1716)

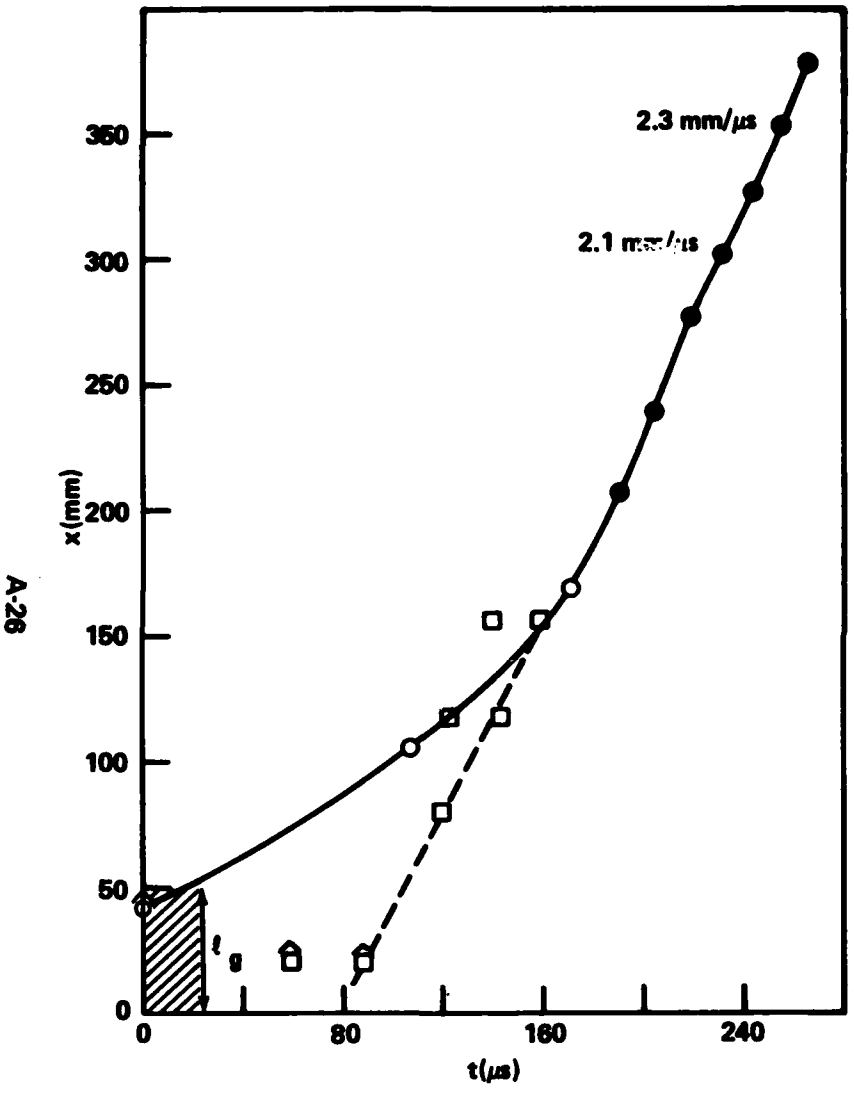

a. DISTANCE-TIME DATA (LEGEND OF FIGURE 3a).

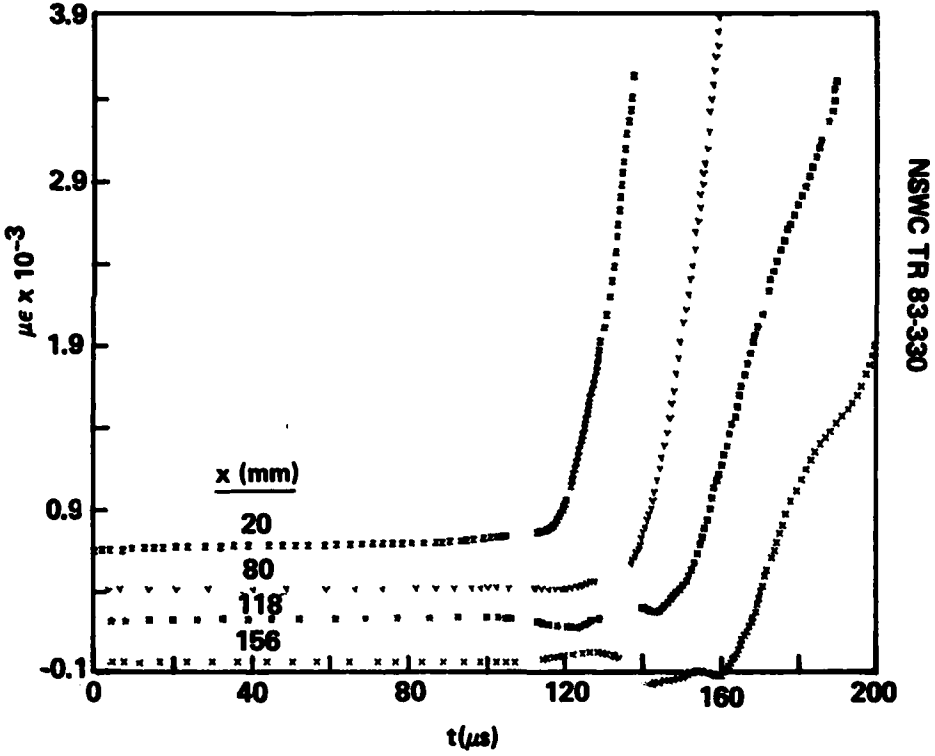

b. STRAIN-TIME DATA (LEGEND OF FIGURE 1b).

FIGURE A-23. DATA FOR 50 mm 95% TMD 94/6 RDX/WAX ON CAST COMP B IN 3 IN. DIA. x 18 IN. LENGTH TUBE (SHOT 1715)

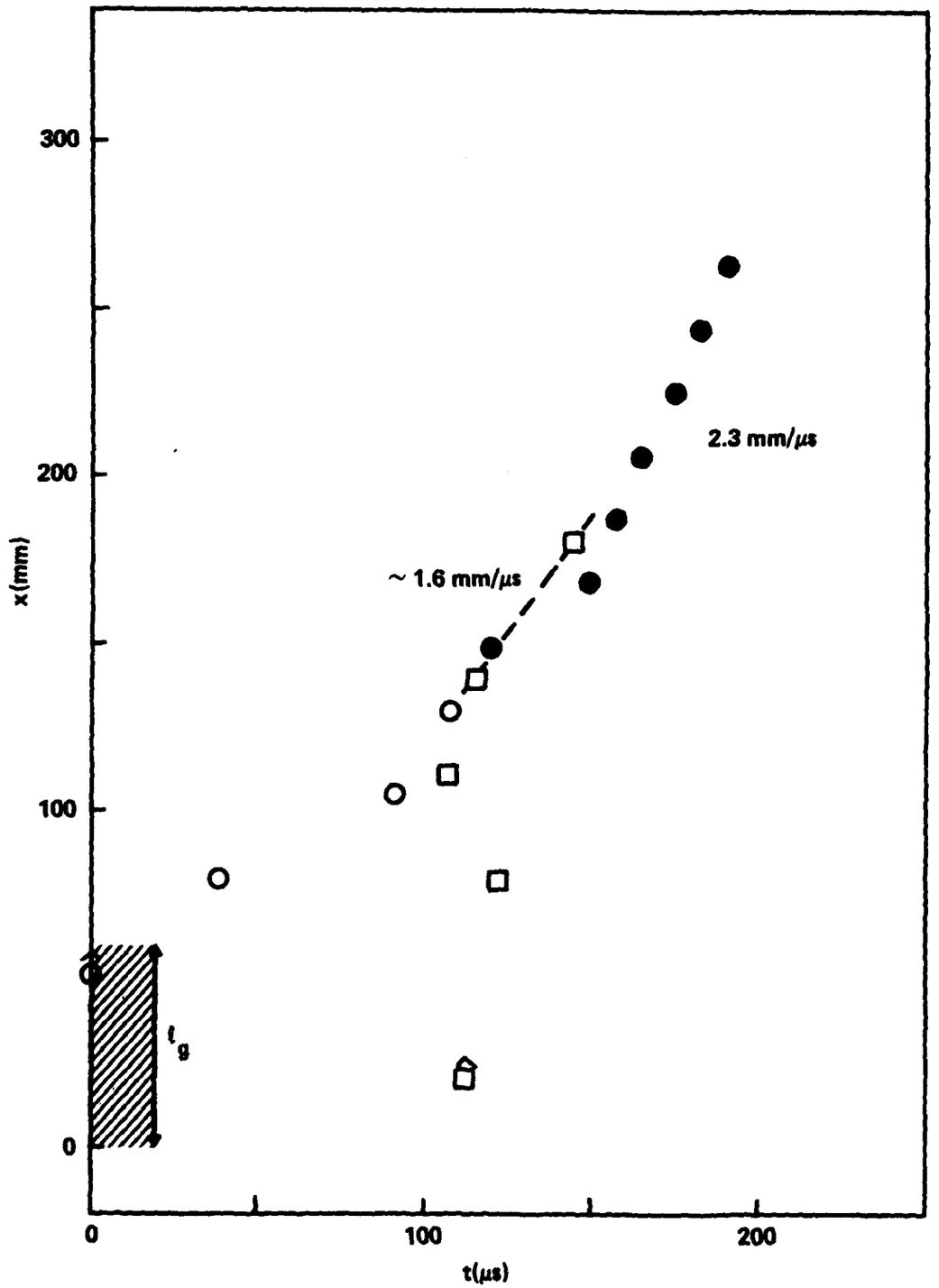

FIGURE A-24. DISTANCE-TIME DATA FOR 60 mm 95% TMD 94/6 RDX/WAX ON CAST PBXN 106 (SHOT 1704)

TABLE A-1. DETAILED DATA FOR GAS LOADING OF PRESSED CHARGES

Shot No.	903		1110		715		814	
HE	Explosive D[a]		Explosive D[a]		TNT[b]		TNT[b]	
ρ_o(g/cm^3)	1.629		1.624		1.553		1.548	
%TMD	94.7		94.4		93.9		93.6	
Loader[c]								
ℓ_g(mm)	38.1		60.3		19.1		28.6	
ρ_o(g/cm^3)	1.616		1.624		1.616		1.611	
%TMD	94.0		94.4		94.0		93.7	
IP Data	x	t	x	t	x	t	x	t
	47.8	0.0*	41.7	0.0*	28.7	0.0*	35.1	0.0*
	79.5	18.3*	60.7	13.0*	41.4	12.0*	66.8	31.3*
	104.9	29.5*	79.8	19.6*	54.2	26.6*	92.2	46.9
	124.0	42.3	105.2	29.1*	79.6	44.5*	111.3	56.2
	143.0	51.6	130.7	42.7	105.0	59.7	130.3	61.3
	162.1	61.8	156.1	54.4	130.3	73.2	149.4	64.7
	181.1	71.4	181.5	67.5	155.7	85.4	168.4	67.8
	200.2	80.9	206.6	79.3	181.2	98.0	187.5	70.5
	219.2	91.0	225.9	87.2	206.8	108.1	206.6	-
	238.3	100.8	245.0	96.9	257.3	119.8	231.9	77.1
	257.3	110.4	264.2	105.9			257.3	81.2
SG Data	x	t	x	t	x	t		
	11.7	No record			11.9	-	Strain-time records lost	
	79.5	11.6	20.8	-	54.5	26.5		
	104.9	22.0	74.8	13-14	79.9	40		
	130.3	36.0	118.0	25,33.5	105.0	48-50.5		
	155.7	49.2	156.0	30.5,49	130.6	62		
			206.6	43,65.5				
$\ell(\ell')$(mm)	F		F		238±1(219)		135±1(106.4)	
Δt_D^{29}(μs)	"		"		117		68	
Δt_P^{29}(μs)	"		"		15.5		-	
Δt_E^{29}(μs)	"		"		101.5		56 est.	
D mm/μs	"		"		-		6.5	

*custom-made probes; a. ρ_V = 1.72 g/cm3 ; b. ρ_V = 1.654 g/cm3 c. ρ_V = 1.72 g/cm3

TABLE A-1. (Cont.) DETAILED DATA FOR GAS LOADING OF PRESSED CHARGES

Shot No.	616		716		702		617	
HE	Explosive D[a]		95/5,TNT/Wax[d]		TNT		TNT	
ρ_o(g/cm^3)	1.508		1.402		1.458		1.473	
%TMD	87.7		87.5		88.2		89.1	
Loader								
ℓ_g(mm)	28.6		19.1		9.5		28.6	
ρ_o(g/cm^3)	1.50		1.515		1.510		1.510	
%TMD	87.2		88.1		87.8		87.8	
IP Data	x	t	x	t	x	t	x	t
	23.9	0*	23.7	0.0*	29.0	0.0*	24.0	0*
	38.5	17.7*	41.5	28.0*	54.2	20.4*	35.2	16.3*
	54.4	27.5*	54.2	39.7*	79.8	41.3*	54.2	43.8*
	79.8	41.0*	79.6	54.6*	105.2	55.5*	66.9	54.9*
	107.0	57.2	105.0	74.2	130.4	71.0	79.6	64.0
	130.4	70.1	130.4	85.7	155.8	76.9	105.0	77.6
	156.0	81.5	155.8	90.5	181.4	80.8	130.4	85.2
	181.4	90.6	181.2	95.1	206.8	84.9	156.0	89.9
	206.8	95.4	206.6	97.9	232.2	89.1	206.8	97.2
	257.6	102.6	257.4	107.0	257.6	92.6	257.6	104.5
SG Data	x	t	x	t	x	t	x	t
	11.7	0.0	SG records lost		20.8	-	11.8	15.2
	54.4	25.0	from late trigger-		41.7	Ringing	41.8	30.0
	79.5	34.3	ing.		66.9	26.1	60.6	43.0
	105.1	46.3			92.2	40.8	79.9	56.3
	143.4	63-68			118.0	54.4	98.8	64.5
$\ell(\ell')$mm	204±3(175.4)		133±4(113.9)		[140±4(130.5)]**		133^{+3}_{-2}(104.4)	
Δt_D^{29}(μs)	81.5		78		[190]**		78.0	
Δt_p^{29}(μs)	-1.0		-		[150]**		14.5	
Δt_E^{29}(μs)	82.5		67-8 est.		[40]**		63.5	
D(mm/μs)	7.1		-		[4.9]**		7.0	

d. ρ_V = 1.60 g/cm^3

*Custom-made probes **metastable detonation

TABLE A-1. (Cont.) DETAILED DATA FOR GAS LOADING OF PRESSED CHARGES

Shot No.	714		1009		1011		708	
HE	Tetryl[e] (coarse)		Ground tetryl X844[e]		RDX[f]		RDX[f]	
ρ_o(g/cm^3)	1.543		1.215		1.244		1.229	
%TMD	87.6		70.0		68.9		68.1	
Loader								
ℓ_g(mm)	19.1		20.1		19.8		19.96	
ρ_o(g/cm^3)	1.515		1.215		1.214		1.210	
%TMD	88.1		70.6		70.6		70.4	
IP Data	x	t	x	t	x	t	x	t
	23.6	0.0*	28.7	0.0*	28.4	0.0*	16.0	0.0*
	41.5	23.4*	54.2	63.6*	41.4	57.8*	28.7	87.4*
	54.2	35.0*	66.9	109.4*	54.2	99.7*	41.5	144.2*
	79.5	48.7*	79.6	139.1*	66.9	136.7*	54.2	184.2*
	104.9	55.0	92.3	161.8*	79.6	Shorted	66.8	223.3*
	130.4	58.0	105.0	192.3	92.3	189.2	79.6	256.7
	155.8	61.4	117.7	204.6	105.0	202.2	92.3	274.4
	181.1	65.3	130.4	209.3	117.7	Shorted	105.0	277.2
	206.6	68.1	155.8	213.8	130.4	205.9	130.4	280.9
	257.4	75.8	181.2	217.9	181.4	213.8	257.6	298.6
			257.6	229.4	257.6	224.4		
SG Data	x	t	x	t	x	t	x	t
	12.1	13.0	11.8	230	11.9	-	12.2	-
	41.9	18.5	50.5	138,219	31.3	141	31.2	250.4-53.6,269.9
	61.0	30.0	69.6	156, -	50.4	154	48.0	247.8
	79.8	40.0	88.4	167,215	69.6	177	67.0	262.6
	98.9	-	107.8	184,202,211	88.5	190	210.1	-
$\ell(\ell')$mm	85^{+5}_{-0}(65.9)		130±2(110)		100±2(80)		93±2(73)	
Δt_D^{29}(μs)	45.5		209		201		74	
Δt_D^{29}(μs)	3.0		120		148		8.5	
$\Delta t_\varepsilon^{29}$(μs)	42.5		89		53		65.5	
$D(\bar{\sigma})$ mm/μs	7.32(0.16)		6.36(0.17)		6.85 (0.12)		7.1	

*Custom-made probes e. ρ_V = 1.73 g/cm^3 f. ρ_V = 1.806 g/cm^3

All x in mm, t in μs. F means failure.

TABLE A-2. DETAILED DATA FOR SELF-LOADING OF CAST 50/50 PENTOLITE IN STANDARD TUBE

Shot No.	1318		1503		1413≠	
HE	Pentolite-c X887		Pentolite-c X887		Pentolite-c	
ρ_o	1.66**		~1.66		~1.66	
%TMD	97.0		97.0		97	
Loader	None		None		None	
Charge length (mm)	295		295		410	
Charge dia. (mm)	16		16		25.4	
IP Data	x	t	x	t	x	t
	41.4	0.0*	41.9	(-49)***	41.5	0.0*
	66.8	41.0*	54.6	0.0*	86.0	-
	92.2	91.9	80.1	42.8*	124.1	61.2*
	111.3	135.6*	105.4	82.7*	155.8	119.25*
	130.3	253.7*	130.8	108.7*	181.4	127.0*
	149.4	268.05*	156.2	128.2*	213.1	131.3*
	168.4	278.3*	175.4	134.0	244.9	135.3
	187.5	282.4*	194.3	145.0	276.6	139.4
	206.5	286.1*	213.4	157.9	308.4	143.9
	232.0	289.4*	238.9	183.3	340.1	147.95
	263.8	293.45*	264.4	194.7	371.9	-
SG Data						
	20.6	173	20.6	-	20.1	77.3
	79.7	192	79.8	7.7,122.7	79.4	93
	105.0	202,237	105.3	-	117.5	82.7,114.7
	130.5	211,254	130.7	32,142	136.5	114.7,121
	155.8	-, 270	155.7	52,159	180.8	125
ℓ(mm)	185		[232][a]		181[b]	
$^{41.5}\Delta t_D$(μs)	280		[180]		127[b]	
$^{41.5}\Delta t_p$	190		[107]		83	
Δt_E	90		[63]		44	
D(mm/μs)	7.8		[2.2][a]		7.6	

**ρ_V = 1.71 g/cm^3 ≠ Large diameter tube a. Metastable b. Probable value, see text
c. Corrected by +104μs to use common zero time for IPs and SGs. ***Conductivity probe.

TABLE A-2. (Cont.) DETAILED DATA FOR SELF-LOADING OF CAST 50/50 PENTOLITE IN STANDARD TUBE

Shot No.	1414 ≠		1508 ≠	
HE	Pentolite-c		Pentolite-c	
ρ_o	~1.66		~1.66	
%TMD	97		97	
Loader	None		None	
Charge length (mm)	410		295	
Charge dia. (mm)	25.4		25.4	
IP Data	x	t	x	t[c]
	41.4	0.0,8.4*	29.1	***
	79.6	31.6*	41.9	-*
	117.7	74.9*	61.0	-*
	143.1	86.35*	80.0	-*
	168.5	89.1*	99.1	-*
	193.9	91.6	118.1	-*
	225.7	95.7	137.2	322.3,328.0
	257.3	100.25	156.2	390.7
	295.5	105.8	181.6	380.1
	333.6	110.65	219.7	424.5
	371.7	Not used	257.8	430.2
SG Data	20.6	47.2,50.4	20.6	304.6,322.5,357.2
	66.8	60.3,69.5	54.1	339.5,352.3
	92.5	69.1,74.3	75.9	348.8,367.4
	117.7	83.9	98.7	362,375.7,381.2
	136.7	84.8	117.6	390.3,369
ℓ(mm)	137[b]		200	
Δt_D(μs)	85[b]		-	
Δt_P	55.5		333	
Δt_E	29.5		69-88	
D(mm/μs)	7.2		6.6	

***Conductivity probe.

TABLE A-3. SELF-LOADING OF CAST H-6

Shot No.	1209	
HE	H-6 c	
ρ_o	~1.75**	
%TMD	~97	
Loader	None	
ℓ_g(mm)		
ρ_o		
%TMD	-	
IP Data	x	t
	35.3	0.0
	79.6	203.1
	105.2	195.8
	130.6	221.5
	156.0	242.8
	181.2	260.9
	206.6	283.1
	225.7	310.2
	244.7	-
	263.8	-
SG Data	x	t
	20.4	138.7,649.8
	73.3	- 657.8
	124.0	138.7
	174.8	223.2
	231.9	223.2
ℓ(mm)	F (no dent)	

**ρ_v = 1.80 g/cm^3

TABLE A-4. DETAILED DATA FOR GAS LOADING OF TNT BASED CAST CHARGES

Shot No.	908		1003		1415		1409	
HE	Pentolite 50/50[a]		Cyclotol 75/25[b]		Cyclotol 75/25[b]		Cyclotol 75/25[b]	
ρ_0(g/cm^3)	1.65		~1.76		1.759		1.706	
%TMD, tube (in.)	96.5, 13.5		~99, 13.5		99, 18		97,18	
Loader	94/6 RDX/wax							
ℓ_g(mm)	40.0		40.0		50.0		60.0	
ρ_0(g/cm^3)	1.60							
%TMD	95.0							
IP Data	x	t	x	t	x	t	x	t
	35.1	0.0*	35.2	0.0*	41.5	0.0*	51.6	0.0*
	47.8	18.3*	79.6	24.3*	79.6	36.4*	79.6	19.4*
	66.8	19.5*	105.0	35.6*	117.7	58.5*	117.7	38.4*
	92.2	36.6*	130.4	48.2*	143.3	70.8**	143.1	46.9*
	111.3	45.4*	155.8	59.4*	168.7	84.2	168.5	61.0
	130.3	48.7*	181.2	70.8*	194.1	95.1	193.9	70.1
	155.7	51.9*	206.6	81.0*	219.3	103.3	219.3	75.7
	181.1	55.7*	225.7	88.0*	244.9	110.6	257.4	81.4
	206.6	59.0*	244.7	95.5*	270.3	115.5	295.5	86.0
	232.0	63.0*	263.8	101.6*	321.1	121.1	333.8	91.7
	257.4	- *			371.9	127.7	371.9	-
SG Data	x	t	x	t	x	t	x	t
	11.9	4.1	12.2	-	20.7	25.0	20.6	5.5
	54.5	2.9	54.6	12	79.6	41.3	79.5	11.9,24.8
	92.3	30.8	105.3	33	130.6	37.5	111.5	- , 30.6
	117.6	37.1-39.0	130.8	43	168.8	78.3	143.0	41.6,45.0
			169.0	56.5,63.0	206.6	73.4	181.1	49.7,56.1
$\ell(\ell')$mm	118.9±2(79)		284±3(244)		262±2(212)		229±3(169)	
$^{35}\Delta t_D$(μs)	47.2		<108		120.5 ext.***		90 ext.	
D(mm/μs)	7.12(0.13)		-		~8.3		~7.4	

a. ρ_V = 1.71 g/cm^3 b. ρ_V = 1.77 g/cm^3 **Conductivity probe ***Extrapolated

≠ Large diameter tube

TABLE A-4. (Cont.) DETAILED DATA FOR GAS LOADING OF TNT BASED CAST CHARGES

Shot No.	1716 ≠		1309		1715	
HE	Cyclotol 75/25		Comp B X738		Comp B X738	
ρ_o(g/cm^3)	1.700		1.744		1.59	
%TMD, tube length (in.)	96, 18		~100, 18		93, 18	
Loader						
ℓ_g(mm)	50.0		50.0		50.0	
ρ_o(g/cm^3)	1.66				1.66	
%TMD	96.5				96.5	
IP Data	x	t	x	t	x	t
	41.4	-*	41.5	0.0*	41.7	0.0*
	105.0	0.0*	79.6	64.5*	105.2	106.7*
	168.5	36.6*	130.6	127.0*	168.7	170.7*
	206.8	52.9	181.4	155.3*	206.9	190.0
	232.2	68.9	219.5	172.2*	238.8	203.7
	257.6	79.2	251.2	187.4*	276.9	219.3
	283.0	90.35	276.6	196.7*	301.8	232.1
	308.4	99.3	302.0	206.6*	327.3	243.8
	340.1	111.0	327.4	216.0*	352.8	255.2
	372.0	116.8	352.8	224.1*	378.3	266.4
			378.2	228.0*		
SG Data	x	t	x	t	x	t
	20.2	-	20.3	16.5,-	20.4	59,88.4
	79.5	6.1	143.3	93.5,142	79.5	120
	117.6	15.0	193.9	Malfunction	117.5	123,144
	155.7	31.3	257.3	74.2,186	155.8	110,140,159
	193.8	45.2	308.2	67.7,210	193.8	-
$\ell(\ell')$mm	365±3(315)		361.4±2(311)		F	
$^{35}\Delta t_D$(μs)	154-172 ext.		237 ext.		F	
D(mm/μs)	-		-		F	

≠ Large diameter tube.

TABLE A-4.(Cont.) DETAILED DATA FOR GAS LOADING OF TNT BASED CAST CHARGES

Shot No.	1206	1102
HE	Comp B X738	TNT X517
ρ_0(g/cm^3)	1.637	1.630
%TMD,tube length (in.)	96,18	98.5,13.5
Loader		
ℓ_g(mm)	60	60

IP Data	1206 x	1206 t	1102 x	1102 t
	52.3	0.0*	41.7	0.0*
	79.6	34.3*	79.8	153.7*
	130.4	73.6*	105.2	199.3*
	168.5	88.8*	130.6	220.6*
	206.6	107.8*	149.6	232.3*
	244.7	122.2*	168.7	242.5*
	270.1	132.4*	187.7	250.9*
	295.5	139.9*	206.9	261.0*
	320.9	145.2*	225.8	-*
	346.3	148.0*	244.9	277.2*
	390.7	154.3*	264.0	285.7*

SG Data	1206 x	1206 t	1102 x	1102 t
	20.6	-	21.1	40
	143.1	74	74.9	190
	187.7	91	105.0	210
	232.2	>101	143.5	228
	283.0	108,133	181.5	242

$\ell(\ell')$mm	313±3(253)	F
$^{35}\Delta t_D$(μs)	153 ext.	F
D(mm/μs)	7.58(0.41)	F

TABLE A-4. (Cont.) DETAILED DATA FOR GAS LOADING OF TNT BASED CAST CHARGES

Shot No.	1105
HE	TNT X517
ρ_o(g/cm^3)	1.623
%TMD, tube length (in.)	98,18
Loader	
ℓ_g(mm)	60

IP Data

x	t
41.7	0.0
79.8	182.8
130.7	241.9
181.5	267.2
219.5	287.0
257.7	303.7
289.4	314.8
314.8	326.6
340.2	338.8
365.6	348.2
391.0	359.6

SG Data

x	t
20.7	50
143.5	248
182.4	261
244.9	291
295.9	311

$\ell(\ell')$mm	F
$^{35}\Delta t_D$(μs)	F
D(mm/μs)	F

TABLE A-5. DETAILED DATA FOR GAS LOADING OF PBX EXPLOSIVES

Shot No.	1316		1704	
HE	PBXN103		PBXN106	
ρ_0(g/cm^3)	~1.89		~1.65	
%TMD, tube length (in.)	~97,18		-, 13.5	
Loader	94/6 RDX/wax		94/6 RDX/wax	
ℓ_g(mm)	60		60	
ρ_0(g/cm^3)	1.60		1.60	
%TMD	95		95	
IP Data	x	t	x	t
	51.8	0.0	51.6	0.0*
	79.8	276.1	79.5	38.5*
	130.7	329.8	104.9	91.2*
	181.5	350.9	130.3	107.9*
	219.5	368.0	149.4	119.1
	251.3	386.0	168.4	148.7
	276.7	397.6	187.5	156.4
	302.3	409.5	206.5	164.2
	327.5	422.2	225.6	173.5
	352.9	435.2	244.6	181.8
	378.5	444.0	263.7	189.6
SG Data	x	t	x	t
	20.6	251	20.6	112.5
	79.6	269	79.5	122.2
	143.3	329	111.3	105.7
	206.5	360	143.0	115.2
	207.0	373	181.1	143.8
	F		F	

DISTRIBUTION

	Copies
Chief of Naval Material Department of the Navy Washington, DC 20360	1
Commander Naval Air Systems Command Attn: AIR-350 AIR-330 Department of the Navy Washington, DC 20361	 1 1
Commander Naval Sea Systems Command Attn: SEA-093B12 SEA-06R SEA-62R2 SEA-06H3 SEA-62R32 SEA-64E Department of the Navy Washington, DC 20362	 2 1 1 1 1 1
Director Strategic Systems Project Office (PM-1) Attn: SP-2731 (E. Throckmorton) Department of the Navy Washington, DC 20376	 1
Chief of Naval Research Attn: ONR-260 ONR-432 (R. Miller) ONR-741 (Technical Library) Department of the Navy Arlington, VA 22217	 1 1 1
Commanding Officer Naval Propellant Plant Attn: Technical Library Indian Head, MD 20640	 1
Office of Naval Technology Attn: MAT-07P (J. Enig) Department of the Navy 800 North Quincy Street Arlington, VA 22217	 1
Commander Naval Weapons Center Attn: Technical Library Code 389 (R. Derr) Code 3835 (R. G. Sewell) Code 3891 (T. Boggs) Code 3891 (H.D. Mallory) Code 3891 (K. Graham) China Lake, CA 93555	 1 1 1 1 1 1
Director Naval Research Laboratory Attn: Technical Information Section Washington, DC 20375	 2
Office of Chief of Naval Operations Operations Evaluation Group (OP03EG) Washington, DC 20350	 1
Director Defense Advanced Research Projects Agency Washington, DC 20301	 1

DISTRIBUTION (CONT.)

	Copies
Commanding Officer Naval Weapons Station Attn: R & D Division Code 50 Yorktown, VA 23691	1 1
Commanding Officer Naval Explosive Ordnance Disposal Facility Attn: Information Services Indian Head, MD 20640	1
McDonnell Aircraft Company Attn: M. L. Schimmel P. O. Box 516 St. Louis, MO 63166	1
Commanding Officer Naval Ammunition Depot Crane, IN 47522	1
Commanding Officer Naval Weapons Evaluation Facility Attn: Code AT-7 Kirtland Air Force Base Albuquerque, NM 87117	1
Commanding Officer Naval Ammunition Depot Attn: QEL Concord, CA 94522	1
Superintendent Naval Academy Attn: Library Annapolis, MD 21402	1
Naval Plant Representative Office Strategic Systems Project Office Lockheed Missiles and Space Co. Attn: SPL-332 (R. H. Guay) P. O. Box 504 Sunnyvale, CA 94088	1
Hercules Incorporated Allegany Ballistics Laboratory Attn: Library P. O. 210 Cumberland, MD 21502	1
AMCRD 5001 Eisenhower Avenue Alexandria, VA 22302	1
Redstone Scientific Information Center U. S. Army Missile Command Attn: Chief, Documents Redstone Arsenal, AL 35809	2
Commanding Officer Army Armament Research and Development Command Energetic Materials Division Attn: DRSMC-LCE-D(D) (N. Slagg) Dover, NJ 07801	1
Commanding Officer Harry Diamond Laboratories Attn: Library Keith Warner 2800 Powder Mill Road Adelphia, MD 20783	1 1
Armament Development & Test Center DLOSL/Technical Library Eglin Air Force Base, FL 32542	1
Commanding Officer Naval Ordnance Station Louisville, KY 40124	1
Director Applied Physics Laboratory Attn: Library Johns Hopkins Road Laurel, MD 20707	1

DISTRIBUTION (CONT.)

	Copies
U. S. Department of Energy Attn: DMA Washington, DC 20545	1
Research Director Pittsburgh Mining and Safety Research Center U. S. Bureau of Mines 4800 Forbes Avenue Pittsburgh, PA 15213	1
Director Defense Technical Information Center Cameron Station Alexandria, VA 22314	12
Goddard Space Flight Center, NASA Glenn Dale Road Greenbelt, MD 20771	1
Lawrence Livermore National Laboratory University of California Attn: Library	1
M. Finger	1
E. Lee	1
P. Urtiew	1
C. Tarver	1
P. O. Box 808 Livermore, CA 94550	
Sandia National Laboratories Attn: R.J. Lawrence, Div. 5166 P. O. Box 5800 Albuquerque, NM 87115	1
Director Los Alamos National Laboratory Attn: Library	1
R. L. Rabie	1
H. Flaugh	1
C. Forest	1
P. O. Box 1663 Los Alamos, NM 87544	

	Copies
Chairman DOD Explosives Safety Board Attn: Dr. T. A. Zaker 2461 Eisenhower Avenue Alexandria, VA 22331	1
Aerojet Ordnance and Manufacturing Company 9236 East Hall Road Downey, CA 90241	1
Thiokol/Huntsville Division Attn: Technical Library Huntsville, AL 35807	1
Zernow Technical Service Center Attn: Dr. L. Zernow 425 W. Bonita Ave., Suite 208 San Dimas, CA 91773	2
SRI, International Attn: D. Curran 333 Ravenswood Avenue Menlo Park, CA 94025	1
Thiokol/Elkton Division Attn: Technical Library P. O. Box 241 Elkton, MD 21921	1
Teledyne McCormick Selph P. O. Box 6 Hollister, CA 95023	1
Lockheed Missiles and Space Co., Inc. P. O. Box 504 Sunnyvale, CA 94086	1
R. Stresau Laboratory, Inc. Star Route Spooner, WI 54801	1

DISTRIBUTION (CONT.)

	Copies
Rohm and Haas Huntsville, Defense Contract Office Attn: H. M. Shuey 723-A Arcadia Circle Huntsville, AL 35801	1
U. S. Army Foreign Service and Technology Center 220 7th Street, N.E. Charlottesville, VA 22901	1
Princeton Combustion Research Laboratories, Inc. 1041 U. S. Highway One North Attn: M. Summerfield N. Messina Princeton, NJ 08540	1 1
Pennsylvania State University Dept. of Mechanical Engineering Attn: K. Kuo University Park, PA 16802	1
Director Ballistic Research Laboratories Attn: Library N. Gerri P. Howe R. Frey D. Kooker Aberdeen Proving Ground, MD 21005	1 1 1 1 1
Paul Gough Associates 1048 South Street Portsmouth, NH 03801	1
Hercules Incorporated, Aerospace Division Attn: B. Hopkins Library 100-H D. Caldwell P. O. Box 98 Magna, UT 84044	1 1 2
Professor H. Krier 144 MEB, University of IL, at U-C 1206 West Green Street Urbana, IL 61801	3
Chemical Propulsion Information Agency The Johns Hopkins University Applied Physics Laboratory Johns Hopkins Road Laurel, MD 20707	1
IIT Research Institute Attn: H. S. Napadensky 10 West 35th Street Chicago, IL 60616	1
Erion Associates, Inc. Attn: W. Petray 600 New Hampshire Avenue, Suite 870 Washington, DC 20037	1
Brigham Young University Dept. of Chemical Engineering Attn: Dr. M. W. Beckstead Provo, UT 84601	1
Library of Congress Attn: Gift and Exchange Division Washington, DC 20540	4
Commanding Officer Naval Underwater Systems Center Attn: LA 151 - Technical Library Newport, RI 02840	1
KAMAN Sciences Attn: J. F. Kincaid 1911 S. Jefferson Highway Suite 1200 Arlington, VA 22202	1

DISTRIBUTION (CONT.)

	Copies
Internal Distribution:	
E36 (GIDEP Office)	1
E431	9
E432	3
R10	1
R13 (Jacobs)	1
R13 (Price)	2
R11 (Kamlet)	1
R10C (Roslund)	1
R10D (Adolph)	1
R10B (Stosz)	1
R11	2
R12	1
R13	2
R14	1
R15	1
R16	1
R10F (Bernecker)	1
R13 (Clairmont)	1
R13 (Sandusky)	1
R13 (Coffey)	1
R12 (Short)	1
R13 (Elban)	1
R13 (Kim)	1
R13 (Forbes)	1
R13 (Coleburn)	1
R13 (Liddiard)	1
R13 (Zerilli)	1
R11 (Hall)	1
R11 (Gotzmer)	1
R11 (Anderson)	1
R12 (Montesi)	1
R13 (DeVost)	1
R13 (Tasker)	1

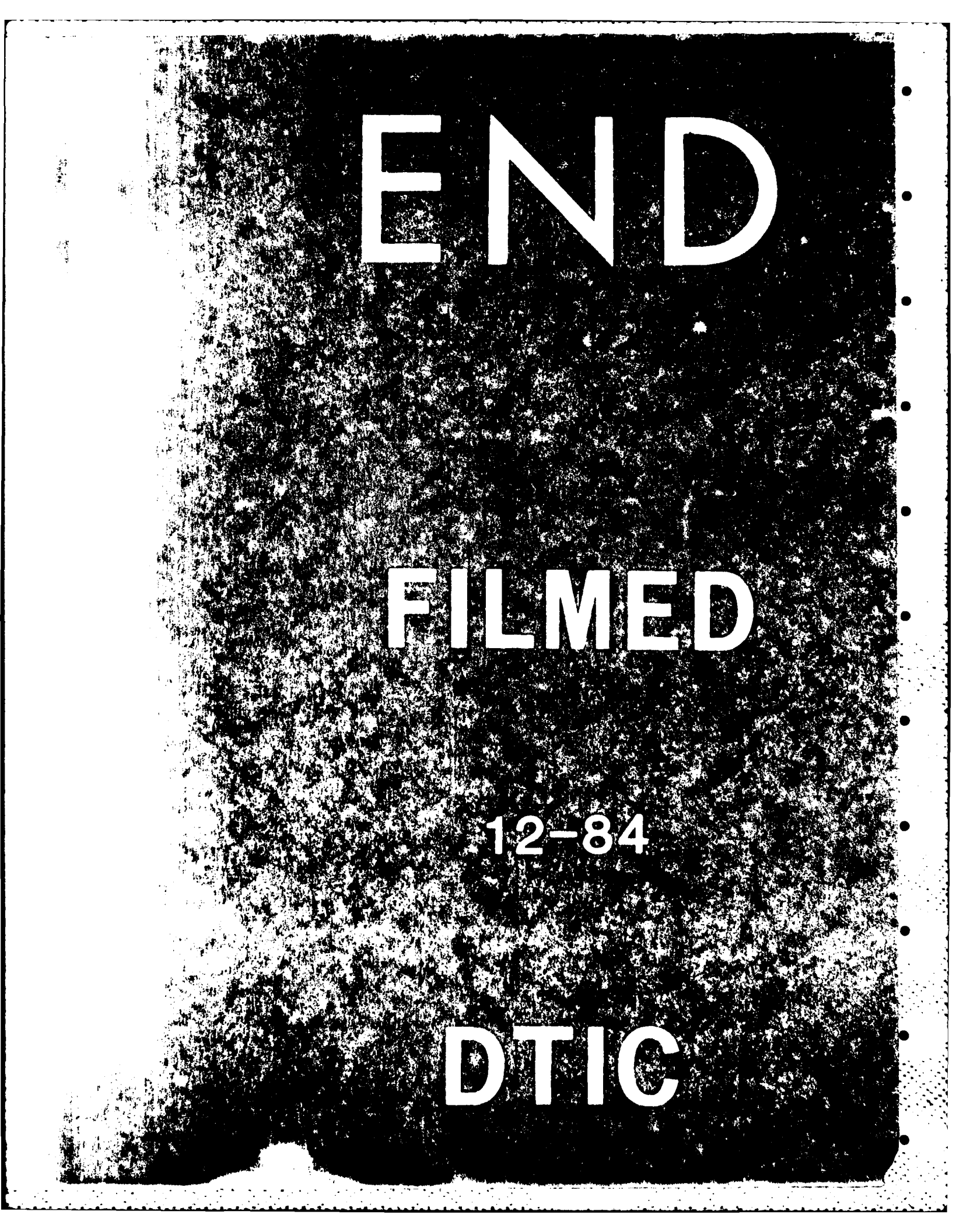
END
FILMED
12-84
DTIC